

**UNIVERSITY OF BOTSWANA**



**FACULTY OF ENGINEERING AND TECHNOLOGY**

**DEPARTMENT OF CIVIL ENGINEERING**

**TITLE**

**CLIMATOLOGICAL DROUGHTS AND THEIR IMPLICATIONS ON WATER  
RESOURCES AND AGRICULTURAL PRODUCTION IN SEMIARID REGIONS:  
THE CASE OF BOTSWANA**

**By**

**Student Name: Jimmy Byakatonda**

**Student Number: 201406683**

**Submitted to the School of Graduate Studies in Fulfilment of the Requirements for the  
Degree of Doctor of Philosophy of Engineering: Civil Engineering**

**Supervisor:**

**Professor B. P. Parida**

**Co-Supervisors:**

**Prof. Piet K. Kenabatho**

**Dr. Ditiro B. Moalafhi**

**September 2018**

## DECLARATION

The work titled **“Climatological droughts and their implications on water resources and agricultural production in semiarid regions: The case of Botswana”** contained in this thesis was completed by the author at the University of Botswana between October 2014 and March 2018. It is original work except where due reference is made and neither has been nor will be submitted for any academic award at University of Botswana or any other University to the best of my knowledge.

Signature: ..... Date: .....

Jimmy Byakatonda

This thesis has been submitted with the approval of the supervisors:

Professor B. P. Parida

Signature: ..... Date: .....

Prof. Piet K. Kenabatho

Signature: ..... Date: .....

Dr. Ditiro B. Moalafhi

Signature: ..... Date: .....

## ACKNOWLEDGEMENT

Sincere gratitude goes to my supervisors Professor B. P. Parida, Prof. Piet K. Kenabatho and Dr. Ditiro B. Moalafhi who have tirelessly rendered academic mentorship from inception to completion of this research. It has been an unwinding journey from the period of shaping the research concept through to producing this thesis. You made me believe in myself after you believed in me. You have developed me not only academically but also in other spheres of life.

My sincere thanks also go the Departments of Meteorological Services and Water Affairs of Botswana together with the Ministry of Agriculture for their kindness and willingness to provide data that were used in this research. The officials in these government entities have kept their offices open for consultations without hesitation.

I also extend my appreciation to Prof. M. Dithinde and Dr. B. Nkwae the former and current head of Civil Engineering Department respectively for their mentorship. Further still gratitude goes to Dr. P.T Odirile and Mr. N.M Subsang for their encouragement during the course this research. To my PhD colleagues you have been a wonderful group thank you very much. I hope we can continue the interaction even after this study as there will be more other exciting opportunities that may require our collaboration.

Special thanks go to the Mobility for Enhancement of Training for Engineering Graduates in Africa (METEGA) for enabling me to undertake this PhD program through the sponsorship they accorded me. I also thank Gulu University for granting me study leave that has allowed me to attend to this program on a fulltime basis.

Last but not least my young family who accepted to stay behind while I pursue this cause. To my youngest son Alban Kihanda Byakatonda who was born while I was away attending this program, may you live to walk in my footsteps and beyond. Thank you family for the support you have exhibited throughout this journey and am not walking alone.

## **DEDICATION**

This thesis is dedicated to my late grandmother **Ms Masika Janeta** who saw me through my early years and passed on just before enrolling on this program. I still hold you dearly. Requiem aeternam dona ei, Domine, et lux perpetua luceat ei. Requiescat in pace. Amen.

## ABSTRACT

In recent years, the frequency of droughts have been increasing due to climate anomalies mostly attributed to climate variability and high water demand brought about by changing lifestyle and urban migration. Although several drought indices have been identified to characterise droughts in various literature and some even recommended by the World Meteorological Organisation (WMO), a more comprehensive index is the one known as Standardised Precipitation and Evapotranspiration Index (SPEI), as an extension of the well-known Standardised Precipitation Index (SPI) to include evapotranspiration in the water balance. Droughts have been described in this research using SPEI values to provide overall reasonable characteristics of different categories of drought at various timescales of 1-, 3-, 6-, 12-, 18- and 24-months. Further to make water resources management meaningful, it requires exploration of the association between SPEI and hydrological droughts represented by Standardised Flow Index (SFI). Climate anomalies leading to climate variability and frequent droughts have been associated with El Niño Southern Oscillation (ENSO) across southern Africa. These anomalies also are attributed to shifts in hydroclimatological factors. Hence it is necessary to carry out in-depth analysis of the onset and cessation of rainfall which otherwise impact agricultural production and food security of the region. These climate anomalies are being felt across the globe but vary to a large extent from one geographical location to another. For this reason, impacts from one location cannot be extrapolated to another. It is therefore necessary to develop location specific mitigation measures towards impacts of climate variability and change. It is on this premise that Botswana, located in the semiarid subtropics and relying mainly on surface water stored in reservoirs, is selected as a case study. Moreover 80% of Botswana's population is engaged in rainfed agriculture as a source of livelihood. In order to arrive at futuristic status of rain onset and cessation dates, Standardised Flow Index (SFI) and cereal yields, an attempt has been made to use artificial intelligence framework in the form of Nonlinear Autoregressive with Exogenous input (NARX) Neural Network (NN) model

to make five (5) years ahead forecasts of the above climatic factors. This research therefore attempts to study the following using meteorological data from 14 synoptic stations for a period 1960-2016: (i) Climatic behavior under ENSO influence including trends in meteorological variables, (ii) determination of onset and cessation of rainfall including dry spell frequency analysis, (iii) determination of SPEI and SFI for climatic and hydrological drought characterisation respectively (iv) determination of the association between climatic indices and cereal yields and (v) providing predictions of stream flow drought in the form of SFI, cereal yields, onset and cessation of rain dates.

In order to achieve the above objectives, this research carried out homogeneity tests and trend analysis using four (4) absolute tests (Standard Normal Homogeneity test, Buishand test, Pettit test, Von Nuemann test) and Man-Kendall test. Results indicate that rainfall time series are fully homogeneous with minimum and maximum temperature showing some years of intervention (i.e. change points). These years of intervention closely followed patterns of ENSO events. Trends also indicate a regionalised decrease in rainfall by 14.7% coupled with 2% increase in temperature across Botswana. The influence of ENSO on local climate was also investigated by determining the degree of association between climatic variables and Sea Surface Temperatures (SSTs) on one hand and Southern Oscillation Index (SOI) on the other hand. Results show negative correlations between SST and rainfall while positive correlations were observed between rainfall and SOI following the ENSO phenomenon. To further understand the influence of summer rainfall on agriculture, seasonal characteristics in the form of dry spell frequency, number of rainy days, onset and cessation of rain were investigated. From these investigations, results show the earliest onset occurring on 30<sup>th</sup>/November in the northeast while the latest on 11<sup>th</sup>/January in the southwest. The cessation of rain dates took an opposite spatial trend with shorter rain season observed in the southwest. Shakawe, Pandamatenga and Kasane were found to have length of the rain season (LRS) of more than 100 days making them suitable for medium maturing cereals. Since droughts have been

identified as a feature of climate variability, their spatiotemporal variability was explored. Botswana was found to be more vulnerable to moderate droughts which showed a high degree of association with ENSO during summer season. A common timescale of 15-months was identified to be suitable for drought monitoring across the study area. It was also observed that climatic droughts take 6 and 7 months to propagate into hydrological droughts in the Okavango and Limpopo river basins respectively. The implication of climate variability on agriculture was further investigated by determining the influence of climatic indices, LRS and ENSO on cereal yields of maize and sorghum. ENSO was found to have the greatest influence on cereal yield accounting for 85% and 78% in maize and sorghum yield variations respectively. Predictions from the three NARX-NN models reveal a likelihood of a shift in the rain season and higher variability in SFI in the near future. Cereal yield projections for the next 5 years reveal a possible yield decline in both maize and sorghum by 52 kg/ha and 126 kg/ha respectively. This research has demonstrated that Botswana's climate is closely associated with ENSO leading to more uncertainty in rainfall and rainfed agriculture. It is envisaged that information generated from this research will enhance agriculture and water resources planning and management especially in semiarid regions where adaptation to climate variability and change is still a challenge.

## TABLE OF CONTENTS

DECLARATION .....	ii
ACKNOWLEDGEMENT .....	iii
DEDICATION .....	iv
ABSTRACT.....	v
TABLE OF CONTENTS.....	viii
LIST OF TABLES .....	xii
LIST OF FIGURES .....	xiv
LIST OF ACRONYMS .....	xvii
CHAPTER–1 .....	1
1. INTRODUCTION .....	1
1.1 BACKGROUND.....	1
1.2 STUDY AREA.....	5
1.2.1 Location of study area .....	5
1.2.2 Population.....	6
1.2.3 Climate profile.....	6
1.2.4 Water resources .....	9
1.2.5 Agriculture.....	10
1.3 PROBLEM STATEMENT .....	10
1.4 OVERALL OBJECTIVE.....	12
1.4.1 Specific research objectives.....	12
1.4.2 Research questions .....	13
1.5 RELEVANCE OF THE STUDY .....	13
1.6 SCOPE OF THE STUDY .....	15
1.7 LAYOUT OF THE THESIS .....	15
CHAPTER–2 .....	17
2. LITERATURE REVIEW .....	17



2.1 INTRODUCTION.....	17
2.2 CLIMATE VARIABILITY AND CHANGE IN SEMIARID REGIONS UNDER GLOBAL WARMING.....	19
2.3 ONSET, CESSATION OF RAIN AND DRY SPELL FREQUENCY IN SEMIARID REGIONS.....	22
2.4 DROUGHT INDICES .....	23
2.5 DROUGHT CHANGES UNDER GLOBAL WARMING .....	25
2.6 ARIDITY AND DROUGHT PROPAGATION .....	26
2.7 MODELING DROUGHT SEVERITY UNDER CLIMATE VARIABILITY .....	29
CHAPTER–3 .....	32
3. DATA AND METHODS USED IN THE RESEARCH .....	32
3.1 INTRODUCTION.....	32
3.2 DATA REQUIREMENTS .....	32
3.2.1 Climatological data.....	32
3.2.2 Hydrological data .....	32
3.2.3 Large scale climatic predictors .....	34
3.2.4 Crop yield data.....	35
3.3 METHODS USED IN THE RESEARCH .....	37
3.3.1 Climatic trends and abrupt changes in meteorological time series .....	37
3.3.2 Onset, cessation of rainfall and dry spell frequency analysis.....	45
3.3.3 Drought severity under climate variability and its relationship with ENSO.....	48
3.3.4 Drought propagation and its influence on water resources .....	52
3.3.5 Influence of climatic indices, length of the rain season on cereal yield.....	57
3.3.6 Modeling climate dynamics and cereal yields using artificial neural network .....	59
CHAPTER–4 .....	65
4. ANALYSIS AND DISCUSSION OF RESULTS .....	65
4.1 GENERAL INTRODUCTION .....	65
4.2 CLIMATIC TRENDS AND ABRUPT CHANGES IN METEOROLOGICAL TIME SERIES.....	65
4.2.1 Tests for homogeneity .....	66
4.2.2 Mann-Kendall (MK) trend analysis and percentage change .....	69
4.2.3 Detection of serial correlation in meteorological variables.....	75
4.2.4 Influence of ENSO on local climatic variables .....	77

4.2.5 Summary.....	79
4.3 ONSET, CESSATION OF RAINFALL AND DRY SPELL FREQUENCY ANALYSIS .....	81
4.3.1 Seasonal rainfall totals.....	81
4.3.2 Number of rainy days .....	84
4.3.3 Onset and cessation of rain dates.....	84
4.3.4 Length of the rain season (LRS).....	88
4.3.5 Dry spell frequency (DSF) analysis.....	90
4.3.6 Summary.....	92
4.4 DROUGHT SEVERITY UNDER CLIMATE VARIABILITY AND ITS RELATIONSHIP WITH ENSO .....	94
4.4.1 Drought occurrence and evolution .....	94
4.4.2 Drought characteristics and their spatial patterns.....	101
4.4.3 Association of ENSO with drought severity .....	108
4.4.4 Summary.....	113
4.5 DROUGHT PROPAGATION AND ITS INFLUENCE ON WATER RESOURCES .	115
4.5.1 Dynamics of climatic and hydrological droughts.....	115
4.5.2 Degree of association between climatic and hydrological droughts .....	120
4.5.3 Timescale for drought monitoring across Limpopo and Okavango river basins ....	123
4.5.4 Rescaled range analysis at 15-months timescale.....	124
4.5.5 Summary.....	125
4.6 INFLUENCE OF CLIMATIC INDICES, LENGTH OF THE RAIN SEASON AND ENSO ON CEREAL YIELDS .....	127
4.6.1 Crop yield data smoothing.....	127
4.6.2 Associations between cereal yields and aridity index (AI) at 1-month timescale...	128
4.6.3 Associations between cereal yields and aridity index (AI) at timescales of 3-, 6- and 12-months timescale .....	130
4.6.4 Associations between cereal yields and Standardised Precipitation Evapotranspiration Index (SPEI) at 1-month timescale .....	134
4.6.5 Associations between cereal yields and Standardised Precipitation Evapotranspiration Index (SPEI) at 3-, 6- and 12-months timescale .....	135
4.6.6 Association between Southern Oscillation Index (SOI) and cereal yields at 1-month timescale .....	141
4.6.7 Association between Length of the rain season (LRS) and cereal yields.....	143
4.6.8 Spatial distribution of correlations (r) between cereal yields and climatic indices .	144
4.6.9 Comparisons between climatic indices and crop yield trends.....	147

4.6.10 Summary.....	148
4.7 MODELING ONSET AND CESSATION OF RAIN, STREAM FLOW DROUGHT AND CEREAL YIELDS USING ARTIFICIAL NEURAL NETWORK.....	150
4.7.1 Prediction of rain onset and cessation dates .....	150
4.7.2 Predictions of Stream flow droughts .....	153
4.7.3 Projections of cereal yields.....	155
4.7.4 Summary.....	158
CHAPTER-5 .....	160
5. CONCLUSIONS AND RECOMMENDATIONS .....	160
5.1 INTRODUCTION.....	160
5.2 CONCLUSIONS .....	160
5.3 CONTRIBUTIONS TO KNOWLEDGE AND RESEARCH OUTPUT .....	164
5.3.1 Contribution to knowledge .....	164
5.3.2 Research outputs.....	165
5.4 LIMITATIONS OF THE STUDY .....	166
5.5 RECOMMENDATIONS FOR FURTHER RESEARCH .....	167
REFERENCES .....	168

## LIST OF TABLES

<b>Table 3-1.</b> Synoptic station locations and length of meteorological variable (rainfall, maximum and minimum temperature) record.....	33
<b>Table 3-2.</b> Agricultural regions with respective synoptic stations .....	36
<b>Table 3-3.</b> Drought severity classifications (Yu et al., 2014) .....	49
<b>Table 4-1.</b> P-Values from four homogeneity tests on rainfall time series.....	66
<b>Table 4-2.</b> P-Values from four homogeneity tests and probable year of intervention for maximum temperature .....	67
<b>Table 4-3.</b> P-Values from four homogeneity tests and probable year of intervention for minimum temperature.....	68
<b>Table 4-4.</b> MK trend and Sen’s Slope estimator results for rainfall .....	70
<b>Table 4-5.</b> MK trend and Sen’s Slope estimator results for maximum temperature.....	72
<b>Table 4-6.</b> MK trend and Sen’s Slope estimator results for minimum temperature .....	74
<b>Table 4-7.</b> Seasonal rainfall characteristics.....	82
<b>Table 4-8.</b> MK trends Z-statistic and Sen’s Slope estimator for rainfall characteristics .....	86
<b>Table 4- 9.</b> Maximum drought severity (SPEI), duration and years of their occurrence .....	99
<b>Table 4-10.</b> Probabilities of occurrence of various drought categories.....	102
<b>Table 4-11.</b> Correlation coefficient between climatic and hydrological droughts .....	121
<b>Table 4-12.</b> Maize and sorghum yield correlations (r) with climatic indices at 1-month timescale .....	129
<b>Table 4-13.</b> Maize and sorghum yield correlations (r) with climatic indices at timescales of 3-, 6- and 12-months .....	137
<b>Table 4-14.</b> Artificial Neural Network (ANN) model performance together with onset and cessation of rain predictions.....	151

**Table 4-15.** Artificial Neural Network (ANN) model performance and crop yield projections  
..... 156

## LIST OF FIGURES

<b>Fig. 1-1.</b> Map of Botswana with spatial distribution of synoptic stations .....	5
<b>Fig. 1-2.</b> Annual rainfall totals (a) Period 1996-2005 (b) Period 2006-2016 .....	8
<b>Fig. 1-3.</b> Rainfall mass curves at selected synoptic stations (a) Ghanzi (b) Letlhakane (c) SSKA and (d) Jwaneng .....	9
<b>Fig. 2-1.</b> Drought propagation (modified from Zargar Yaghoobi (2012)) .....	29
<b>Fig. 3-1.</b> Location of synoptic stations and river gauging stations used in hydrological drought analysis.....	33
<b>Fig. 3-2.</b> Spatial distribution of crop yield data locations across agricultural zones and rainfall coefficient of variation .....	35
<b>Fig. 3-3.</b> Nonlinear auto regressive with exogenous input (NARX) ANN architecture.....	63
<b>Fig. 4-1.</b> Annual rainfall MK-Z trends .....	71
<b>Fig. 4-2.</b> Maximum temperature MK-Z trends .....	73
<b>Fig. 4-3.</b> Minimum temperature MK-Z trends.....	75
<b>Fig. 4-4.</b> Serial correlation effect on annual rainfall time series .....	76
<b>Fig. 4-5.</b> Serial correlation effect on annual (a) Maximum (b) Minimum temperature series ..	76
<b>Fig. 4-6.</b> Proportions of stations with significant correlation between ENSO and local climatic variables .....	78
<b>Fig. 4-7.</b> Annual maximum temperature normalised at Mahalapye and Nino 3.4 SST time series .....	78
<b>Fig. 4-8.</b> Seasonal rainfall totals with coefficient of variation at each station.....	82
<b>Fig. 4-9.</b> MK trends and dates for (a) Rain onset and (b) Rain cessation.....	87
<b>Fig. 4-10.</b> Spatial trends of length of rain season (LRS) and values of LRS.....	89

<b>Fig. 4-11.</b> Dry spell frequency (DSF) trends (Figures at the stations indicate DSF values) for October-April season .....	91
<b>Fig. 4-12.</b> Temporal evolution of SPEI of 3-, 6-, 12- and 24-month at a) Francistown and b) Ghanzi .....	96
<b>Fig. 4-13.</b> Temporal evolution of SPEI of 3-, 6-, 12- and 24-month at c) Maun and d) Tsabong .....	97
<b>Fig. 4-14.</b> Spatial patterns of vulnerability towards a) SPEI-1 severe drought, b) SPEI-1 moderate drought, c) SPEI-3 severe drought d) SPEI-3 moderate drought, e) SPEI-6 severe drought f) SPEI-6 moderate drought.....	105
<b>Fig. 4-15.</b> Spatial patterns of vulnerability towards a) SPEI-12 severe drought, b) SPEI-12 moderate drought, c) SPEI-18 severe drought d) SPEI-18 moderate drought, e) SPEI-24 severe drought f) SPEI-24 moderate drought.....	107
<b>Fig. 4-16.</b> Box and whisker plots of the Pearson's correlation coefficients between SPEI and SSTs.....	110
<b>Fig. 4-17.</b> Box and whisker plots of the Pearson's correlation coefficients between SPEI and SOI.....	112
<b>Fig. 4-18.</b> Dynamics of climatic (red dotted line) and hydrological droughts ( blue shaded area) in the Limpopo basin at timescales of a) 3-months, b) 6-months, c) 12-months, d) 15-months and e) 18-months.....	117
<b>Fig. 4-19.</b> Dynamics of climatic (red dotted line) and hydrological droughts (blue shaded area) in the Okavango basin at timescales of a) 3-months, b) 6-months, c) 12-months, d) 15-months and e) 18-months.....	119
<b>Fig. 4-20.</b> Moderate drought probability across timescales.....	124
<b>Fig. 4-21.</b> H-Coefficient for the two river basins (a) Limpopo (b) Okavango .....	125
<b>Fig. 4-22.</b> Maize and sorghum yields (recorded and detrended) in selected regions (a) maize-northern, (b) maize-central, (c) sorghum-eastern, (d) sorghum-central.....	128

<b>Fig. 4-23.</b> Spatial distribution of correlations (r) (significant values are shown) between maize yield and (a) Aridity Index (AI), (b) Southern oscillation index (SOI), (c) Standardised Precipitation Evapotranspiration Index (SPEI) and (d) Length of the rain season (LRS).....	145
<b>Fig. 4-24.</b> Spatial distribution of correlations (r) (Significant values are shown) between sorghum yield and (a) Aridity Index (AI), (b) Southern oscillation index (SOI), (c) Standardised Precipitation Evapotranspiration Index (SPEI) and (d) Length of the rain season (LRS).....	146
<b>Fig. 4-25.</b> Comparisons between time series of climatic indices and crop yield anomalies (a) AI and maize yield, (b) SOI and maize yield (c) SPEI and maize yield, (d) LRS and sorghum yield.....	148
<b>Fig. 4-26.</b> Artificial Neural Network (ANN) model outputs and targets for onset and cessation dates at selected station. Onset dates predictions at (a) Kasane, (b) SSKA, (c) Ghanzi and cessation dates predictions at (d) Kasane, (e) SSKA, (f) Ghanzi .....	152
<b>Fig. 4-27.</b> Artificial Neural Network (ANN) model outputs and targets for standardised flow index (SFI) at the two river basins (a) Limpopo (b) Okavango.....	154
<b>Fig. 4-28.</b> Artificial Neural Network (ANN) crop yield projection model outputs and targets in selected regions (a) Maize yield-northern, (b) Maize yield-eastern, (c) Maize yield-central, (d) Sorghum yield-southern, (e) Sorghum yield-eastern and (f) Sorghum yield-western.....	157



## LIST OF ACRONYMS

AI	Aridity Index
AMSL	Above Mean Sea Level
ANN	Artificial Neural Network
ARIMA	Autoregressive integrated moving average
ASCE	American Society of Civil Engineers
CDF	Cumulative Density Function
CV	Coefficient of Variation
DRNN	Dynamic Recurrent Neural Network
DWA	Department of Water Affairs
ENSO	El Niño Southern Oscillation
ESS	Effective Sample Size
ET <sub>0</sub>	Potential Evapotranspiration
FAO	Food and Agricultural Organisation
GEV	Generalised Extreme Value
GLO	Generalised logistic
GOB-MEWT	Government of Botswana- Ministry of Environment, Wildlife and Tourism
ICID	International Commission on Irrigation and Drainage
ICPAC	Climate Prediction and Applications Centre

IGAD	Intergovernmental Authority for Development
IPCC	Intergovernmental Panel on Climate Change
ITCZ	Inter Tropical Convergence Zone
LRS	Length of the Rain Season
MARIMA	Multiplicative Autoregressive Integrated Moving Average
MK	Mann-Kendall
MSE	Mean Squared Error
MWEWR	Ministry of Minerals, Energy and Water Resources
NARX	Nonlinear Autoregressive with Exogenous input
NOAA	National Oceanic and Atmospheric administration
PDF	Probability Density Function
PDSI	Palmar Drought Severity Index
PET	Potential Evapotranspiration
PWM	Probability Weighted Moments
R/S	Rescaled Range Analysis
RMSE	Root Mean Square Error
RNN	Recurrent Neural Network
SARIMA	Seasonal Autoregressive Integrated Moving Average
SFI	Standardised Flow Index

SNHT	Standard Normal Homogeneity Test
SOI	Southern Oscillation Index
SPEI	Standardised Precipitation and Evapotranspiration Index
SPI	Standardised Precipitation Index
SST	Sea Surface Temperatures
WMO	World Meteorological Organisation

## **CHAPTER-1**

### **1. INTRODUCTION**

#### **1.1 BACKGROUND**

Over the years, it has been established that anthropogenic effects on the environment are having a substantial contribution towards global warming and variations in climate patterns (Cooper et al., 2008; Khan et al., 2009; IPCC, 2012). These effects even worsen the otherwise naturally occurring variations, some of which are also in teleconnection with El Niño southern oscillation (ENSO) events in the Equatorial Pacific (Zaroug et al., 2013; Hoell et al., 2015). Climate models have predicted an average global temperature rise of more than 2 °C, with higher than the projected temperature in semiarid areas exacerbating climate variability in these regions (Feidas et al., 2004; Engelbrecht et al., 2015; Rahman and Lateh, 2015). The increased incidences of climate variability have resulted in frequent droughts and floods in different locations in recent times. Thus droughts have become frequent and pose challenges to water resources and rainfed farming as a whole, particularly in semiarid regions. These challenges are a threat to efforts towards achieving Sustainable Development Goals (SDG) 2 and 13 (eradication of all forms of hunger and taking actions towards addressing effects of climate change respectively) especially in semiarid regions.

Challenges brought about by climate change and increased incidences of climate variability call for new strategies in order to increase agricultural output and hence guarantee food security (Rowhani et al., 2011). Farming practices and water resources utilisation will therefore need to adapt to this high variability in rainfall, more severe and frequent droughts (Tirado and Cotter, 2010; Nath et al., 2017). It was reported by Pachauri and Reisinger (2008) and Rowhani et al. (2011) that in semiarid areas which are already seasonally dry, crop productivity is projected to decrease even for small local temperature increases between 1 to 2

°C, which would increase the risk of hunger, poverty and disease. Studies by Cancelliere et al. (2007) and Naumann et al. (2014) suggest that drought monitoring and prediction are important ingredients in implementing appropriate drought mitigation measures. Equally a study in Botswana reported how spatial and temporal representation of drought severity is essential in drought vulnerability assessment and hence monitoring (Batisani, 2011).

Gommes and Petrassi (1994), Malesu et al. (2007) and more recently Masih et al. (2014) reported chronology of drought events that have ravaged agriculture and water resources on the African continent. They indicated a long history of variations in rainfall which have become more diverse both in length and intensity over time. The most devastating droughts were reported in the 1910s, affecting both East and West Africa. This followed periods of higher rainfall and then in 1950 onwards, rainfall decreased, culminating in a drought in West Africa in 1984. They went ahead to state that the decade of 1960 to 1970 inclined towards wetter years as compared to the two subsequent decades of 1970 to 1990. Nevertheless, years when rainfall was below normal were 1973, 1984 and 1992 with many of them following El Niño events. The first episode of 1973 succeeded good years of above normal rainfall and hence caught most countries off guard causing far adverse impacts as compared to 1984 because countries had developed coping mechanisms. The 1992 Southern African drought was moderately limited in its geographical extent as compared to the Sahel drought episode. The southern African region has been reported by Gommes and Petrassi (1994) and Malesu et al. (2007) as exhibiting a relatively low rainfall index with variability exceeding that of the Sahel region. The collective features between this region and the southern-central Africa and Madagascar region in the drought phenomena are the dry years of 1973, 1982, 1983 and 1992, with also some notable differences, such as in 1985 and 1993. The countries in this region were severely affected by the 1991/92 droughts, which were the most severe after the 1981 to 1985 droughts. The recent drought of 2015/16 was even more devastating in southern Africa leading to total crop failure and drying up of major water storage reservoirs including

Gaborone dam, the main source of water supply to Botswana's capital city Gaborone. All these drought episodes are attributed to climate anomalies (Mishra and Singh, 2011; Dai, 2013).

Two important features controlling the climate of southern Africa were reported in Nicholson et al. (2001) and Batisani (2011) as the semi-permanent sub-tropical high pressure systems located in the southeast Atlantic (St. Helena anticyclone) and southwest Indian Ocean (Mascarene high). These subtropical high pressure systems are associated with widespread and persistent subsidence. The other feature was from studies by Richard et al. (2000), Nicholson et al. (2001) and Edossa et al. (2014) which revealed ENSO's influence on rainfall over southern Africa given that it triggers an atmospheric response that influences sea surface temperatures (SSTs) in the Indian and Atlantic Oceans on the South African coast. These atmospheric responses are reported to be responsible for droughts during the El Niño phases and heavy rains during the La Niña periods. For these foregoing reasons, a greater part of southern Africa has been classified as semiarid and prone to high drought severities. The rain season across most of these semiarid locations is as a result of cold fronts occurring from the months of October through to April. December and January are the peak rainfall months occurring as a result of the downward movement of the Inter-Tropical Convergence Zone (ITCZ) and warm episodes blowing over the Atlantic, Pacific and Indian Oceans (Byakatonda et al., 2018c). This period coincides with the summer season during which high rates of evapotranspiration (ET) are experienced. The local climate is believed to be moderated by ENSO episodes, however the degree of their association has not been well established (Nicholson et al., 2001) which calls for further investigation.

Drought severity is best represented by indices which integrates various parameters of the water balance (rainfall, temperature, ET and runoff) to arrive at a broad picture for operational decision making in drought disaster management within the context of agricultural and water resources sectors (Sivakumar, 2010). It may be necessary to investigate the spatial extent of

droughts by way of interpolation of these indices over a given region at various timescales. Drought severity prediction have also been reported by Morid et al. (2007) and Byakatonda et al. (2016) as an important factor in drought preparedness as well as mitigation.

To further understand effects of climate variability, Botswana has been selected as a study area due to its characterisation as semiarid with highly erratic rainfall and high evapotranspiration rates (Batisani, 2012). Global warming has already hit Botswana as expressed through frequent and more severe droughts resulting in declining agricultural production and water resources that are unable to meet the current demand (Botswana Central Statistics, 2009; Byakatonda et al., 2018b). Studies of drought severity which were conducted in Botswana (Batisani, 2011) considered absence of rainfall as the only indicator triggering drought. However in the advent of global warming that has been widely reported (Pachauri and Reisinger, 2008; Huang et al., 2016), temperature cannot be ignored in climate change studies. Also, the declining agricultural yields threaten the food security situation of Botswana. There is thus an urgent need to improve performance in cereal production in Botswana to reduce the high levels of food imports, reduce rural urban migration and even avoid total abandonment of this subsector. To achieve this, it is necessary to investigate evolution of drought under climate variability in an effort to devise climate change adaptation strategies. Comprehensive studies of drought severity incorporating both precipitation and temperature are not documented for the study area. Equally the influences of large climatic predictors such as ENSO have also not been incorporated in studies of climate variability in Botswana. It is on this background that a comprehensive research is necessary to investigate the impact of drought under climate variability on water resources and rainfed farming over the study area taking into consideration the effects of global warming and influence of ENSO.

## 1.2 STUDY AREA

### 1.2.1 Location of study area

Botswana is centrally located in southern Africa, north of South Africa also bordering Zimbabwe, Namibia and Zambia as shown in Fig. 1-1. Botswana has land boundaries of combined length totalling 4,013 km, of which the constituent boundaries are shared with Namibia, for 1,360 km; South Africa, 1,840 km; Zimbabwe, 813 km and Zambia, 150 m. The country lies between latitude  $20.8^{\circ}$  S and  $26.8^{\circ}$  S and between longitude  $20.0^{\circ}$  E and  $29.4^{\circ}$  E. Botswana occupies an area of 600,370 km<sup>2</sup>, of which 581,730 km<sup>2</sup> is land (Batisani, 2011).

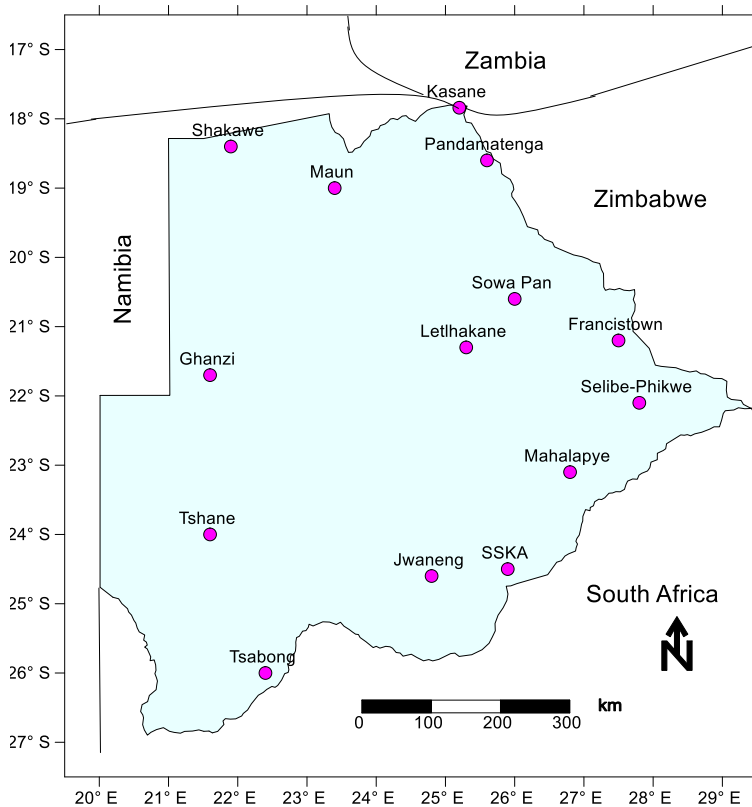


**Fig. 1-1.** Map of Botswana with spatial distribution of synoptic stations

Botswana completely lies within the shallow basin formed by the high-lying interior plateau of southern Africa. Three-quarters of the land surface is covered by the Kalahari sands, which fill the basin to a depth of up to several hundred meters. The land surface is nearly flat, with a mean altitude of 1000 m AMSL. The lowest point in Botswana is at the confluence of the



Limpopo and Shashe rivers at an altitude of 537 m while the highest point is found at the Otse Hill in the southeast, at 1491 m (GOB-MEWT, 2012).

### **1.2.2 Population**

The population figures from the most recent national census of 2011 stood at 2,024,787, with a growth rate of 2.0% relating to 2001 as the base year. Majority of this population is concentrated along the railway line in the east of the country at about 3 persons per km<sup>2</sup>. The population distribution is related to both historical factors, and availability of water and arable soils (Ministry of Finance and Development Planning, 2017).

### **1.2.3 Climate profile**

The country is arid to semiarid with low annual rainfall, the highest of 650 mm is registered in the northeast and lowest of 250 mm in the southwest (Tsheko, 2004; GOB-MEWT, 2012; Byakatonda et al., 2018d). Most of the rain occurs from November to April, and falls as localised showers and thunderstorms. The main features of the climate are determined by Botswana's inland location, spanning the subtropical high-pressure belt. In the summer period, the Inter-Tropical Convergence Zone (ITCZ) moves southward to about 20° S in November/December bringing moisture to the northern parts of the country resulting in rain onset in those locations. The rest of the subcontinent is influenced by a thermal low pressure cell. Moist air associated with the ITCZ, and the moist air which is fed in to the eastern parts of the country from the Indian Ocean, is warmed by the intense solar radiation, leading to convective storms. The air becomes gradually drier westwards as most of the moisture is shed over the eastern and northern parts of the country. From the months of May to September the stable high pressure cell and solar shift displaces the ITCZ together with its associated thermal lows northwards, resulting in drier conditions in winter. Once every few weeks during the dry season, westerly waves displace the cell northward, drawing in cold air from the south and causing light frontal clouds (GOB-MEWT, 2012).

The mean monthly maximum and minimum temperature ranges from 29 °C to 35 °C and 15 °C to 20 °C in summer respectively. The winter mean maximum and minimum temperatures are 20 °C to 29 °C and 3 °C to 12 °C respectively. The high solar radiation, low humidity and high temperatures lead to very high open water evaporation rates, ranging from 1800 to 2200 mm/year, way above the rainfall, signaling shortness of water (Byakatonda et al., 2016). The high variability in rainfall coupled with high potential evapotranspiration, exacerbates the challenge of water shortage in the already water stressed country (GOB-MEWT, 2012).

The study area is highly susceptible to increased incidences of climate variability because of its location in a semiarid region (Byakatonda et al., 2018c). It is also vulnerable to variations in climate induced by global sea-surface temperature anomalies. In particular, El Niño events in the Equatorial Pacific lead to negative departures from the normal in respect to rainfall, while La Niña events tend to enhance rainfall amounts. Rainfall over the study area is highly linked to the global El Niño Southern Oscillation phenomenon (Nicholson et al., 2001; Moalafhi et al., 2012). During strong El Niño years, the rainfall over most of the study area is severely depressed. These conditions may persevere for several years in succession. The perseverance of drought always bring a host of social problems like famine and diseases (GOB-MEWT, 2012). Botswana has over the years experienced dwindling water resources and frequent crop failures mainly attributed to erratic rainfall and declining totals.

Preliminary studies across the study area indicate that rainfall in dry locations of southwest is decreasing. During the same time period, the dry area is expanding from southwest towards northeast as shown in Figure 1-2. For example rainfall below 400 mm/yr that was concentrated in the southwestern locations between 1996 and 2006 (Figure 1-2a) has now spread to the central region during the period of 2006-2016 (Figure 1-2b). The area under these conditions is

observed to increase from 12.4% (Figure 1-2a) to 18.0% (Figure 1-2b) over the two time periods. This could imply increasing desertification which requires urgent mitigation measures.

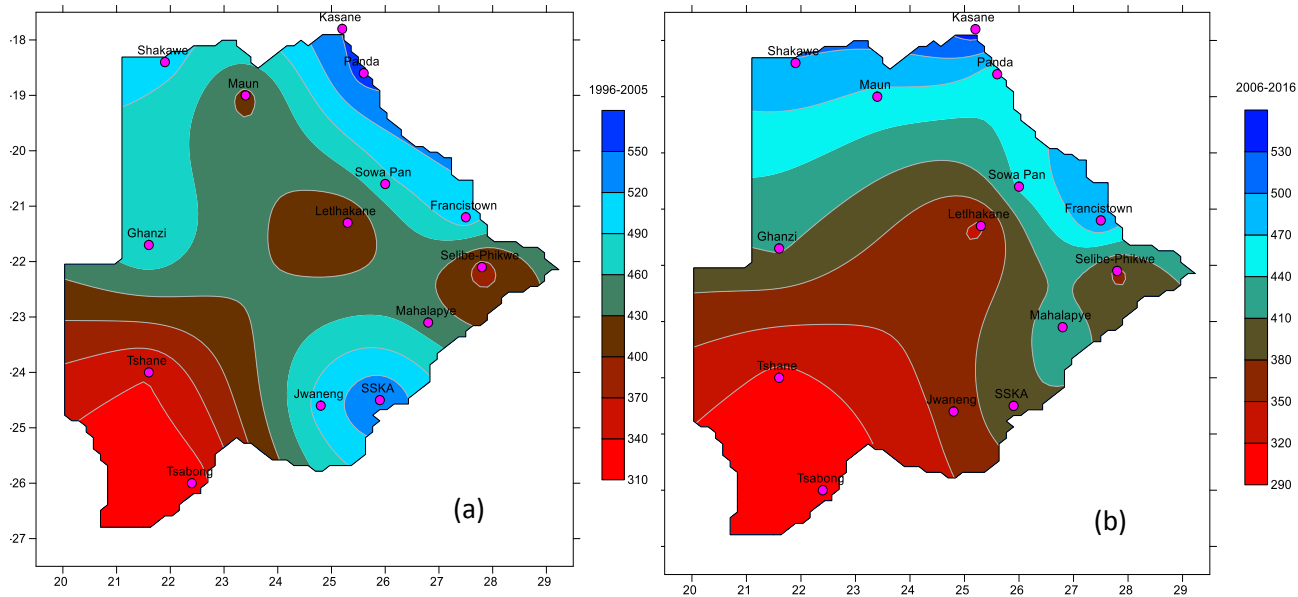


**Fig. 1-2.** Annual rainfall totals (a) Period 1996-2005 (b) Period 2006-2016

Further to this, the drop in rainfall below the 20 year average during the last decade is demonstrated with rainfall mass curves at selected locations across the study area (Figure 1-3). From these plots, it is evident that majority of Botswana's rainfall received during summer months from October to April have been decreasing. This decreasing rainfall and increasing dry area (Figure 1-2) could be corroborating the notion that dry semiarid locations will get even drier with the advent of climate change and increased variability (Pachauri and Reisinger, 2008). This makes it necessary to embark on studies that can help generate interventions in an effort to adapt to the impacts of droughts under climate variability.

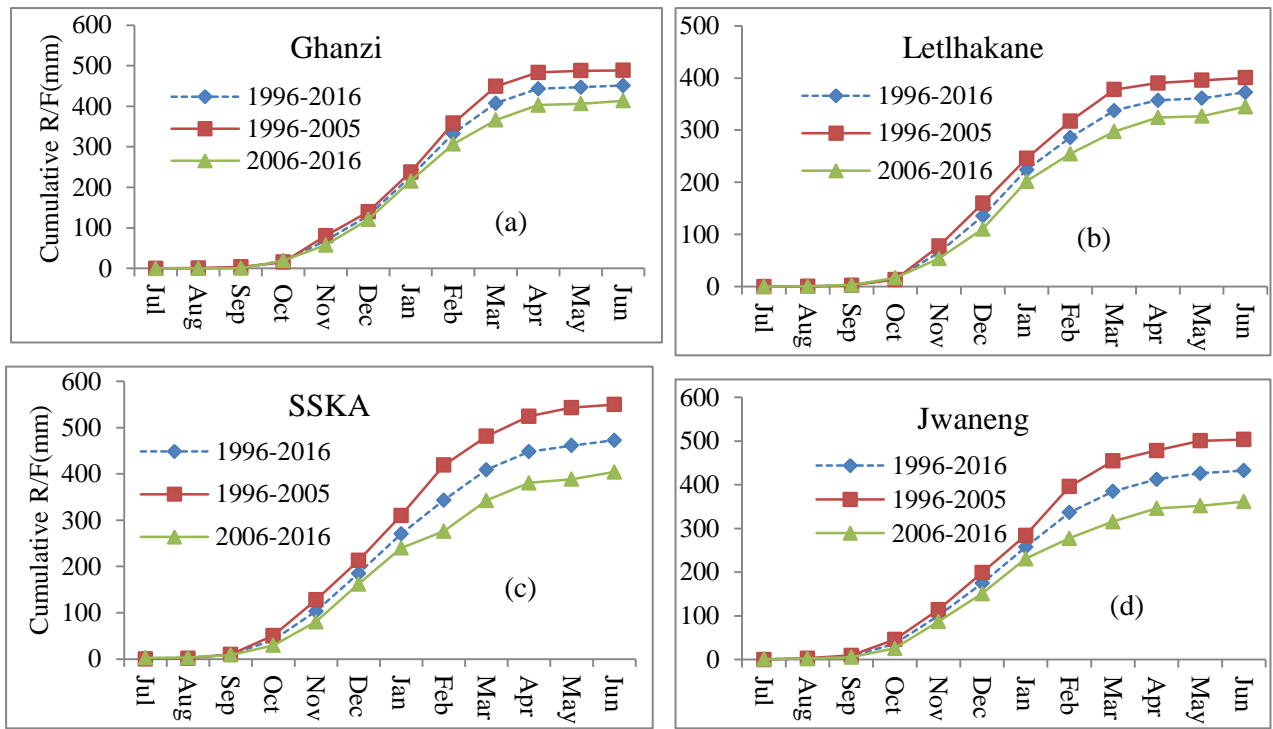


**Fig. 1-3.** Rainfall mass curves at selected synoptic stations (a) Ghanzi (b) Letlhakane (c) SSKA and (d) Jwaneng

#### 1.2.4 Water resources

Water is a key resource in the study area, affecting many aspects of national development (Ministry of Finance and Development Planning, 2017). Increasing demands for consumptive water uses for domestic, mining, industrial, commercial and agricultural sectors makes water a very valuable commodity that necessitates careful planning for its sustainable utilisation and conservation. Groundwater is the main source of potable water supply in the study area with exception of urbanised settlements and a few major villages (GOB-MEWT, 2012). The water resources in the study area are mainly confined in five river basins viz: Okavango, Makgadikgadi, Limpopo, Chobe-Kwando-Linyanti and Orange (GOB-MMEWR, 2006). The main rivers in Botswana are trans-boundary making water resources development a multi stakeholder involving process. The Okavango, Chobe-Kwando-Linyanti and Limpopo which are trans-boundary have more perennial water sources on which Botswana depends. Most of the inland water sources drain to the Limpopo river basin which is used for water supply.

### **1.2.5 Agriculture**

Crop production is limited by traditional farming techniques, recurrent drought, erosion, pests and diseases. Most of the arable land is located in the eastern and northeastern parts of the study area. The principal crops for domestic use are sorghum and maize (Ministry of Finance and Development Planning, 2009). A continued decline in cultivated area has also been recorded since 1979 mainly attributed to persistent crop failures (Statistics Botswana, 2015). This threatens the rural livelihood and the country's economy. The Ministry of Finance and Development Planning (2017) in the National Development Plan 11 of Botswana reports that 80% of the rural households in Botswana derive their livelihood from rainfed farming. They further report that cereal production has been declining over time with average yield of 0.3 t/ha from small traditional farm holdings as opposed to 2.5 t/ha from commercial farms in the same geographical area. A remarkable decrease in yield of 2.4% was reported in 2011/12 season attributed to multiyear drought (Statistics Botswana, 2015). In spite of this decline in food production, Botswana population has continued to rise posing more pressure on the already limited water resources and threatening rural livelihoods. The decline is highly attributed to increased incidences of climate variability with notable declining rainfall and temperature rise being experienced across the study area (Parida and Moalafhi, 2008).

### **1.3 PROBLEM STATEMENT**

In lieu of rising global temperatures and increasing population, both agricultural water demand and human water consumption is on the increase. This poses challenges of improving yields that are much needed to feed the population under strained natural resources (Rockström et al., 2009). In Sub-Saharan Africa, where assimilation of improved technologies is still slow to counter the effects of the changing environmental conditions, climate variations and especially droughts are the main factors that hinder regular supply of water and food availability, a key to sustainable development (Sivakumar, 2010; Byakatonda et al., 2018b). With uncertainties of rainfall patterns and more incidences of droughts in semiarid areas, there is need for research

into avenues that can improve drought early warning systems and drought monitoring. According to the IPCC in Pachauri and Reisinger (2008), the world has been more prone to drought during the past 25 years and that climate projections indicate increased incidences in the near future. This variability in climate will be worse in drier arid and semiarid areas as compared to humid and sub-humid regions (Füssel, 2009; Batisani and Yarnal, 2010). This carries significant consequences for water resources and agricultural production, especially in the developing countries and semiarid regions in particular. White and Walcott (2009) suggested a number of natural pointers that should be monitored routinely including dry spell frequency (DSF), onset and cessation of rain together with their spatial characteristics. They further argue that drought severity needs to be appraised at frequent time steps. Even though most drought categories originate from insufficiency of precipitation, it is inadequate to rely solely on this climate variable to assess drought severity and resultant impacts. Indices based solely on precipitation data do not take into consideration other factors such as ambient temperature and evapotranspiration required in a comprehensive drought early warning system. Comprehensive drought monitoring systems are a significant component of national drought strategies that provide early warning of the onset and cessation of rain, provide drought vulnerability assessment and transfer that information to the users in a timely manner (WMO, 2009). With this information available, the impacts of climate variability can be mitigated or even avoided in many instances.

The Intergovernmental Authority for Development (IGAD), through its climate prediction arm, the Climate Prediction and Applications Centre (ICPAC) has been mandated with drought monitoring and prediction for the Horn of Africa region since 1989. This region has been ravaged by droughts in the past decades. Drought has previously been monitored using the Standardised Precipitation Index (SPI) combined with GIS mapping techniques over this region (Omondi, 2011). Over southern Africa the link between El Niño and drought has been established in studies by Richard et al. (2000), Nicholson et al. (2001) and Edossa et al. (2014).

In spite of this, the degree of association with local climate is not well established and there is no evidence of using ENSO as a suitable predictor of drought severity in this region.

In Botswana, decreasing precipitation has been reported in the most recent studies (Parida and Moalafhi, 2008; Batisani and Yarnal, 2010; Batisani, 2011). Besides, there is no information in Botswana to the effect that other climatic predictors other than rainfall have been incorporated in the determination of drought severity. Still in Botswana, an attempt has been made to estimate the length of the growing season but using rainfall as the only input variable (GOB-MMEWR, 2012). It is therefore necessary to develop a criteria for determining onset and cessation of rain that incorporates both rainfall and temperature as part of an early warning system for the country. It is also essential to determine drought indices which are region specific since they are not transferrable from one region to the other (Heim Jr, 2002). Moreover there is also need for periodical appraisal due to spatial and temporal variations in these indices. This hence calls for informed research to develop indices not limited to precipitation but encompassing other climate variables that are region specific. Also it is necessary to develop prediction models to support long term mitigation measures for reduction of drought impacts due to increased incidences of climate variability.

#### **1.4 OVERALL OBJECTIVE**

To assess the impact of droughts under climate variability on water resources and cereal yields in semiarid regions using Botswana as a case study.

##### **1.4.1 Specific research objectives**

1. To investigate the monotonic trends and abrupt changes in meteorological time series as a result of climate variability under ENSO influence.
2. To determine the dry spell frequency, onset and cessation of rainfall dates, their variability and trends.

3. To determine drought severity using SPEI and its influence on hydrological systems under ENSO scenarios.
4. To determine the degree of association between climatic indices, length of the rain season and ENSO on cereal yield.
5. To provide predictions of hydrological droughts, cereal yields, onset and cessation of rain dates across the study area.

#### **1.4.2 Research questions**

1. What are the monotonic trends and abrupt changes in meteorological time series as a result of climate variability under the influence of ENSO?
2. What is the dry spell frequency, onset and cessation of rainfall dates, their variability and trends?
3. What is the magnitude of drought severity and its influence on hydrological systems under ENSO?
4. What is the degree of association between climatic indices, length of the rain season, ENSO and cereal yield over the study area?
5. What is the futuristic behavior of hydrological droughts, cereal yields, onset and cessation of rain dates across the study area?

#### **1.5 RELEVANCE OF THE STUDY**

High population pressures coupled with increasing number of smallholder farmers under rainfed agriculture in southern Africa is putting pressure on environmental systems. Both surface and ground water productivity is on a decline due to limited recharge as a result of decreased rainfall amounts (Parida and Moalafhi, 2008). Further still, yields of cereals which are mainly subsistence are on a decline. To compound the problem, a good number of the farmers lack capacity to adopt modern farming techniques making them vulnerable to climate variability (Tadross et al., 2005). Their main apprehension is for the rains to be dependable enough to assure sufficient water availability and that those conditions are sustained or



enhanced in the course of the rain season. This confirms the observation that variability in seasonal characteristics such as onset, cessation, number of rainy days, dry spell frequency and drought severity are injurious to agriculture and water availability. Equipped with information on the seasonal distribution of rainfall, dry spell frequency and drought indices, a farmer can choose to plant a more or less drought resistant crop, while information on the onset and cessation of rain facilitates the choice of a long or short season cultivar. Knowledge of drought severity and their spatial distribution could aid partitioning the country into homogenous zones based on drought vulnerability. The required information for drought planning in the context of semiarid climate begins with the study of climatic indices such as aridity index, rain onset, cessation and dry spell frequency (Usman and Reason, 2004). This research seeks to investigate the association of these indices with agriculture and water resources in Botswana. Short term scale prediction models for drought severity, cereal yields, onset and cessation of rain dates are also developed to facilitate planning.

Supplementing the growing competencies in providing seasonal and interannual climate predictions is necessary in mitigating the effects of drought and desertification. Research into causes and impacts of climate variations and climate indices prediction with a view to providing early warning is an essential component of this study. The proposed research seeks to determine dry spell frequency, onset and cessation of rainfall dates, aridity index (AI) and also drought severity based on SPEI. It further examines the degree of association between SPEI, AI, length of rain season (LRS) and cereal production in addition to predicting its future trends under ENSO scenarios. This information is expected to feed into the National Risk and Disaster Management Plan of Botswana to support drought monitoring strategies. These measures are geared at creating community drought resilience and devise mitigation measures for the disaster response organs in the country. Prediction of onset and cessation of rain helps to determine the length of the rain season which informs research on the right cultivars for different drought regimes and maturity periods.

## **1.6 SCOPE OF THE STUDY**

The scope of the research is limited to studying climatological and hydrological droughts over the study area for the period of 1960 to 2016. It examines climate variability through explanatory data analysis of meteorological data of Botswana from 14 synoptic stations. The study also determines the magnitude and spatial distribution of drought severity based on SPEI under ENSO influence. Dry spell frequency, rain onset and cessation of rain dates are determined together with their trends. Predictions of drought severity, cereal yields, onset and cessation of rain dates under the influence of ENSO are made through ANNs. For meteorological data analysis, only variability in temperature and rainfall is investigated as the main drivers affecting local climates in semiarid locations. The variations in cereal yields are limited to climatic factors and any other agronomical practices that may influence yield are smoothed out. At the end, the current research generates knowledge and/or information on mitigating effects of drought under climate variability on rainfed farming and water resources in semiarid areas using Botswana as a case study. The findings from this research relate more to climate variability rather than change.

## **1.7 LAYOUT OF THE THESIS**

This thesis is organised into five Chapters, with Chapter 1 giving a general introduction. After the general introduction, the study area is introduced and its choice justified. The study area is described in terms of its climate profile, agricultural activities and current water resources situation. The problem statement, research objectives, relevance of the study and the scope are also covered under chapter 1. Chapter 2 reviews the relevant and recent literature that discusses the effects of climate variability on water resources and agricultural production. The Chapter further discusses drought classification using the suggested drought indices. As part of drought management and monitoring, this Chapter also explores the extent to which ANN has been used in hydrological modeling and drought management in particular.

Chapter 3 describes the data and methods used throughout this research. This Chapter describes the methods used in understanding climatic characteristics for the study area. It further explores the dry spell frequency, rain onset and cessation. Drought severity under ENSO influences is also discussed in this Chapter. Methods of determining a suitable timescale across the study area that can be used in drought monitoring have been explained. The influence of drought severity on water resources at the identified timescale is also investigated in this Chapter. The Chapter further describes the procedure for determining influence of climatic indices on cereal yields. The Chapter ends by providing avenues for predicting stream flow droughts, cereal yields, onset and cessation of rain dates to aid planning. Chapter 4 presents the analyses and discussion of results generated from the methods described in Chapter 3. The analyses and discussions encompasses aspects presented in Chapter 3. The thesis ends with Chapter 5 on conclusions and recommendations. This Chapter also presents research contribution to knowledge while giving recommendations for future studies. Most of the work contained in this thesis has already been published and or have been accepted for publications in peer reviewed international journals.

## CHAPTER-2

### 2. LITERATURE REVIEW

#### 2.1 INTRODUCTION

Climate variability and change have become a global concern due to the natural hazards that are associated with them (Wilhite et al., 2007; Yu et al., 2014; Wang et al., 2015). These hazards in the form of droughts and floods have increased in frequency and magnitude in recent times especially in low lying areas which are prone to floods and semiarid areas which are susceptible to droughts (Zaroug et al., 2013; Hoell et al., 2015). The increased incidences of natural hazards have been attributed to increasing concentrations of atmospheric carbon dioxide (CO<sub>2</sub>) over the recent past that has been singled out as the main cause of global warming (Some'e et al., 2012; Stocker et al., 2013). The fifth assessment report (AR5) of the intergovernmental panel on climate change (IPCC) shows a close positive association between CO<sub>2</sub> concentration and global temperature rise (Stocker et al., 2013). Also climate variability and change is thought to be influenced by the large scale climate predictors in the form of ENSO. It is reported that the first decade of the 21<sup>st</sup> century has been the warmest ever, coinciding with the strongest El Niño in 100 years (Rahman and Latch, 2015; Hansen et al., 2016). These climatic changes could lead to a shift in meteorological variables such as rainfall and temperature (Yue and Hashino, 2003; Costa and Soares, 2009a; Hänsel et al., 2016). These anticipated changes are not uniformly spread globally, with different regions experiencing impacts at varying degrees. It is further projected that arid and semiarid regions could experience higher than global average warming levels (Modarres and da Silva, 2007; Khan et al., 2016). Hence there is need to shift focus towards semiarid locations where adaptation measures to these extreme weather conditions are a big challenge. Various studies have pointed out that arid and semiarid areas are finding challenges coping with dwindling water resources and declining crop yields (Dai, 2013; Huang et al., 2016).

It has been reported that slightly over 60% of the world's food production emanates from rainfed agriculture that cover almost 80% of the world's croplands (Guha-Sapir et al., 2011). In Sub-Saharan Africa for example where climate variability already limits agricultural production, 95% of food comes from rainfed farming (FAO Statistics, 2009). Brown and Funk (2008) reported that since the 1990s, rising commodity prices and declining acreage of cultivated area have led to decreases in food production, eroding food security in many communities and this is particularly due to persistent crop failure attributed to inadequate rains. It was also discovered that a number of regions in the world lack food self sufficiency and mainly rely on local agricultural production to meet their food demands. The majority of these regions lie in the tropics and subtropics which are substantially affected by climate variations and increasing commodity price instabilities. In these regions, many farmers have very little options other than consume their produce and sell the surplus on local and regional markets to acquire essential commodities remaining with no buffer (World Bank, 2005). This makes the farmers more vulnerable to climate variations, because when there is decreased production, the household incomes deep low while their costs go up to maintain basic consumption demands. Investigations on climate risks and adaptation were carried out by Lobell et al. (2008) and Li et al. (2009) for crops in twelve food-insecure regions in the world to identify mitigation measures. Based on statistical crop models and climate projections for 2030 from 20 general circulation models, their results identified south Asia and southern Africa as two regions that without sufficient attempts are more vulnerable to negative impacts of climate change as several crops that are important to ensure food-secure human populations will greatly be affected.

Studies across southern Africa have indicated that the region is prone to pronounced weather extremes including drought associated with climate variability (Tsheko, 2004; Usman and Reason, 2004). This region has been reported by Preece (2008) and Batisani (2012) as one finding difficulties coping with climate variability. It was also demonstrated that southern

African agriculture and water resources require steady inputs of precipitation, rather than highly varied frequency of wet/dry cycles (Rocha and Simmonds, 1997; Rowhani et al., 2011). Recent investigations have pointed out that warming sea surface temperatures (SSTs) coupled with local feedbacks are the main drivers for drought conditions over southern Africa (Nicholson et al., 2001; Heim Jr, 2002; Pachauri and Reisinger, 2008). Studies on long term changes in rainfall and temperature are necessary for sustainable land and water resources planning and management especially under climate variability and change (Shahid, 2010; Tabari and Talaei, 2011). This Chapter intends to examine the available recent studies in regards to climate variability and change in relation to water resources and rainfed agriculture especially in semiarid regions. It also identifies gaps on avenues of minimising climate risk in semiarid areas. The Chapter specifically looks at literature on studies of long term trends in meteorological variables in an effort to trace the climate change signal. It also examines work so far done on the effect of dry spells, onset and cessation of rain on agricultural and water resources. Recurrent droughts and aridity under global warming are scrutinised in this Chapter. Various literatures on drought severity modeling techniques are examined to enhance planning for both agricultural and water resources.

## **2.2 CLIMATE VARIABILITY AND CHANGE IN SEMIARID REGIONS UNDER GLOBAL WARMING**

Investigation of surface temperature trends on the African continent, reveal warming tendencies at magnitudes more than twice the global rate (Engelbrecht et al., 2015). Further to this, it has been shown that temperature rise is likely to impact on rainfall quantities and hence livelihood at large (Heim Jr, 2002; Kenabatho et al., 2012). Thus, climate variability and change is projected to compromise agricultural productivity and water resources availability on the African continent due to her low economic and human capacity. Impacts of this variability are expected to be more severe on the peripherals of semiarid and arid areas with an expected reduction in rainfed yields of up to 50% (Parry, 2007; Solomon, 2007). Therefore, for any

meaningful study on climate variability and change, these meteorological variables should not be ignored. Of recent, interest has increased in investigating long term trends in rainfall and temperature in quest for tracing the climate change signal (Menzel et al., 2006; Giorgi and Lionello, 2008; Kenabatho et al., 2012).

Several studies have since been conducted globally and regionally to investigate climate variability by analysing trends in rainfall and temperature time series. Such of these investigations have been conducted in semiarid locations such as Iran by Some'e et al. (2012) and Tabari and Talae (2011). Results from their studies indicate both increasing and decreasing trends in meteorological variables for a period of 1966-2006, with significant trends mainly observed during winter period. In Nigeria, Akinsanola and Ogunjobi (2015) reported decreasing trends in both annual and winter seasonal rainfall while using the Mann-Kendal (MK) test statistic. In Portugal Costa and Soares (2009b) reported high rainfall variability by examining trends in aridity and standardised precipitation index (SPI). Their study revealed high climatic uncertainty in the south of the country. In Turkey, Partal and Kahya (2006) applied the MK test and Sen's Slope estimator to study the direction and magnitude of trends in meteorological variables. Their study identified the months of January, February and September to be exhibiting decreasing trends especially in the south and west of Turkey for the period from 1929 to 1993. Climatic changes for a period of 1980 to 2010 were investigated in Serbia by Gocic and Trajkovic (2013) using the MK trend analysis and Sen's Slope estimator. Their results indicated increasing trends in both annual and seasonal temperature with no significant trends in rainfall. Some attempts have been made to study climate variability and change in Botswana by Parida and Moalafhi (2008) and Batisani and Yarnal (2010) who both reported decreasing rainfall and increasing incidences of drought over the study area. However these studies only analysed rainfall as the only precursor of climate variability and change.

Studies in climate variability have showed that generally, the four absolute homogeneity tests (Standard Normal Homogeneity test, Buishand test, Pettit test, Von Nuemann test) and trend

analysis are suitable tests for identifying breaks in meteorological time series and trend detection (Wijngaard et al., 2003; Partal and Kahya, 2006; Reza et al., 2011; Tabari et al., 2011). Likewise, the nonparametric tests of Mann-Kendall and Sen's Slope estimator have good capability for nonlinear trend detection in climatological data series. It is recommended that more than one statistical test be applied for trend detection in data series to decrease uncertainty of incorrect detection and interpretation as compared to use of a single test (WMO, 2000). The Mann-Kendall test has been used in Botswana to determine mean annual stream flow and annual rainfall trends. The results showed that stream flow is highly variable but its relationship with rainfall was low (Batisani, 2011). Different studies have shown that positive serial correlation increases the variance of the MK statistic which in turn increases the probability of detecting a significant trend, whereas in fact none may exist. The existence of serial correlation influences the magnitude of the trend estimate (Yue et al., 2002; Yue and Wang, 2004). The effective sample size (ESS) approach has been found to remove the serial correlation effect on the time series (Yue and Wang, 2004; Tabari and Talaei, 2011).

Climate variability has also been closely linked with El Niño Southern Oscillation (ENSO) that is attributed to hydroclimatic extremes in the form of droughts and floods. ENSO is identified as the main source of climate variability in the Equatorial Pacific (Morán-Tejeda et al., 2016). This climate variability has teleconnections with the Indian and Atlantic Oceans (Nicholson et al., 2001; Nyenzi and Lefale, 2006). Influences of ENSO on the local climate may not be ignored since a number of studies over southern Africa have reported its close association with rainfall patterns and onset of droughts (Nicholson et al., 2001; Usman and Reason, 2004; Edossa et al., 2014). With advent of climate change and increased incidences of climate variability, it is imperative to periodically update studies on change detection in meteorological time series.



### **2.3 ONSET, CESSATION OF RAIN AND DRY SPELL FREQUENCY IN SEMIARID REGIONS**

Rainfall has been identified as the most one single factor that influences agricultural yields as well as quantities of surface, ground water and soil moisture storage (Sivakumar, 1988; Mugalavai et al., 2008; Amekudzi et al., 2015). In many instances, average conditions are used in planning and management of both agricultural and water resources (Usman and Reason, 2004). However, a rain season classified as near normal may still record poor harvest due to high variability and short rainfall episodes punctuated with relatively longer dry spells. For better crop yields, well distributed rains just enough to meet crop water requirements is sufficient than intermittent heavy showers that registers high rainfall totals (Usman and Reason, 2004; Kebede et al., 2016).

Various studies in regards to analysis of onset and cessation of rain conducted in both West and East Africa showed high association between rain onset and length of rain season (Sivakumar, 1988; Odekunle, 2006; Mugalavai et al., 2008; Amekudzi et al., 2015). They associated early rain onset with longer seasonal rains. However in these studies, trends in onset and cessation of rain were not investigated to determine the direction and magnitude of any possible changes in these features of rainfall over time.

Since variability in seasonal rainfall totals alone may not explain the relationship between rainfall and crop yields, dry spell frequency analysis has usually been undertaken for different parts of the globe as a means of further investigating the implications of changing climate on food security (Usman and Reason, 2004; Araya et al., 2010; Ngetich et al., 2014). A number of definitions exist for dry spells, but for this research, it is taken as extended periods with no rainfall within a rain season (Ngetich et al., 2014). Dry spells are crucial in this research since they are directly linked to crop moisture stress. Studies in semiarid environments in Sub-Saharan Africa have indicated that dry spells range between 5 and 15 days (Usman and

Reason, 2004; Ngetich et al., 2014). Regionally, studies analysing dry spells have been conducted in the southern Africa using gridded data of 2.5°X2.5° resolution by Usman and Reason (2004). However this gridded data was somewhat coarse and lacked site specific attributes.

A number of techniques have been employed to determine the onset and cessation of rains in Sub-Saharan Africa ranging from water balance techniques (Mugalavai et al., 2008; Ngetich et al., 2014) to the use of rainfall amount and rainy days (Odekunle, 2006). The interannual variability of the rain onset was investigated for maize growing season across China, West Africa, Kenya, Zimbabwe and South Africa as a starting point in an effort to predict this important seasonal characteristic (Le Barbé et al., 2002; Tadross et al., 2005; Jiang et al., 2011; Mupangwa et al., 2011; Recha et al., 2012). Findings from these studies were instrumental in providing farmers with projected length of the rain season before sowing. Further still, results from these predictions are required by the farmers for better agricultural management especially in the selection of optimal planting dates (Laux et al., 2010). Studies on the onset and cessation criteria in semiarid Botswana are none existent hence a motivation for this research.

## **2.4 DROUGHT INDICES**

Due to complexities of droughts, their direct measurement is not readily available and hence various components of the hydrological cycle are currently used as proxies to characterise droughts. These proxies are indicators that can reveal the effect of droughts on various components of the hydrological cycle such as, stream flow, soil moisture and evapotranspiration which are also part of the climate cycle (Wilhite, 2000; Heim Jr, 2002; Dai, 2013; WMO and GWP, 2016). Since droughts are also an integral part of the climate cycle, they may not be avoidable but their impacts can be mitigated through preparedness and monitoring (Narasimhan and Srinivasan, 2005; Morid et al., 2006). In an effort to lessen drought impacts, the World Meteorological Organisation (WMO) has recommended use of

drought indices for drought monitoring (WMO, 2009). However attainment of successful drought monitoring is dependent on how drought is characterised and quantified in both spatial and temporal extents (Iglesias et al., 2009; Nalbantis and Tsakiris, 2009; Lloyd-Hughes, 2012; Mbululo and Nyihirani, 2012).

A number of drought indices for quantification of drought in terms of magnitude, duration and intensity exists and have been applied in various studies investigating drought occurrences (Alley, 1984; McKee et al., 1993; Heim Jr, 2002; Keyantash and Dracup, 2002; Vicente-Serrano et al., 2010; Beguería et al., 2014; Stagge et al., 2014; WMO and GWP, 2016; Byakatonda et al., 2018a). Three of the indices which are commonly under use and recommended by the World Meteorological Organisation (WMO) are the Palmer Drought Severity Index (PDSI), Standardised Precipitation Index (SPI) and Standardised Precipitation and Evapotranspiration Index (SPEI) (Sivakumar, 2010; Hayes et al., 2011; Byakatonda et al., 2016). This research employs SPEI to characterise drought by duration, severity and intensity. The choice of SPEI was premised on the fact that it retains attributes of both PDSI and SPI while taking care of global warming tendencies (Vicente-Serrano et al., 2010; McEvoy et al., 2012; Beguería et al., 2014). The SPEI is a generally accepted drought index because it accounts for effects of global warming that cannot be ignored in studies of drought severity. Drought indices have been used over time in drought early warning systems by applying them in drought severity predictions (Morid et al. (2007; Mishra and Singh, 2011). For proper water resources management, predictions ranging from a few months to a few years play a vital role in giving futuristic conditions (Dastorani and Afkhami, 2011; Mishra and Singh, 2011). A number of statistical tools and techniques for drought severity prediction have been suggested by various authors ranging from the Markov chains by Li-hua (2006) to regressions models for drought severity prediction using SPI and PDSI time series (Maier and Dandy, 2000; Illeperuma and Sonnadara, 2009; Mishra and Singh, 2011). However there is no evidence on record that SPEI under influence of ENSO has been used in the prediction of drought severity.

## **2.5 DROUGHT CHANGES UNDER GLOBAL WARMING**

Drought is a form of hydrological extreme that is wide spread in temporal and spatial extent often referred to as ‘creeping disaster’ (Kundzewicz and Kaczmarek, 2000; Mishra and Singh, 2010; Van Loon, 2013). Impacts of droughts are likely to increase with the current rise in global temperature and reduction in precipitation (Solomon, 2007; Dai, 2011; Wada et al., 2011; Dai, 2013). Drought is not region specific, however most severe impacts of drought on population are seen to occur in arid and semiarid areas where available water resources are scarce even under normal conditions and the dwellers have limited adaptability options (De Stefano et al., 2012; Van Loon, 2013). This calls for research into drought characteristics which will help in formulation of effective management strategies specific to these areas.

Droughts have various definitions and classifications according to Wilhite (2000) and Sheffield et al. (2012). For purposes of this research, the scope is limited to two common classifications viz: climatological and hydrological droughts. Climatological drought is defined as below normal precipitation coupled with increase in potential evapotranspiration covering large spatial extents for prolonged time period (Rimkus et al., 2013; Van Loon, 2013; Van Loon and Laaha, 2015). Climatological drought can be further subdivided into meteorological and agricultural droughts. The latter is mainly linked to low soil moisture content unable to meet crop water requirements. Hydrological drought on the other hand is associated with below average surface water flow for prolonged periods (Smakhtin and Hughes, 2004; Feyen and Dankers, 2009; Mishra et al., 2015). Hydrological droughts depend on a number of processes including the atmosphere and a host of other factors in the terrestrial part of the hydrological cycle that govern moisture transport (Mishra and Singh, 2010; Rimkus et al., 2013; Van Loon, 2013). The atmospheric processes that govern both climatological and hydrological droughts are believed to be linked to climate variability and change (Jung et al., 2010; Lorenzo-Lacruz et al., 2010; Van Loon, 2013). Response of hydrological systems are closely associated with climatic conditions in that decrease in precipitation with rising

temperatures, increases potential evapotranspiration which leads to depletion of water and moisture storage (Vicente-Serrano and López-Moreno, 2005; Lorenzo-Lacruz et al., 2010; Van Loon, 2013). All these interactions between climatic and hydrological process are a function of a timescale.

In as much as global warming has been associated with increased drought severity, many researches have also established that ocean-atmosphere dynamics triggered by activities in the equatorial Pacific basin referred to as ENSO are also closely linked with global warming (Nicholson and Kim, 1997; Nicholson et al., 2001; Fauchereau et al., 2003; Nyenzi and Lefale, 2006; Jones et al., 2007; Vicente-Serrano et al., 2011). In recent findings, some of which are presented in Vicente-Serrano et al. (2011), the effect of ENSO on drought severity at a global scale using gridded data are documented. However there is high uncertainty in global gridded data due to low spatial extent and hence cannot be solely relied upon. There is also inherent spatial variability in rainfall, largely resulting from towering isolated cumulus clouds (Yuan and Hartmann, 2008). Wang et al. (2015) found differing trends in dryness conditions over China while using ground observed data as compared to other results reported by Dai (2013) and Vicente-Serrano et al. (2011) who used gridded data over the same area. The first attempt to assess drought vulnerability across the study area by Batisani (2011) used SPI for a period between 1974 and 2005. With resounding evidence of global warming and ENSO influences on the local climate, it is necessary to incorporate temperature in any climate variability and change studies.

## **2.6 ARIDITY AND DROUGHT PROPAGATION**

Aridity is a common phenomenon in the subtropics where anticyclone weather patterns are frequent and likely to have direct influence on the evaporation rates from surface reservoirs and hence affecting other aspects of the hydrological cycle (Galarneau Jr et al., 2008; Some'e et al., 2013). On the other hand droughts are usually associated with the dryness conditions in a

region due to climate anomalies such as decreased rainfall, increased temperature and evapotranspiration. Although aridity and droughts are in many ways associated, the main difference between them is in their scale in the sense that aridity arises from long term persistent dry conditions (Maliva & Missimer, 2012). In other words aridity could be referred to as an extreme manifestation of droughts.

Climate variability being closely related to the warming of the earth, is likely to cause frequent droughts and even make semiarid regions arid or hyper arid (Zhang et al., 2009; Some'e et al., 2013; Byakatonda et al., 2016). For these foregoing situations, it has become imperative to understand not only the aridity trends due to the ongoing climate variability but also to determine the association between the aridity and cereal yields across the study area.

Drought being a complex natural hazard, its onset may not easily be established because it propagates in different forms over time (Vicente-Serrano et al., 2012; Van Loon, 2013). Drought originates from atmospheric dynamics that affect rainfall circulation and other components of the hydrological cycle such as surface runoff, soil moisture and relative humidity (Zargar Yaghoobi, 2012; WMO and GWP, 2016). The longer drought conditions persist, the more spatial extent it covers triggering aridity. It normally propagates in the following sequence; meteorological, agricultural and hydrological drought with prolonged conditions resulting into aridity (Nalbantis and Tsakiris, 2009; Shukla et al., 2011; Zargar Yaghoobi, 2012). The interrelationships between these sequences are illustrated in Fig. 2-1.

Standardised flow index (SFI) which is analogous to SPEI and SPI in their multiscalar nature is used to quantify hydrological droughts. This drought index has been used in various studies evaluating hydrological droughts and also recommended by the WMO (Nalbantis and Tsakiris, 2009; Lorenzo-Lacruz et al., 2010; WMO and GWP, 2016). Establishing relationships between climatological and hydrological droughts are crucial in planning and management of water resources especially under global warming conditions. These relationships do not exist

currently for the study area hence it may be necessary to determine an association between climatological and hydrological droughts and establish a common timescale at which SPEI and SFI are closely related. However in recent times, it has also been observed that droughts often extend over longer timescales sometimes over the year with continued dry spells into the next hydrological year hence impacting on stream flow and over-the-year reservoir storage. It then becomes imperative to study the long term persistence or possible reversion in characteristics of such determined indices using the Hurst phenomenon which at the same time is a measure of climate variability (Hurst, 1951; Koutsoyiannis, 2003).

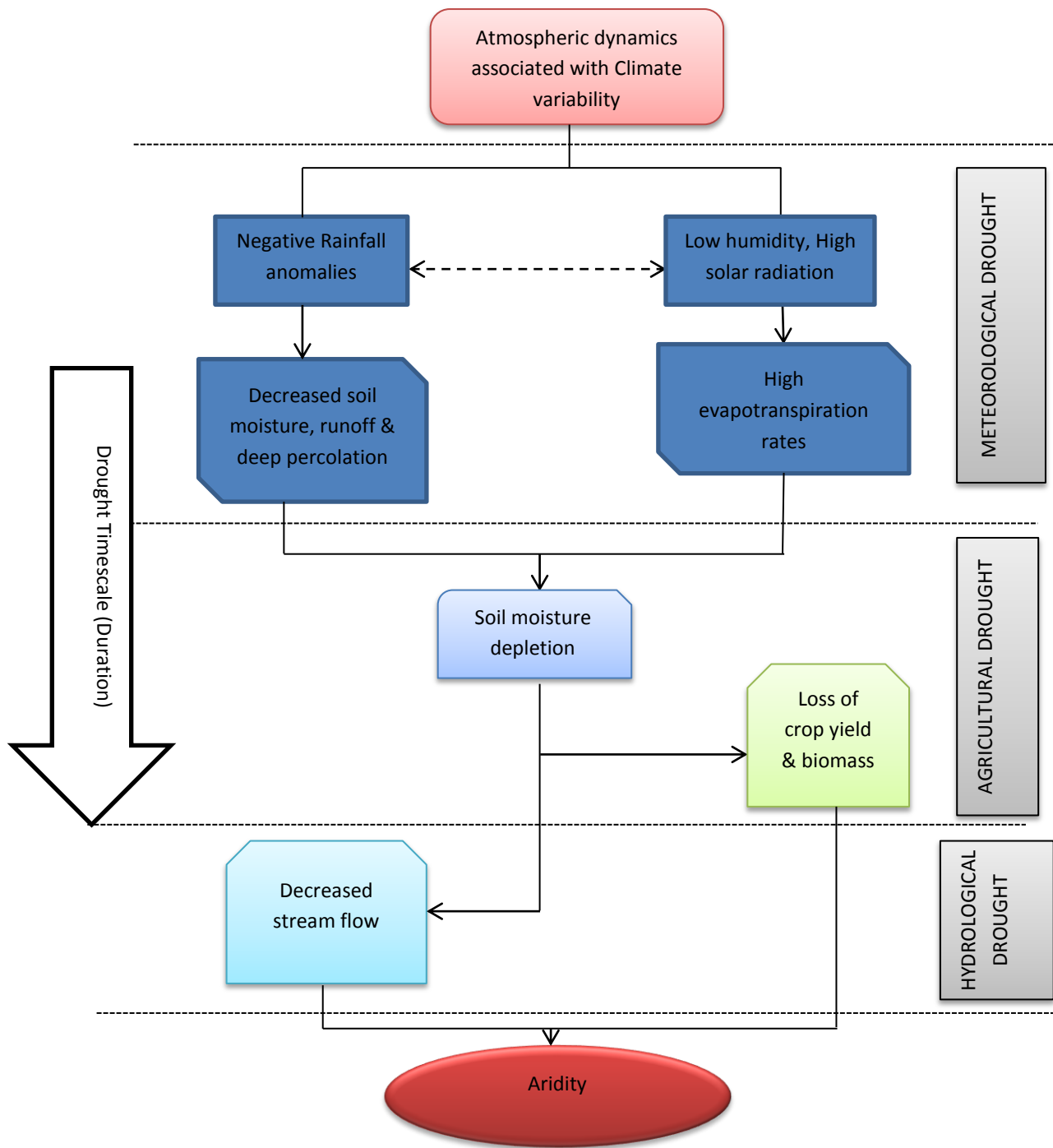


**Fig. 2-1.** Drought propagation (modified from Zargar Yaghoobi (2012))

## 2.7 MODELING DROUGHT SEVERITY UNDER CLIMATE VARIABILITY

As part of limiting the impacts of droughts hazards, drought severity modeling is of paramount importance for drought risk assessment and mitigation. Over time, statistical models have been applied to predict droughts dating back to 1970 by Saldarriaga and Yevjevich (1970) who started incorporating time series analysis in drought severity predictions. Markov chains were



later introduced in drought prediction using PDSI by Rao and Padmanabhan (1984). They investigated the ability of predicting and simulating PDSI time series as a form of drought severity modeling. More robust stochastic models such as autoregressive integrated moving average (ARIMA) and seasonal autoregressive integrated moving average (SARIMA) were employed by Mishra and Desai (2005). Studies conducted to compare the use of stochastic and Artificial Neural Network (ANN) in prediction found that ANNs were more robust (Zealand et al., 1999; Mishra et al., 2007). Considerable application of ANNs in time series prediction resurfaced from 1980s after it emerged that they had a suitable network predictor (Diaconescu, 2008). ANN are considered nonparametric when applied in time series prediction in that it is not required to ascertain the processes that generate the signals (Parlos et al., 2000). It has been demonstrated that recurrent neural network (RNN) with sufficient number of neurons is a realisation of the multiplicative autoregressive integrated moving average (MARIMA) process (Gao and Meng Joo, 2005; Diaconescu, 2008; Menezes and Barreto, 2008; Kenabatho et al., 2015). Studies into the use of various combinations of different ANNs configurations are ongoing but the race is between static ANN (Back propagation neural network) and the dynamic ANN (Recurrent neural network) (Menezes and Barreto, 2008; Lahmiri, 2016). Results from various prediction models reveal that, dynamic ANN which incorporates a time delay through feedback connections mimics accurately neural biological information which is key in time series modeling (Maier and Dandy, 2000; Chang et al., 2014; Chang et al., 2015; Byakatonda et al., 2018a). With continued uncertainties in climate patterns and frequent extreme weather conditions globally, the use of ANNs in climate variability studies has increased in the recent past in an attempt to understand these unmeasurable nonlinear conditions (Chen et al., 2005; Mishra and Desai, 2006; Liu et al., 2010). ANNs have been found to give reasonable results when applied to short term predictions. It is a tool capable of learning any data combination regardless of the process that generated it (Chang et al., 2015; Byakatonda et al., 2016).

This research develops a multistep ahead drought severity, rain onset/cessation dates and cereal yield prediction models. Multistep predictions are more complex than a one step ahead as it requires more model memory (Sorjamaa et al., 2007; Chang et al., 2014). For this reason, the Nonlinear autoregressive with exogenous input (NARX) network a class of dynamic recurrent neural networks (DRNN) is selected for use in this research since it has been found to outperform static ANNs in water resources and drought modeling (Gao and Meng Joo, 2005; Mishra et al., 2007; Menezes and Barreto, 2008; Lahmiri, 2016).

## **CHAPTER-3**

### **3. DATA AND METHODS USED IN THE RESEARCH**

#### **3.1 INTRODUCTION**

Data used in this research comprised of observed climatological, hydrological, cereal yields recorded in the study area and records of large scale climatic predictors in form of SOI and SST. The methods used for analysis and interpretation of the data have been arranged in the order of objectives as stated in Chapter 1 and presented in Section 3.3 of this Chapter.

#### **3.2 DATA REQUIREMENTS**

##### **3.2.1 Climatological data**

Records of rainfall, minimum and maximum temperature at daily and monthly timescale were obtained from the Department of Meteorological Services of Botswana (DMS) at fourteen synoptic stations with the longest record being 1960-2016. The stations have a good spread over the study area and are spatially represented in Figure 1-1. Details of their locations and length of data available at each station have been provided in Table 3-1.

##### **3.2.2 Hydrological data**

The hydrological data were provided by the Department of Water Affairs of Botswana (DWA). The data consisted of monthly discharge recorded at Mohembo on river Okavango for a period between 1975 and 2016. The second gauging station was recorded at Buffel drift on river Limpopo (Fig. 3-1) with data spanning from 1997 to 2016. These stations were selected due to availability of consistent data with less than 10% missing values. To facilitate study of the association between climatic and hydrological droughts, equally six (6) synotic stations were selected to quantify climatic droughts in the Limpopo and Okavango river basins. Three (3) stations were selected in each of the river basins as shown in Figure 3-1.

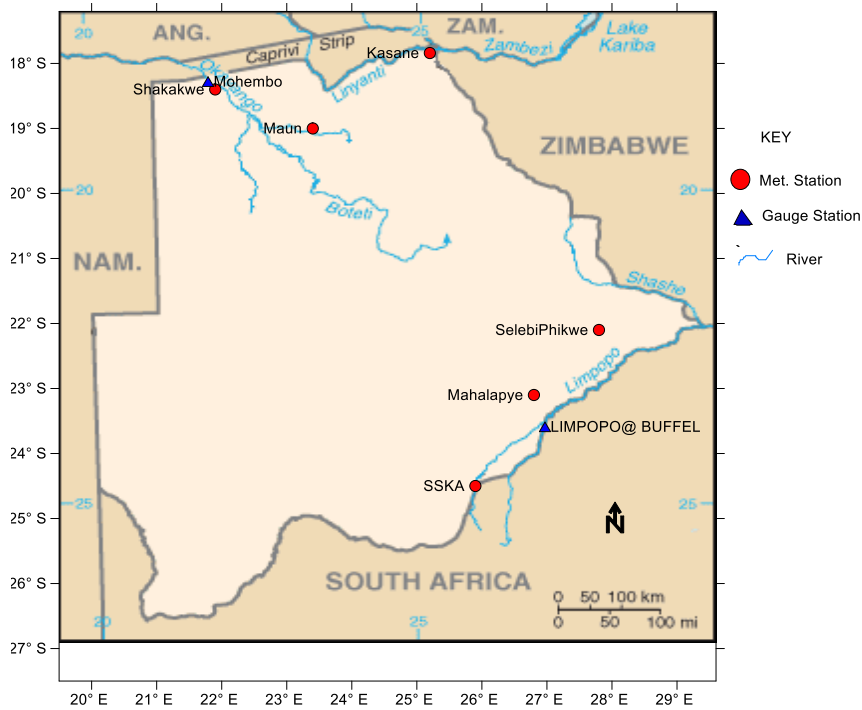


**Fig. 3-1.** Location of synoptic stations and river gauging stations used in hydrological drought analysis

**Table 3-1.** Synoptic station locations and length of meteorological variable (rainfall, maximum and minimum temperature) record

SN	Station ID	Station Name	Latitude	Longitude	Elevation Amsl (m)	Period of record		
			°S	°E		Rainfall	Max Temp	Min Temp
1	033-FRAN	Francistown	21.2	27.5	968	1960-2016	1960-2016	1960-2016
2	039-GANT	Ghanzi	21.7	21.6	1131	1960-2016	1961-2016	1960-2016
3	053-JWAN	Jwaneng	24.6	24.8	935	1988-2016	1989-2016	1989-2016
4	064-KASA	Kasane	17.8	25.2	960	1968-2016	1983-2016	1983-2016
5	093-LET2	Letlhakane	21.3	25.3	991	1993-2016	1994-2016	1994-2016
6	106-MAHA	Mahalapye	23.1	26.8	1005	1960-2016	1971-2016	1971-2016
7	130-MAUN	Maun	19	23.4	945	1960-2016	1965-2016	1965-2016
8	183-PAN2	Pandamatenga	17.8	28.6	1071	1998-2016	1998-2016	1998-2016
9	213-SEL2	Selibe-Phikwe	23.1	37.8	892	1998-2016	2000-2016	2000-2016
10	223-SHAK	Shakawe	18.4	21.9	1030	1960-2016	1965-2016	1965-2016
11	035-SSKA	SSKA	24.7	25.9	975	1985-2016	1985-2016	1985-2016
12	033-SUAP	Sowa Pan	20.6	26	908	1992-2016	2000-2016	2000-2016
13	244-TSAB	Tsabong	26	22.4	960	1960-2016	1961-2016	1961-2016
14	251-TSHA	Tshane	24	21.6	1118	1960-2016	1961-2016	1960-2016

### **3.2.3 Large scale climatic predictors**

The large scale climatic predictors used for this research are in the form of El Niño Southern Oscillation (ENSO). ENSO has been reported in Chapter 2 to be responsible for variant climate behaviour across southern Africa. The ENSO phenomenon is represented by Sea surface temperature (SST) anomalies and Southern Oscillation Index (SOI).

#### **3.2.3.1 Sea surface temperature (SST) anomalies**

Data of monthly Sea Surface Temperature (SST) anomalies from the El Niño 3.4 region were obtained from the climate prediction center of the National Oceanic and Atmospheric Administration (NOAA-NCEP, 2016) for a concurrent period of 1960-2016. El Niño southern oscillation (ENSO) is closely associated with oceanic-atmospheric dynamics that influence variations in ocean currents and SSTs with teleconnections up to the Antarctic (Bromwich et al., 2000). The ENSO phenomena consist of two components of El Niño and La Niña. The latter is linked with cooler SSTs in the east of the equatorial Pacific and for this condition to occur, this event coincides with a strong Walker circulation (Rojas et al., 2014). The El Niño conditions results from warm SSTs in the western Pacific progressing to the east and this phase coinciding with a weak Walker circulation. The main activity of the El Niño (La Niña) occurs when the central equatorial Pacific Ocean is warm (cool) covering regions 3 and 4. Strong positive anomalies signify El Niño whereas strong negative is a precursor to La Niña events.

#### **3.2.3.2 Southern Oscillation Index (SOI)**

Data of monthly Southern Oscillation Index (SOI) were obtained from the National Climate and Data Center of NOAA (NOAA-NCDC, 2016) also for a period of 1960-2016. Southern Oscillation Index (SOI) also called the Walker circulation defines the east-west atmospheric movement. SOI is applied in the quantification of the ENSO magnitude based on atmospheric pressure. It is computed from the difference between sea level pressure measurement at Tahiti and Darwin (Troup, 1965; Rojas et al., 2014). Negative values of SOI are associated with El

Niño while strong positive values are La Niña events. Various studies have associated climatic disasters such as droughts, floods, tsunamis, hurricanes to ENSO/SOI that influence variant atmospheric and oceanic behaviors (Usman and Reason, 2004; Jones et al., 2007; Morid et al., 2007; Vicente-Serrano et al., 2011; Edossa et al., 2014).

### 3.2.4 Crop yield data

Yields of two main cereal crops in Botswana Viz; maize and sorghum were obtained from the Ministry of Agriculture for a period between 1978/79 and 2015/16. The crop yield data were aggregated according to agricultural zones as indicated in Table 3-2. Locations where crop yield data were obtained are also spatially presented in Figure 3-2. The synoptic stations situated in the respective agricultural zones were used to quantify climatic droughts in the respective regions. The agricultural zones are denoted as northern, western, central, southern and eastern.

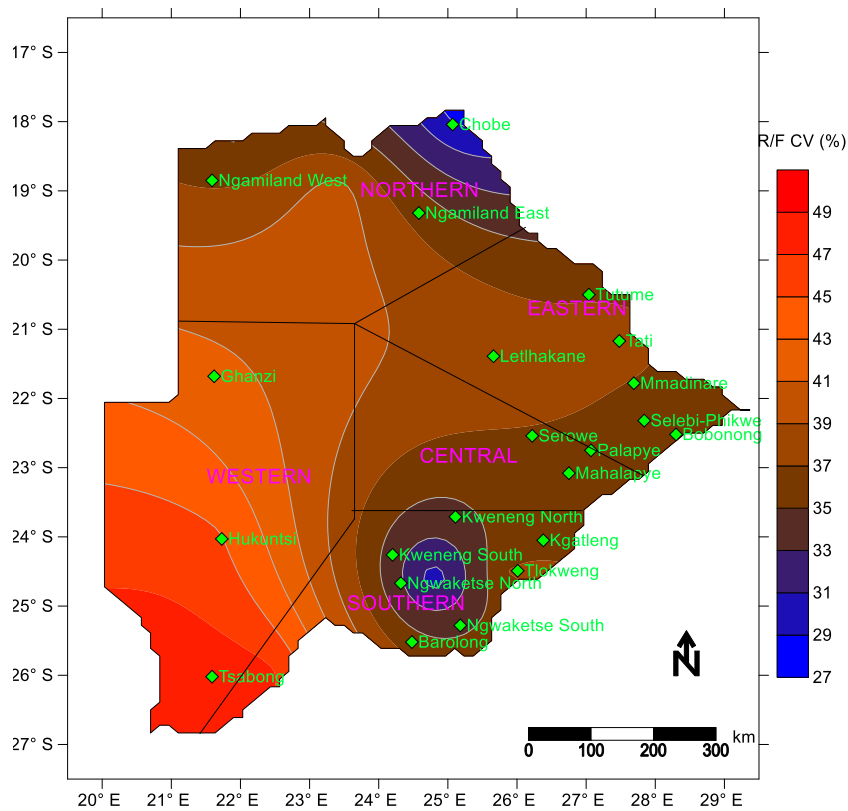


**Fig. 3-2.** Spatial distribution of crop yield data locations across agricultural zones and rainfall coefficient of variation

The growing season starts November/December ending April/May depending on onset and cessation of rains which vary between locations. Both maize and sorghum are rainfed with yields in most cases closely following rainfall patterns. A case in point was the above normal rain year of 1995/96 which resulted in sudden increase in yields as shown in Figure 4-22. That year was also characterised as a La Niña year by Golden gate weather services (2017), indicating a high possibility of ENSO influence on yields over the study area. The mean maize yield varies from 142 kg/ha in the southern region to 43 kg/ha in the western region. Sorghum yields range from 184 kg/ha in the southern region to 19 kg/ha in the western region shown in Table 3-2. Just as the case of rainfall, cereal yields experience even higher variability. The western region located in the Kalahari desert exhibits coefficients of variability (CV) of 130% while the lowest of 75% in maize yields is experienced in the southern region. Sorghum yields show the highest CV of 127% in northern region, while the lowest CV of 73% is recorded in the southern region.

**Table 3-2.** Agricultural regions with respective synoptic stations

Agricultural Region	Maize yield		Sorghum yield		Synoptic Stations
	Mean (kg/ha)	CV (%)	Mean (Kg/ha)	CV (%)	
Southern	141.6	75.0	183.6	72.8	SSKA, Jwaneng and Tsabong
Central	72.0	138.3	143.3	124.7	Mahalapye
Eastern	63.4	85.5	140.0	89.0	Francistown, Letlhakane and Selibe-Phikwe
Northern	109.5	84.4	113.7	126.8	Shakawe, Maun and Kasane
Western	42.8	129.0	18.8	98.5	Ghanzi, Tshane and Tsabong

#### *Cereal yield data smoothing*

Since the aim of this study is to investigate the influence of climatic factors on cereal yields, attempts are made to minimise effects of other technological interventions that could influence yield trends. This is achieved through detrending crop yield data. The technique used in this research is the Holt-Winters double exponential smoothing. This technique is suitable as it takes care of time dependent trend which is inherent in crop yield time series resulting from rainfed agriculture. As a result it assigns exponentially decreasing weights resulting in recent

observations having more effect on data smoothing (Lim and McAleer, 2001; LaViola, 2003). The formulation as suggested by Lim and McAleer (2001) and applied in Croarkin and Tobias (2006) states that, for a given period  $t$ , the smoothed cereal yields  $C_t$  is obtained from,

$$C_t = \alpha y_t + (1 - \alpha)(C_{t-1} + a_{t-1}) \text{ for } 0 \leq \alpha \leq 1 \quad (3.1)$$

Where  $a_t$  takes care of the trend in the data at time  $t$  and is given by;

$$a_t = \beta(C_t - C_{t-1}) + (1 - \beta)a_{t-1} \text{ for } 0 \leq \beta \leq 1 \quad (3.2)$$

Whereas  $y_t$  are observed cereal yields at any time  $t$ ,  $\alpha$  and  $\beta$  are smoothing constants obtained via the nonlinear optimization of Levenberg-Marquardt algorithm through the damped least squares as detailed in Lourakis (2005). The initial values of  $C_{t=1} = y_1$  and  $a_1$  is given by;

$$a_1 = \frac{(y_n - y_1)}{(n-1)} \quad (3.3)$$

Where  $n$  is the total number of years under observation.

### **3.3 METHODS USED IN THE RESEARCH**

The methods under this subsection relate to each of the specific objectives as stated in Chapter 1. The first objective is answered under methods listed in subsection 3.3.1 while the second objective is addressed under 3.3.2. Subsections 3.3.3 and 3.3.4 are answering objective 3 of this research. The objective in regard to the influence of climatic indices on cereal yields is covered in subsection 3.3.5 with the last objective addressed in subsection 3.3.6.

#### **3.3.1 Climatic trends and abrupt changes in meteorological time series**

The subsections below cover methodologies for detecting possible long term changes in the climate of the study area. The methodologies covered here are tests for homogeneity, trend analysis of meteorological time series, detection of persistence, influence of ENSO on local climatic variables and spatial presentation of rainfall variables and their trend.



### 3.3.1.1 Tests for homogeneity

Data used in long term climatological studies are required to be homogeneous in that, they should belong to the same population with mean of no temporal variation (Akinsanola and Ogunjobi, 2015). Data is considered homogeneous if any changes are only attributed to natural occurrences. Homogeneity testing in this research involves a number of stages. The first stage comprises of data quality checks to identify recording errors using both visual and graphical techniques. The second stage involves applying of absolute homogeneity testing techniques that includes the Standard Normal Homogeneity Test (SNHT) (Alexandersson, 1986), Pettit test (Pettit, 1979), Buishand range test (Buishand, 1982) and the Von Neumann ratio test (Von Neumann, 1941). Wijngaard et al. (2003) in a comprehensive study of European climate systems, recommended no discardment of stations with suspected nonhomogeneities but rather classify them. Absolute tests were selected over relative tests due to the somewhat sparse and skew towards the east (Figure 1-1) meteorological network across the study area. The following classification by Wijngaard et al. (2003) and Hänsel et al. (2016) is used in this research viz: ‘useful’, ‘doubtful’, and ‘suspect’ at 1% significant level. A station is classified as ‘useful’ if it is homogenous in at least three of the four tests, ‘doubtful’ is used when homogeneity is reported for two tests and ‘suspect’ when station fails in three or more of the tests (Wijngaard et al. 2003; Costa and Soares 2009b; Hänsel et al. 2016). For further studies of variability and trend analysis, stations classified as ‘useful’, their complete data record is used. If a station is labeled ‘doubtful’, the whole data record is used but trend in the data is further scrutinised by comparing with trends before and after the suspected year of intervention. For stations classified as ‘suspect’, the record before the suspected year of intervention was excluded from the analysis.

The null hypothesis for the four absolute tests assumes that the time series are homogeneous. For the alternative hypothesis, the SNHT, Pettit and Buishand tests suppose an intervention in the time series. These tests are able to locate the year of intervention and its statistical

significance. The Von Neumann test under the alternative hypothesis assumes persistence in the time series. Formulations of the four tests are presented below:

*Standard normal homogeneity test (SNHT)*

The SNHT as presented by Alexandersson (1986) and Alexandersson and Moberg (1997), gives a statistic that compares the means of the first  $m$  series with the  $(n-m)$  series of meteorological variable at an annual scale. If  $W_i$  denotes meteorological time series for  $i=1,2,3,\dots,n$ , then the test statistic is given by;

$$T(m) = m\bar{y}_1^2 + (n - m)\bar{y}_2^2 \quad \text{for } m = 1,2, \dots, n \quad (3.4)$$

Where,

$$\bar{y}_1 = \frac{1}{m} \sum_{i=1}^m \frac{(W_i - \bar{W})}{\sigma} \quad (3.5)$$

and

$$\bar{y}_2 = \frac{1}{(n-m)} \sum_{i=m+1}^n \frac{(W_i - \bar{W})}{\sigma} \quad (3.6)$$

Where,  $\bar{W}$  and  $\sigma$  are the expected value and standard deviation of the time series respectively.

A plot of  $T(m)$  against  $m$  reaches its maximum at the suspected year of intervention. The test statistic at the suspected point is given by;

$$T_0 = \underbrace{\text{Max}}_{1 \leq m \leq n} T(m) \quad (3.7)$$

The null hypothesis is rejected if  $T_0$  exceeds a given threshold which is a function of the sample size at a given level of significance. A Table of critical  $T_0$  values is presented in Wijngaard et al. (2003).

*Pettit test*

This is a non parametric rank based test presented by (Pettit, 1979) and applied in Akinsanola

and Ogunjobi (2015) and Wijngaard et al. (2003). It states that if  $r_1, r_2, \dots, r_n$  are ranks of a given meteorological variable  $W_i$ , then the order statistic is given by

$$X_m = 2 \sum_{i=1}^m r_i - m(n + 1) \quad \text{for } m = 1, 2, \dots, n \quad (3.8)$$

If intervention is suspected to occur at year  $K$ , the plot of  $X_m$  against time will exhibit a minimum or maximum at  $m=K$  and

$$X_K = \underbrace{\text{Max}}_{1 \leq m \leq n} |X_m| \quad (3.9)$$

The significant values of  $X_K$  are provided in Tables as a function of sample size at a given significant level.

#### *Buishand test*

The Buishand test as presented by Buishand (1982) utilises adjusted partial sums given by;

$$S_0^* = 0 \text{ and } S_m^* = \sum_{i=1}^m (W_i - \bar{W}) \quad \text{for } m = 1, 2, \dots, n \quad (3.10)$$

The null hypothesis is accepted if the plot of  $S_m^*$  against time fluctuates around  $S_0^*$ . Gradual rise or fall in the plot is an indication of suspected point of intervention corresponding to a particular year  $M$ . The test of significance is achieved through rescaled range  $R$  given by;

$$R = \left( \frac{\underbrace{\text{Max}}_{1 \leq m \leq n} S_m^* - \underbrace{\text{Min}}_{1 \leq m \leq n} S_m^*}{\sigma} \right) \quad (3.11)$$

The critical values of  $R/\sqrt{n}$  are given in Buishand (1982). If the computed  $R/\sqrt{n}$  is greater than the tabulated value, then the null hypothesis is rejected.

#### *Von Neumann test*

The Von Neumann test is a complementary test to the three preceding homogeneity tests characterised by ratios of successive mean square difference to the variance of the time series (Von Neumann, 1941; Wijngaard et al., 2003). It is given by;

$$N = \frac{\sum_{i=1}^{n-1} (W_i - W_{i+1})^2}{\sum_{i=1}^n (W_i - \bar{W})^2} \quad (3.12)$$

The test gives no information on the point of intervention even though it exists. Significant values of N are tabulated in Von Neumann (1941).

### 3.3.1.2 Trend analysis of meteorological time series

Following classification of meteorological stations as ‘useful’, ‘doubtful’, and ‘suspect’ in subsection 3.3.1.1, analysis of trend is made. This research applies two non parametric statistics, the Mann-Kendall to determine the direction of the trend and Sen’s Slope for the magnitude of the trend. The Sen’s Slope is also used to determine the percentage change in the variable for the period of analysis.

#### *Mann-Kendall (MK) trend statistic*

The MK statistic as presented by Mann (1945) and Kendall (1975) applied in Tabari et al. (2011) and Akinsanola and Ogunjobi (2015) is given by;

$$S = \sum_{i=1}^{n-1} \sum_{k=i+1}^n \text{Sgn}(W_k - W_i) \quad \text{for } k > i \quad (3.13)$$

Where Sgn is the sign function given by;

$$\text{Sgn}(W_k - W_i) = \begin{cases} +1 & \text{if } (W_k - W_i) > 0 \\ 0 & \text{if } (W_k - W_i) = 0 \\ -1 & \text{if } (W_k - W_i) < 0 \end{cases} \quad (3.14)$$

The statistical significance of the trend is tested using the Z-statistic which is obtained from;

$$Z_w = \begin{cases} \frac{S-1}{\sqrt{\text{Var}(S)}} & \text{if } S > 0 \\ 0 & \text{if } S = 0 \\ \frac{S+1}{\sqrt{\text{Var}(S)}} & \text{if } S < 0 \end{cases} \quad (3.15)$$

Where Var(S) is the variance of the S statistic obtained from Equation (3.13). The Var(S) is computed from;

$$\text{Var}(S) = \frac{n(n-1)(2n+5) - \sum_{i=1}^q p_i(p_i-1)(2p_i+5)}{18} \quad (3.16)$$

Where  $q$  and  $p_i$  are the total number of tied groups and ties of extend  $i$  respectively. Positive values of  $Z_w$  designate upwards trends while negative values otherwise. The null hypothesis assumes that no trend exists in the time series and the alternative hypothesis assumes trend exists. The significance of the trend is tested by comparing the resulting p-value with a significant value  $\alpha$ . When the computed p-value is greater than  $\alpha$ , the null hypothesis is accepted. In this research  $\alpha=0.05$  is used to accept or reject the null hypothesis. The MK test has successfully been applied in a number of hydroclimatic studies (Yue and Hashino, 2003; Some'e et al., 2012; Gocic and Trajkovic, 2013; Sabzevari et al., 2015).

#### *Trend slope magnitude estimation*

The Sen's Slope method is used to test the magnitude of the MK trend. This method examines whether the regression slope between ordered pairs is significantly different from zero. The slope is estimated from the procedure proposed by Thiel (1950) and Sen (1968). The slope of  $N$  ordered pairs of data points is given by;

$$Q_i = \frac{(W_k - W_i)}{k-i} \text{ for } i=1,2,\dots,N \quad (3.17)$$

The median slope of  $Q_i$  arranged in ascending order gives the Sen's Slope and computed from;

$$Q_{\text{med}} = \begin{cases} \frac{Q_{\frac{(N+1)}{2}}}{2} & \text{if } N \text{ is odd} \\ \frac{Q_{\frac{N}{2}} + Q_{\frac{[N+2]}}{2}}{2} & \text{if } N \text{ is even} \end{cases} \quad (3.18)$$

For trend comparisons among different meteorological locations, the percentage change in slope is preferred as proposed by Yue and Hashino (2003) and applied in Akinsanola and Ogunjobi (2015). The percentage slope is given by;

$$\Delta S = \frac{Q_{\text{med}} \times T}{\bar{W}} \cdot 100 \quad (3.19)$$

For regionalisation, the total change over the study area is obtained from

$$\Delta S_R = \frac{1}{b} \sum_{i=1}^b \Delta S \quad (3.20)$$

Where  $\Delta S$  is the percentage change over a period of record  $T$ ,  $b$  is the total number of stations over the study area and  $\Delta S_R$  the regionalised change in a given meteorological variable.

### 3.3.1.3 Detection of persistence

Parametric trend tests of climatological data series require that they are serially independent and random in nature (Tabari et al., 2011; Gocic and Trajkovic, 2013). An auto correlation is applied to detect non-randomness in data. Presence of persistence in the time series increases chances of accepting the null hypothesis even when trend exists (Yue et al., 2002; Tabari and Talaei, 2011). For meteorological time series that exhibits significant serial correlation at  $\alpha=0.05$ , the effective sample size (ESS) method suggested by Lettenmaier (1976) and used in Tabari and Talaei (2011) and Akinsanola and Ogunjobi (2015) is applied to correct the influence of the serial correlation on the Mann-Kendall test.

The autocorrelation lag 1 is used in this research since the main interest is to examine the possibility of none randomness in the data series. Possibility of statistically significant correlations in sample data series  $W_1 + W_2 + W_3 + \dots + W_n$  is tested using the following procedure as stated in (Gocic and Trajkovic, 2013):

- i. The lag-1 serial correlation coefficient of sample data  $W_i$  is computed as applied in Croarkin and Tobias (2006)

$$r_1 = \frac{\frac{1}{n-1} \sum_{i=1}^{n-1} (W_i - \bar{W})(W_{i+1} - \bar{W})}{\frac{1}{n} \sum_{i=1}^n ((W_i - \bar{W}))^2} \quad (3.21)$$

- ii. If the computed  $r_1$  in (i) above is not significant at  $\alpha=0.05$ , the variance of the Mann-Kendall is used as earlier determined in Equation (3.16).
- iii. Should the calculated  $r_1$  be significant at  $\alpha=0.05$ , the variance of the Mann-Kendall statistic is modified using ESS.

The modified variance  $\text{Var}^*(s)$  is given by;

$$\text{Var}^*(s) = \text{var}(s) \cdot \frac{n}{n^*} \quad (3.22)$$

Where  $n$  is the actual sample size of the time series and  $n^*$  is the ESS. The ration of  $n/n^*$  is the correction factor. Matalas and Langbein (1962) and Akinsanola and Ogunjobi (2015) proposed a formula to determine  $n^*$  from the lag-1 serial correlation;

$$n^* = \frac{n}{1 + 2 \cdot \frac{r_1^{n+1} - nr_1^2 + (n-1)r_1}{n(r_1-1)^2}} \quad (3.23)$$

By replacing the  $\text{Var}(s)$  with  $\text{Var}^*(s)$  in the Mann-Kendall's Equation, a modified test statistic  $Z_w$  is computed by,

$$Z_w^* = Z_w \sqrt{\frac{n^*}{n}} \quad (3.24)$$

The null hypothesis being tested is that, the sequence was produced in a random manner.

#### **3.3.1.4 Influence of ENSO on local climatic variables**

The degree of association between ENSO and local climatic variables is investigated using multivariate analysis. The degree of association is tested at 5% significant level under the null hypothesis that there is no correlation between ENSO and local climatic variables. Monthly SSTs and SOI data is averaged at annual scale using the same criteria as that of meteorological variables. Correlations between SSTs and climatic variables on one hand and SOI on the other hand are determined.

#### **3.3.1.5 Spatial presentation of rainfall variables and their trends**

After obtaining climatic characteristics at each gauge station in the study area, they are interpolated to enable spatial representation for further scrutiny. The Kriging geostatistic technique in SURFER is used to interpolate these point characteristics into surface maps for the study area. It must however be noted that density of the synoptic stations over large parts of Botswana which constitutes the heart of the Kalahari Desert is very low. This means that

spatial representation of rainfall and temperature characteristics should be interpreted with caution over these areas. In effect the interpolation results over this region may not be as accurate as the rest of the locations. The east and northeast to northern parts of the country, however, have relatively better coverage by synoptic stations.

### **3.3.2 Onset, cessation of rainfall and dry spell frequency analysis**

After investigating possible changes in meteorological time series in section 3.3.1, it was hence necessary to determine how these changes have affected the onset and cessation of rainfall across the study area. In this Section the methodologies for determining potential evapotranspiration, dry spell frequency, onset and cessation of rain dates are presented.

#### **3.3.2.1 Determination of potential evapotranspiration ( $ET_0$ )**

From numerous existing  $ET_0$  equations, the FAO-56 method of the Penman-Monteith (P-M) equation (Allen et al., 1998) is currently widely used and recommended by Food and Agricultural Organization (FAO), International Commission on Irrigation and Drainage (ICID) and American Society of Civil Engineers (ASCE) as a standard because it is predominately a physically based approach (Vicente-Serrano et al., 2010). A major challenge to the application of the P-M however, is the relatively high data demand in form of air temperature, wind speed, relative humidity and solar radiation. A number of meteorological stations in the study area do not possess all this range of dataset. For this reason, an alternative approach developed by Hargreaves (1994) where only mean maximum and mean minimum air temperature and extraterrestrial radiation are required is used in this research. The extraterrestrial radiation component is calculated for a certain day and location. The Hargreaves equation as applied in Droogers and Allen (2002) for computation of  $ET_0$  is given by:

$$ET_0 = 0.0023(T_{\text{mean}} + 17.8)(T_{\text{max}} - T_{\text{min}})^{0.5} \cdot 0.408R_a \quad (3.25)$$

Where,



$T_{\text{mean}}$  the mean air temperature ( $^{\circ}\text{C}$ ),

$T_{\text{max}}$  the maximum air temperature ( $^{\circ}\text{C}$ ),

$T_{\text{min}}$  the minimum air temperature ( $^{\circ}\text{C}$ )

$R_a$  extraterrestrial radiation [ $\text{MJ m}^{-2} \text{day}^{-1}$ ] and is given by

$$R_a = \frac{24(60)}{\pi} G_{\text{sc}} d_r [\omega_s \sin(\varphi) \sin(\delta) + \cos(\varphi) \cos(\delta) \sin(\omega_s)] \quad (3.26)$$

Where,

$G_{\text{sc}}$  solar constant =  $0.0820 \text{ MJ m}^{-2} \text{ min}^{-1}$ ,

$d_r$  inverse relative distance Earth-Sun (Equation 3.27),

$\omega_s$  sunset hour angle (Equation 3.30) [rad],

$\varphi$  latitude [rad],

$\delta$  solar declination (Equation 3.28) [rad].

The inverse relative distance Earth-Sun,  $d_r$ , and the solar declination,  $\delta$ , are given by:

$$d_r = 1 + 0.033 \cos\left(\frac{2\pi}{365} J\right) \quad (3.27)$$

$$\delta = 0.409 \sin\left(\frac{2\pi}{365} J - 1.39\right) \quad (3.28)$$

Where J is the average Julian day of the month M given by

$$J = \begin{cases} \left(\frac{275M}{9} - 30 + D\right) - 2 & M > 3 \\ \left(\frac{275M}{9} - 30 + D\right) & M < 3 \\ \left(\frac{275M}{9} - 30 + D\right) + 1 & M > 2 \text{ for leap year} \end{cases} \quad (3.29)$$

D=15 for average month representing calendar day

The sunset hour angle,  $\omega_s$ , is given by:

$$\omega_s = \cos^{-1}[-\tan(\varphi)\tan(\delta)] \quad (3.30)$$

### 3.3.2.2 Identification of onset and cessation of rain

Numerous methods exist for determining onset and cessation of rain dates as presented in Sivakumar (1988), Recha et al. (2012), Ngetich et al. (2014) and Amekudzi et al. (2015). However, most of these methods rely only on rainfall data to determine the onset and cessation dates. Due to the important role  $ET_0$  plays in plant moisture deficit, the rainfall-evapotranspiration relationship as described in Araya and Stroosnijder (2011), Kebede et al. (2016) and Byakatonda et al. (2016) is used in this research to formulate a criteria for identifying onset and cessation of rain dates.

Onset is assumed to occur when pentad rainfall equals or exceeds half of the pentad  $ET_0$  (Araya and Stroosnijder, 2011; Byakatonda et al., 2016). This is true under the following objective criteria; 1) these conditions are maintained for the next 10 days with rainfall totals exceeding 25 mm and 2) no dry spell exceeding two pentads occur within 30 days of identified onset date.

Conversely cessation is assumed to occur after the onset date when the pentad rainfall totals falls below half the pentad  $ET_0$  under the following objective criteria; a dry spell exceeding two pentads occurs after the deficit is recorded and cessation date is then taken as the 7<sup>th</sup> day from the day the deficit started. The length of the rain season is computed as the number of days between onset and cessation dates. Number of rainy days in a season is determined as the total number of days that registers rainfall more than 1 mm.

Time series of onset, cessation dates and length of growing season are generated for further analysis of trends and determination of coefficient of variation (CV). Mean onset and cessation dates are determined for each station over the study area.

### **3.3.2.3 Dry spell frequency analysis**

Knowledge on the frequency of dry spells is crucial for successful rainfed venture farming. Dry spells were aggregated at different intervals of 10 and 15 days in West Africa by Sivakumar (1992) and 5, 10 and 15 days by Ngetich et al. (2014) in East Africa. Aggregation at 5 day (Pentads) intervals is made for this research to include finer and lower bounds of dry spells. Dry spell frequency is determined as the number of pentads with rainfall less than 5 mm. Time series of dry spell frequency is generated at each station for further analysis.

The homogeneity of rainfall variables time series in the form of onset, cessation, length of the rain season, dry spell frequency is tested using the four absolute tests as presented in subsection 3.3.1.1. This was to allow the generated time series to undergo trend analysis as explained in subsection 3.3.1.2.

### **3.3.3 Drought severity under climate variability and its relationship with ENSO**

Drought severity is closely associated with climate variability, with the advent of global warming, it is imperative that the drought evolution and characteristics are explored. This subsection quantifies drought severity in form of magnitude, duration and intensity.

#### **3.3.3.1 Drought severity characterisation using Standardised precipitation**

##### **evapotranspiration index (SPEI)**

The determination of SPEI is summarised in the following steps (Beguería et al., 2014; Edossa et al., 2014; Stagge et al., 2015).

1. Determination of potential evapotranspiration ( $ET_0$ )
2. Generation of the climatic water balance ( $W_j$ ) which is the difference between monthly rainfall amounts ( $R$ ) and potential evapotranspiration ( $ET_0$ ).
3. Aggregation of the climatic water balance ( $W_j$ ) from step (2) over a period of  $n$  months, where  $n$  is drought time scale.

4. The aggregated climatic water balance time series obtained in step (3) are then standardised through a Gaussian transformation.

The potential evapotranspiration was determined using the procedure as presented in subsection 3.3.2.1. For purposes of determining drought vulnerability across the study area, classifications proposed by Yu et al. (2014) are used in this research and presented in Table 3-3.

**Table 3-3.** Drought severity classifications (Yu et al., 2014)

Drought severity	Drought severity classes
<-2	Extreme Drought
-1.99 to -1.50	Severe Drought
-1.49 to 1.00	Moderate Drought
-1.00 to 1.00	Near Normal
1.00 to 1.49	Moderately Wet
1.50 to 1.99	Severely Wet
> 2.00	Extremely Wet

#### 3.3.3.1.1 Aggregation of climate water balance ( $W_j$ ) series

The  $W_j$  series are accumulated at different timescales of n=1-, 3-, 6-, 12-, 18- and 24-months. Twelve independent series are generated one for each month in order to maintain the homogeneity of the accumulated  $W_j$  series ( $W_{i,j}^n$ ) (Vicente-Serrano et al., 2010; Zargar Yaghoobi, 2012; Stagge et al., 2015), the  $W_{i,j}^n$  in a given month j and year i is dependent upon a selected timescale n. For illustration purposes, the accumulated series for one month j in a particular year i is determined from;

$$W_{i,j}^n = \sum_{l=13-n+j}^{12} W_{i-1,l} + \sum_{l=1}^j W_{i,l} \text{ if } j < n \text{ and} \quad (3.31)$$

$$W_{i,j}^n = \sum_{l=j-n+1}^j W_{i,l} \text{ if } j \geq n \quad (3.32)$$

#### 3.3.3.1.2 Standardisation of the water balance series

In determining SPEI values, a 3-parameter distribution was utilised since  $W_{i,j}^n$  values can have both negative values in periods of low rainfall and positive values in periods of above normal

rainfall (Potop et al., 2010; Vicente-Serrano et al., 2010). L-Moments as linear combinations of ordered  $W_{i,j}^n$  series were used for fitting an appropriate probability distribution function on to the original series. L-moments were selected because they are believed to give least bias estimates and performs well even with data sets containing outliers (Hosking and Wallis, 2005; Beguería et al., 2014; Byakatonda et al., 2016).

The L-moments allow comparison of various candidate frequency distributions that can fit the  $W_{i,j}^n$  series. To identify the candidate distributions, L-moments ratios of L-Skewness ( $\tau_3$ ) and L-Kurtosis ( $\tau_4$ ) were used since they are a summary of probability distributions in terms of the shape, location and scale parameters (Hosking and Wallis, 2005). L-Skewness  $\tau_3$  and L-Kurtosis  $\tau_4$  are presented in Equations (3.33) and (3.34);

$$\tau_3 = \frac{\lambda_3}{\lambda_2} \quad (3.33)$$

$$\tau_4 = \frac{\lambda_4}{\lambda_2} \quad (3.34)$$

Where,  $\lambda_1, \lambda_2, \lambda_3$  and  $\lambda_4$  are first to fourth order linear moments obtained from  $W_{i,j}^n$  arranged in ascending order. They are computed from Equations (3.35-38) (Hosking and Wallis, 2005; Parida and Moalafhi, 2008)

$$\lambda_1 = E \left[ W_{i,j(1:1)}^n \right] \quad (3.35)$$

$$\lambda_2 = \frac{1}{2} E \left[ W_{i,j(2:2)}^n - W_{i,j(1:2)}^n \right] \quad (3.36)$$

$$\lambda_3 = \frac{1}{3} E \left[ W_{i,j(3:3)}^n - 2W_{i,j(2:3)}^n + W_{i,j(1:3)}^n \right] \quad (3.37)$$

$$\lambda_4 = \frac{1}{4} E \left[ W_{i,j(4:4)}^n - 3W_{i,j(3:4)}^n + 3W_{i,j(2:4)}^n - W_{i,j(1:4)}^n \right] \quad (3.38)$$

The notations  $W_{i,j}^n(q:r)$  denotes the  $q^{\text{th}}$  smallest value from a data set of  $r$  elements.

From the L-moment ratio diagram, the 3-parameter generalised logistic distribution function was identified to fit the  $W_{j,i}^n$  series at all the selected timescales. The GLO is given by Equation (3.39) (Hosking and Wallis, 2005);

$$f(W_{i,j}^n) = \frac{\alpha^{-1} \exp[-(1-k)Y]}{[1 + \exp(-Y)]^2} \quad (3.39)$$

Where,

$$Y = \begin{cases} -k^{-1} \log \left[ 1 - \frac{k(W_{i,j}^n - \xi)}{\alpha} \right], & k \neq 0 \\ \frac{(W_{i,j}^n - \xi)}{\alpha}, & k = 0 \end{cases} \quad (3.40)$$

and  $\xi$  denotes location,  $\alpha$ -scale and  $k$ -shape parameters which are obtained as functions of L-moments as follows;

$$k = -\tau_3 \quad (3.41)$$

$$\alpha = \frac{\lambda_2 \sin k\pi}{k\pi} \quad (3.42)$$

$$\xi = \lambda_1 - \alpha \left( \frac{1}{k} - \frac{\pi}{\sin k\pi} \right) \quad (3.43)$$

The cumulative density distribution function from which probabilities of non-exceedance are derived is given by;

$$F(W_{i,j}^n) = \frac{1}{[1 + \exp(-Y)]} \quad (3.44)$$

From Equation 3.44, the probability of exceedance  $P$  of a given  $W_{i,j}^n$  value can be determined.

The  $P$  value is obtained from;

$$P = 1 - F(W_{i,j}^n) \quad (3.45)$$

The probabilities  $P$  of exceedance are then standardised through a Gaussian transformation into a normal variable using the following approximation by Abramowitz and Stegun (1964)

$$\text{SPEI} = Z - \frac{2.516+0.803Z+0.0103Z^2}{1+1.433Z+0.189Z^2+0.0013Z^3} \quad (3.46)$$

$$\text{Where, } Z = \left[ \ln \left( \frac{1}{p^2} \right) \right]^{\frac{1}{2}} \quad (3.47)$$

SPEI series are standardised with mean of zero and standard deviation of one for easier comparison on temporal and spatial scales. At each timescale, SPEI events which are continuously negative signify drought conditions. The SPEI values define duration, magnitude and intensity of each drought event.

### **3.3.3.2 Association of ENSO with drought severity**

The degree of association between ENSO and drought severity is investigated using bivariate correlation analysis at each timescale. The correlation is performed between drought severity and SSTs on one hand and SOI on the other hand at 5% significant level. This is done on a monthly basis to identify which season of the year presents with the highest associations and its implications on agricultural and water resources. The results from this analysis are represented in box and whisker plots.

### **3.3.4 Drought propagation and its influence on water resources**

#### **3.3.4.1 Study sites**

Water resources in the study area are mainly confined in five river basins viz: Okavango, Makgadikgadi, Limpopo, Chobe-Kwando-Linyanti and Orange (GOB-MMEWR, 2006) with the main rivers being transboundary. This makes water resources development a multi stakeholder involving process. The Okavango, Chobe-Kwando-Linyanti and Limpopo which are transboundary have more perennial water sources on which Botswana depends. Most of the inland water sources drain to the Limpopo river basin which provides majority of the water supply. To understand the influence of drought on water resources, this research uses Limpopo and Okavango river basins as study sites.

### *Okavango river basin*

The main river that supplies this basin is River Okavango which enters Botswana from Angola at Mohebo (Figure 3-1) and ends up as a delta. The river basin has been classified as a Ramsar site and therefore has restrictions on the extent of water resources development and abstractions (Byakatonda et al., 2016). This basin mainly meets local water demand of the Panhandle with the remainder of the resource reserved for ecological functions. It can be considered as a natural storage type river basin where only losses are through evaporation and seepage.

### *Limpopo river basin (Botswana sub basin )*

Majority of seasonal and permanent inland streams drain into the Limpopo river basin including Notwane, Metsimotlhaba, Mahalapwe, Shashe, Tati, Ntshe, Ramokgwebana, Taupye, Bonwapitse, Thune and Lotsane (GOB-MMEWR, 2006). Most of these streams are heavily regulated with surface dams managed by Ministry of Minerals Energy and Water Resources (GOB-MMEWR) for domestic, industrial supply and irrigation. These river sub basins have no clear topographical divide as they are characterised by a flat terrain (FAO, 2001). The river basin receives its inflows during the wet months and generally is dry the remainder of year. It can be classified as a non-storage type of river basin (except storage in artificial storage structures).

#### **3.3.4.2 Determination of hydrological drought index**

Hydrological drought is expressed through Standardised Flow Index (SFI) which takes care of seasonality in the flows other than assuming that hydrological droughts are based on low flow thresholds (Smakhtin and Hughes, 2004; Lorenzo-Lacruz et al., 2010). For Botswana's case, flow is highly seasonal as it is linked to the summer rainfall (GOB-MMEWR, 2006), it requires relating monthly anomalies to long term average conditions (Vicente-Serrano and López-Moreno, 2005; Nalbantis and Tsakiris, 2009). In lieu of this, the research used the



procedure of standardisation of time series at timescales of 1-, 3-, 6-, 12-, 18- and 24-months. This procedure has been applied in studies by Byakatonda et al. (2016), Lorenzo-Lacruz et al. (2010) and Shukla et al. (2011). The technique of L-moments is employed as explained in subsection 3.3.3.1. This research identified that the Generalised Extreme Value (GEV) function best models the flow data most of the time in the two river basins. This is in agreement with findings of Dikgola (2015) who identified GEV to fit well River Okavango flow time series. The probability density function (pdf) of the GEV category of a function S representing flow time series according to Hosking and Wallis (2005) is given by;

$$f(S) = \alpha^{-1} \exp[-(1 - k)y - \exp(-y)] \quad (3.48)$$

Where,

$$y = \begin{cases} -k^{-1} \ln \left[ 1 - \frac{k(s-\xi)}{\alpha} \right], & k \neq 0 \\ \frac{(s-\xi)}{\alpha}, & k = 0 \end{cases} \quad (3.49)$$

The cumulative density function is given by;

$$F(S) = \exp[-\exp(-y)] \quad (3.50)$$

Where  $\xi$ ,  $\alpha$ , and  $k$  are location, scale and shape parameters, respectively, for S ranging from:

$$S: \begin{cases} -\infty < s \leq \xi + \frac{\alpha}{k} & \text{if } k > 0 \\ -\infty < s < \infty & \text{if } k = 0 \end{cases} \quad (3.51)$$

The Parameters are computed as a function of L-moment ratios as follows;

Shape parameter,

$$k = 7.859c + 2.9554c^2 \quad (3.52)$$

$$\text{Where, } c = \frac{2}{3+\tau_3} - \frac{\ln 2}{\ln 3} \quad (3.53)$$

Scale parameter,

$$\alpha = \frac{\lambda_2 k}{(1-2^{-k})\Gamma(1+k)} \quad (3.54)$$

Location Parameter,

$$\xi = \lambda_1 - \frac{\alpha[1-\Gamma(1+K)]}{k} \quad (3.55)$$

The cumulative density function  $F(S)$  in Equation (3.50) is then standardised to the Z-value using the same procedure discussed in subsection 3.3.3.1. At every timescale, the hydrological droughts were defined by indices below zero. The value of the index at any point also defines the magnitude and intensity of the hydrological drought.

### **3.3.4.3 Association between climatological and hydrological droughts**

To assess the inter linkages between climatological and hydrological droughts, statistical analysis were performed. A degree of association is determined through bivariate correlation analysis at 5% level of significance. Correlations are determined at each identified timescale to come up with the most suitable period for the respective river basins that could be used in drought monitoring and management. The correlation analysis is done for both monthly (seasonal) and combined drought severity time series. This is handy in investigating seasonality while identifying months of the year with significant association between indices. Evolutions of climatic and hydrological droughts were superimposed to identify possible time lags that may exist between the two drought classifications. Any identified time lag was further confirmed using lag correlations between SPEI and SFI. This time lag is considered as the period taken for climatological drought to propagate to hydrological drought. To identify the timescale which can be used by operational hydrologists and water managers in Botswana's drought management, plots of probabilities of experiencing a given droughts category against timescale from individual river basins were also superimposed to delineate the region of their interaction. The joint identified timescale for the study area is used to investigate future drought severity variability through rescaled range analysis and modeling using artificial neural network (ANN). Drought occurrence probability is determined from the ratio of the

frequency of occurrence of that drought category to the total SPEI events during the historical period (Byakatonda et al., 2016).

#### **3.3.4.4 Rescaled range (R/S) analysis of hydrological drought index (SFI)**

Drought indices aid understanding of dynamics of droughts and their variability. In this research, their long term persistence or reversion is investigated through the rescaled range analysis (R/S) (Sakalauskiene, 2003; Voss, 2013). Linked with rescaled range analysis is the Hurst coefficient (H) which is an expression of long term dependence and also a measure of variability (Koutsoyiannis, 2003; Sakalauskiene, 2003; Granero et al., 2008). The H-coefficient ranges from  $0 \leq H \leq 1$ ,  $H > 0.5$  indicates persistence in the time series while  $H = 0.5$  is an indicator of randomness in the data.  $H < 0.5$  is a sign of reversion in the trend of the time series in the next time period.

Below are the steps undertaken for rescaled range analysis to enable estimation of the H-coefficient;

1. Drought severity at identified timescale for drought monitoring were denoted as a stationery stochastic process  $Z_i$  with  $i=1,2,3,\dots,N$ , where  $i$  denotes months of length  $N$  and  $Z$  are SFI values determined from subsection (3.3.4.2).
2. The  $Z_i$  time series are divided into multiple regions of ranges with varying lengths ( $i=1,2,3,\dots,n$ ) with  $n$  being length of a given sub series. For this research the dataset is split into six ranges of sub series categorised as follows;
  - a. First range includes complete drought severity series ( $n=N$ )
  - b. Second range, data are split into 2 sub series ( $n \approx N/2$ )
  - c. Third range data are split into 4 sub series ( $n \approx N/4$ )
  - d. For the fourth range, the time series are divided into 8 sub series of equal length ( $n \approx N/8$ )
  - e. Fifth range data are divided into 16 multiple units ( $n \approx N/16$ )

- f. For the last range, series are split into 32 different series ( $n \approx N/32$ )
3. The expected values of each of the time series above is then determined from
 
$$\bar{Z} = E(Z_i)$$
  4. The expected value from 3 above for each range is used to generate series of deviations as follows;  $Y_i = Z_i - \bar{Z}$  for  $i=1,2,3,\dots,n$ 

$$(3.56)$$
  5. The minimum and maximum values from the deviation series are then determined. An adjusted range is computed from  $R^* = \text{Max}(Y_1, Y_2, \dots, Y_n) - \text{Min}(Y_1, Y_2, \dots, Y_n)$ 

$$(3.57)$$
  6. The standard deviation for each range is computed from
 
$$SD = \sqrt{\frac{\sum_{i=1}^n (Z_i - \bar{Z})^2}{n-1}}$$

$$(3.58)$$
  7. The rescaled range is computed from  $R/S = \frac{R^*}{SD}$ , for each sub range an average R/S is computed.
  8. Rescaled range is related to H-coefficient through  $(R/S) \approx kn^H$
  9. The H-coefficient is then obtained by running a regression following the expression,
 
$$\ln(R/S) = \ln(k) + H \cdot \ln(n)$$

$$(3.59)$$
  10. A slope of the regression plot of  $\ln(R/S)$  against  $\ln(n)$  results from the H-coefficient, which is a measure of future variability in the time series describing long term dependence process of Z-series.

This procedure has been applied in studies of trends in hydrological time series and financial markets (Sakalauskiene, 2003; Granero et al., 2008; Voss, 2013; Munshi, 2014).

### 3.3.5 Influence of climatic indices, length of the rain season on cereal yield

The climatic indices being considered are standardised precipitation and evapotranspiration index, southern oscillation index and aridity index. All the afore stipulated climatic indices

except aridity index have been discussed in preceding subsections. The computation procedure of the aridity index is presented in subsection 3.3.5.1.

### **3.3.5.1 Determination of aridity index (AI)**

Aridity index is used in this study to understand the effect of long term moisture deficiency over the study area. It is used to measure the extent of dryness of a given climate and sometimes used in climate classifications (Maliva and Missimer, 2012). The aridity index relates the available rainfall with  $ET_0$ . For applications of AI to soil moisture deficit and hence agriculture, the De Mortone formula is used.  $AI_i$  for a given year  $i$  as defined by De Martonne (1926), applied in Livada and Assimakopoulos (2007) and Zhang et al. (2009) is presented as;

$$AI_i = \frac{12P_i}{10+T_i} \quad (3.60)$$

Where  $P_i$  is the monthly rainfall for year  $i$  and  $T_i$  is the monthly mean air temperature. When aridity index falls below 20, the actual evapotranspiration starts to drop below potential evapotranspiration and hence periods of moisture deficit leading to plant water stress. Prolonged periods under deficit conditions may lead to yield loss. Time series of AI are smoothed to minimise fluctuations over different timescales of 3-, 6- and 12-months used in analysis with cereal yields. The original and smoothed series are then used for correlation analysis with detrended cereal yields. The different moving average window periods is also used to identify the timescale that closely associates with cereal yields.

### **3.3.5.2 Association of climatic indices and length of the rain season with cereal yield**

The effects of climatic variables on cereal yields are investigated through statistical analysis. Due to the complexities in climate dynamics and sometimes nonlinearity in the relationships between cereal yields and climate variables coupled with small samples, a non parametric Spearman rank correlation is used in this research to establish monotonic relationships. Bivariate statistical analysis is used to investigate the degree of association between climatic

indices and cereal yields of maize and sorghum. The Spearman rank correlation  $C_Y$  provided by Kottegoda and Rosso (2008) was applied. The correlation is given by;

$$C_Y = 1 - \frac{6 \sum_{i=1}^n Y_i^2}{n(n^2-1)} \quad (3.61)$$

Where  $Y_i$  is the difference in ranks of the climatic indices and cereal yields under investigation while  $n$  is the length of the time series. The test for significance is accomplished by computing the  $Z$  statistic given by;

$$Z_{\text{stat}} = C_Y \sqrt{\frac{(n-2)}{(1-C_Y^2)}} \quad (3.62)$$

The correlation is considered significant when the  $Z_{\text{stat}}$  value obtained in Equation (3.62) is greater than the critical  $Z$  value obtained from standard normal Table.

The degree of the association between cereal yields and climatic indices such as AI, SPEI, SOI and LRS is determined through correlation analysis. A correlation matrix of different pairs is then built to identify significant associations at 95% confidence level. Even where strong associations exist, projections cannot be made based on these relationships due to the complexity of climatic dynamics. For this reason, ANNs are employed to project cereal yields using climatic indices as predictors.

### **3.3.6 Modeling climate dynamics and cereal yields using artificial neural network**

Neural networks comprises of inter linkages of process nodes that enable learning of input and output processes (Rajasekaran et al., 2011; Masinde, 2014; Byakatonda et al., 2016). To develop future dynamic situations, the NARX model is utilised. The NARX model is a class of recurrent neural network (RNN) equipped with tapped delay lines that provides additional dynamic memory to aid learning of complex nonlinear multivariate processes. The network comprises of the input and output regressor with feedback connectors from the output layer for

better learning and eventual generation of dynamic patterns of the target output. The NARX model construction process and prediction criteria can be summarised in the following steps:

1. Data preprocessing by standardising both input and target series using the Mapminmax option
2. Building the network in form of exogenous input nodes and autoregressive target nodes.
3. Choosing the number of hidden layers that can adequately learn the input-target relationships.
4. Training of the network in an open loop mode using Levenberg-Marquardt optimization function with termination based on multi criteria including performance, gradient and number of epoch.
5. Prediction is then conducted in the closed loop mode and its performance evaluated through coefficient of correlation (r) and mean square error (MSE) between model outputs and target series.

### **3.3.6.1 Data preprocessing**

In an effort to optimise predictions, time series of target and input predictors are inspected for consistency. The exogenous inputs are selected based on the fact that they are known factors that can externally affect the outcome of the target series (Huang et al., 2006; Diaconescu, 2008). The target series is the autoregressive component of the model.

The selected data are then rescaled to a standardised range between -1 and 1 for easier learning of the network. This is achieved through the Mapminmax function in the ANN toolbox through the following Equation by Morid et al. (2007) and applied in Masinde (2014);

$$X_p = C_{\min} + \frac{(X_t - X_{t\min})}{(X_{t\max} - X_{t\min})} \cdot (C_{\max} - C_{\min}) \quad (3.63)$$

Where,  $X_p$  is the rescaled data series,  $X_t$  is the original series,  $C_{\min} \geq -1$  and  $C_{\max} \leq 1$ ,  $X_{\min}$  minimum value of  $X_t$  series and  $X_{\max}$  is maximum value of  $X_t$  series.

### 3.3.6.2 NARX construction, training and learning

The NARX model consists of input, one hidden and output layers with two tapped delay elements originating from input and output regressors. Hidden layer neurons are chosen based on various network combinations with the final number following the procedure proposed by Hecht-Nielsen (1987), applied in Maier and Dandy (2001), Stathakis (2009) and Byakatonda et al. (2016) which states that  $H_L \leq 2X_p + 1$  where  $H_L$  are the number of neurons in the hidden layer and  $X_p$  number of predictors. This dynamic recurrent neural network with feed forward back propagation utilises a sigmoid transfer function in the hidden layer and a linear transfer function in the output layer. The Levenberg-Marquardt optimisation function is used to update the weights and bias values during the training mode. This function keeps to minimum the squared errors and weights while the right combination that generalises well the network is being generated (Demuth et al., 2009; Byakatonda et al., 2016). Different training algorithms are used and the one adopted in this research (Levenberg-Marquardt) gives the best performances with the lowest Mean Squared Error (MSE) and highest regression coefficient between the model outputs and actual targets.

The model topology is presented in Figure 3-3. The recurrent connections from the outputs may delay a number of unit times to form new inputs. The nonlinear system for n-steps predictions ( $n \geq 1$ ) can be represented mathematically as;

$$\hat{y}(t+n) = f\left\{[X_1(t+n-1), \dots, X_1(t+n-d); X_2(t+n-1), \dots, X_2(t+n-d) \dots; \dots X_p(t+n-1), \dots, X_p(t+n-d)]; [\hat{y}(t+n-1), \dots, \hat{y}(t+n-d)]\right\} \quad (3.64)$$

Where  $d$  is the input and output delay (memory orders)  $\geq 1$ ,  $p$  is the number of predictors available at the input regressor.  $y(t+n)$  is output value at  $(t+n)$  time step,  $\hat{y}$  are estimated target series,  $X_p(t)$  input vector with  $p$  arrays where  $p = 1, 2, 3, \dots$  Whereas  $f(\cdot)$  is a nonlinear mapping



function that is approximated by the learning algorithm. The network has two regressors; the regressor  $y(t+n-d)$  acts as an autoregressive model while  $X_p(t+n-d)$  is the implicit exogenous variable in the time series. In this model, the target series are predicted using their past values to generate future values. Their prediction is assisted by exogenous inputs  $X_p(t+n-d)$  which are external predictors that influence the outcome of the target series.

Training of the network and its application in prediction is achieved in two ways. The training mode is the series-parallel connection (Open loop), where the outputs regressor at the input layer is comprised of only actual values of target series and the network only makes a one-step ahead prediction. In the training mode, Equation 3.64 is modified as;

$$\hat{y}(t+1) = f\{[X_1(t), \dots, X_1(t+1-d); X_2(t), \dots, X_2(t+1-d) \dots; \dots X_p(t), \dots, X_p(t+1-d)]; [y(t), \dots, y(t+1-d)]\} \quad (3.65)$$

Where  $y(t)$  are actual measured target values at the output's regressor.

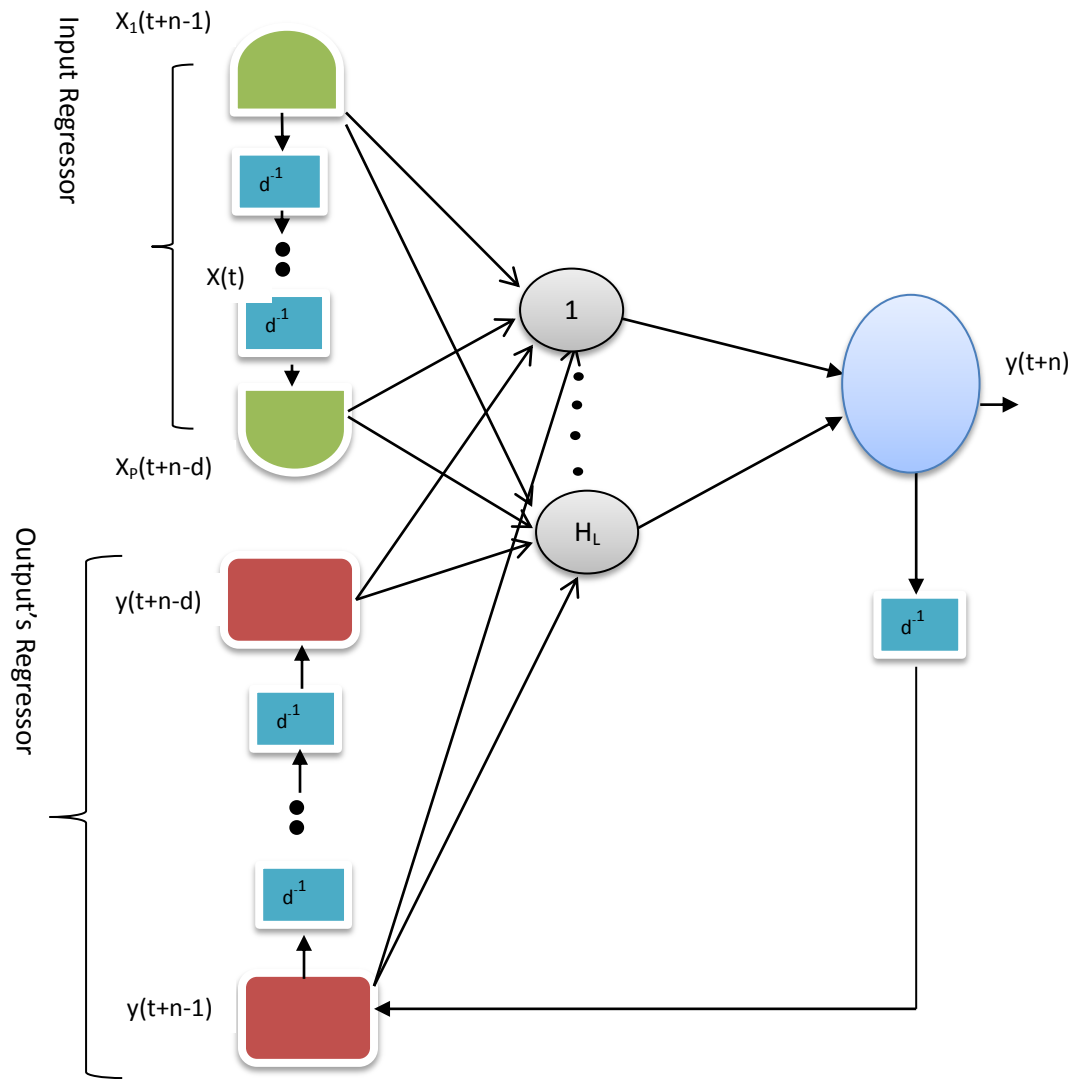


**Fig. 3-3.** Nonlinear auto regressive with exogenous input (NARX) ANN architecture

### 3.3.6.3 NARX prediction and performance criteria

In a multistep prediction mode, the parallel mode (Closed loop) is used. In this mode, the estimated outputs are fed back to the output's regressor as presented mathematically in (3.64). When the network is in the prediction mode, the input and target time series are divided into two groups. The first group is without the most recent time series data whose length is equivalent to the prediction horizon. For input series  $X_p(t)(1,2,3,\dots,M) \in X$  and  $M$  is the total number of data series, the length of the first group is considered as  $(M-n)$  used in training and testing the network. This arrangement allows the model to learn the input-output relationship without recorded data. The second group of input dataset is equivalent to  $n$  most recent

historical values used for simulation of the model and generating of new target series, whereas the actual target series is responsible for validation of the predicted values. In this research 5 years prediction of standardised flow index, cereal yields, onset and cessation of rain for 2017 to 2022 are made.

Model performance is evaluated based on errors from training, validation, and testing phases. In this research, the Mean Squared Error (MSE) and correlation coefficient (r) between the targets and model outputs (Diaconescu, 2008; Chang et al., 2014; Chang et al., 2015) are used in the evaluation as follows:

$$\text{MSE} = \frac{1}{n} \sum_{i=1}^n e_i^2 = \frac{1}{n} \sum_{i=1}^n (y_i - \hat{y}_i)^2 \quad (3.66)$$

$$r_{y\hat{y}} = \frac{\sum_{i=1}^n (y_i - \bar{y}_i)(\hat{y}_i - \bar{\hat{y}}_i)}{\sqrt{\sum_{i=1}^n (y_i - \bar{y}_i)^2} \sqrt{\sum_{i=1}^n (\hat{y}_i - \bar{\hat{y}}_i)^2}} \quad (3.67)$$

Where  $y_i$  and  $\hat{y}_i$  are the observed and model outputs respectively and  $n$  is the prediction horizon.  $\bar{y}_i$  and  $\bar{\hat{y}}_i$  are average values of observed and model outputs respectively.

## **CHAPTER-4**

### **4. ANALYSIS AND DISCUSSION OF RESULTS**

#### **4.1 GENERAL INTRODUCTION**

This Chapter presents results, their analysis and discussion following the methodology developed in Chapter 3. These results emanate from analysis of hydroclimatological variables and their relationship with maize and sorghum crop yields in Botswana. The chapter is comprised of 6 subsections corresponding to each specific objective in chapter 1. The chapter begins with results from explanatory data analysis which included homogeneity testing and trend analysis. After the climatic trends in meteorological variables were established, it was necessary to establish further rainfall characteristics in form of onset and cessation of rain together with dry spell frequency analysis. This analysis is pivotal to this research since it reveals the effects of climate variability on agricultural production. These results are presented in subsections 4.2 and 4.3. From objective 3, two subsections were derived with 4.4 presenting the relationship between drought severity and ENSO while subsection 4.5 presents propagation of climatological drought to hydrological drought. Under these subsections a common timescale for drought monitoring is presented. Subsection 4.6 presents the influence of climate variability expressed through climatic indices on crop yields of maize and sorghum. The last subsection 4.7 deals with modelling of climatic indices and crop yields for purposes of identifying their future behaviour to facilitate planning and management of water and agricultural resources.

#### **4.2 CLIMATIC TRENDS AND ABRUPT CHANGES IN METEOROLOGICAL TIME SERIES**

Establishment of long term climatic trends is one measure towards development of climate change adaptation strategies. This chapter presents results from analysis of rainfall, minimum and maximum temperature time series. Results from the four absolute homogeneity tests

(Standard normal homogeneity test, Pettit test, Buishand range test and Von Neumann ratio test), trend analysis test, tests for persistence and influence of ENSO on local climate are presented in this section.

#### 4.2.1 Tests for homogeneity

Data used in climate change studies are necessary to be homogeneous to ensure that any climatic changes observed are as a result of natural occurrence. This subsection presents results from temporal homogeneity analysis of climatic data used in this study.

##### 4.2.1.1 Annual rainfall time series

Table 4-1 presents homogeneity tests results on annual rainfall totals for the stations in the study area. The p-values are compared with a critical value  $\alpha$  at 1% level of significance ( $\alpha = 0.01$ ). The results reveal that all the stations in the study area are homogeneous and hence classified as ‘useful’ for further trend and variability analysis.

**Table 4-1.** P-Values from four homogeneity tests on rainfall time series

Station	Pettitt's test	SNHT	BHD's test	von's test	Classification
	p-value	p-value	p-value	p-value	
Francistown	0.562	0.722	0.870	0.800	Useful
Ghanzi	0.237	0.586	0.904	0.852	Useful
Jwaneng	0.158	0.017	0.078	0.055	Useful
Kasane	0.097	0.040	0.068	0.269	Useful
Letlhakane	0.550	0.512	0.422	0.436	Useful
Mahalapye	0.698	0.650	0.602	0.253	Useful
Maun	0.548	0.222	0.106	0.836	Useful
Pandamatenga	0.045	0.204	0.058	0.352	Useful
Selibe-Phikwe	0.480	0.436	0.548	0.140	Useful
Shakawe	0.822	0.837	0.610	0.846	Useful
SSKA	0.330	0.116	0.194	0.419	Useful
Sowa Pan	0.166	0.919	0.749	0.502	Useful
Tsabong	0.119	0.953	0.793	0.112	Useful
Tshane	0.877	0.869	0.637	0.571	Useful

$\alpha = 0.01$

#### 4.2.1.2 Maximum temperature time series

P-values from homogeneity tests on maximum temperature series are presented in Table 4-2. Results reveal that majority of the stations are homogenous except for three stations that failed three out of the four tests and hence classified as 'suspect'. These stations are Francistown, in the east, Maun in the north and Shakawe in the northwest of Botswana. At Francistown and Maun, the suspected year of intervention is 1980/81 for all the absolute tests.

**Table 4-2.** P-Values from four homogeneity tests and probable year of intervention for maximum temperature

Station	Pettitt's test		SNHT		BHD's test		von's test	Classification
	p-value	Year	p-value	Year	p-value	Year	p-value	
Francistown	0.000*	1980/81	0.0003*	1980/81	0.000	1980/81	0.002*	Suspect
Ghanzi	0.074	Homo	0.070	Homo	0.024	Homo	0.202	Useful
Jwaneng	0.450	Homo	0.029	Homo	0.144	Homo	0.044	Useful
Kasane	0.187	Homo	0.104	Homo	0.064	Homo	0.181	Useful
Letlhakane	0.197	Homo	0.660	Homo	0.858	Homo	0.43	Useful
Mahalapye	0.086	Homo	0.011	Homo	0.032	Homo	0.110	Useful
Maun	0.000*	1980/81	0.000*	1980/81	0.000*	1980/81	0.024	Suspect
Pandamatenga	0.650	Homo	0.248	Homo	0.701	Homo	0.408	Useful
Selibe-Phikwe	0.420	Homo	0.320	Homo	0.657	Homo	0.404	Useful
Shakawe	0.000*	1985/86	0.000*	1980/81	0.000*	1988/89	0.000*	Suspect
SSKA	0.986	Homo	0.430	Homo	0.397	Homo	0.099	Useful
Sowa Pan	0.289	Homo	0.978	Homo	0.980	Homo	0.417	Useful
Tsabong	0.129	Homo	0.182	Homo	0.072	Homo	0.397	Useful
Tshane	0.148	Homo	0.091	Homo	0.037	Homo	0.280	Useful

$\alpha = 0.01$ , Homo=Homogeneous

#### 4.2.1.3 Minimum temperature time series

Results from tests of homogeneity in minimum temperature are presented in Table 4-3. It can be observed that, at 43% of the stations minimum temperature series are homogeneous. However at Letlhakane and Shakawe the minimum temperature series failed in two of the tests and hence classified as 'doubtful'. The change years reported at these stations were 2000/01 and 1990/91 respectively. Similarly 43% of the stations failed in at least three of the tests and are classified as suspect. These stations are Ghanzi with a change year of 1984/85, Kasane with

a change in 1992/93 and Mahalapye in 1981/82. The Other stations are Maun in 1983/84, Tsabong in 1996/97 and Tshane in 1988/89.

**Table 4-3.** P-Values from four homogeneity tests and probable year of intervention for minimum temperature

Station	Pettitt's test		SNHT		BHD's test		von's test	Classification
	p-value	Change year	p-value	Change year	p-value	Change year	p-value	
Francistown	0.268	Homo	0.094	Homo	0.042	Homo	0.000*	Useful
Ghanzi	0.000*	1984/85	0.047	Homo	0.001*	1984/85	0.006*	Suspect
Jwaneng	0.412	Homo	0.208	Homo	0.218	Homo	0.011	Useful
Kasane	0.000*	1991/92	0.000*	1991/92	0.000*	1991/92	0.000*	Suspect
Letlhakane	0.013	Homo	0.110	Homo	0.007*	2000/01	0.006*	Doubtful
Mahalapye	0.001*	1981/82	0.000*	1981/82	0.000*	1981/82	0.000*	Suspect
Maun	0.000*	1991/92	0.000*	1983/84	0.000*	1991/92	0.000*	Suspect
Pandamatenga	0.534	Homo	0.126	Homo	0.072	Homo	0.266	Useful
Selibe-Phikwe	0.507	Homo	0.214	Homo	0.366	Homo	0.041	Useful
Shakawe	0.020	Homo	0.016	Homo	0.004*	1990/91	0.001*	Doubtful
SSKA	0.912	Homo	0.052	1986/87	0.429	Homo	0.127	Useful
Sowa Pan	0.060	Homo	0.019	Homo	0.058	Homo	0.019	Useful
Tsabong	0.000*	1996/97	0.000*	1997/98	0.000*	1996/97	0.000*	Suspect
Tshane	0.000*	1990/91	0.000*	1988/89	0.000*	1988/89	0.000*	Suspect

$\alpha = 0.01$ , Homo=Homogeneous

The four absolute homogeneity tests demonstrated their ability in detecting inconsistencies and breaks in meteorological time series. The results from these tests have enabled categorisation of meteorological stations as 'useful', 'doubtful' and 'suspect'. This is particularly helpful for future climatic studies over the region as station classified as suspect may be excluded from further trend analysis. Results indicated that rainfall time series are fully homogenous. Similarly 78.6% of the stations for maximum temperature and 43% for minimum temperature time series were found homogeneous. These results of homogenous rainfall series are consistent with findings of Wijngaard et al. (2003) and Hänsel et al. (2016) who indicated difficulties in identifying breaks in rainfall time series with high variability which is the case for semiarid climates (Modarres and da Silva, 2007). It was easier to detect breaks in temperature time series due to their lower variability as compared to rainfall series. However in absence of metadata, it was difficult to conclusively state if the reported interventions or lack

of is as a result of climatic changes or nonhomogeneities in the time series. For the foregoing reason, it was not possible to discard any station but consciously examined the data prior and after the suspected year of intervention. In those stations classified as ‘suspect’, only those series after the intervention were used in trend analysis.

El Niño years of 1986/87, 1991/92, 1997/98 and 2004/05 at the same time La Niña years of 1983/84 and 1984/85, were also identified as years of intervention in the temperature time series. This revelation may further strengthen the assertion that inter annual variability over southern Africa is influenced by ENSO activities in the Equatorial Pacific that has been reported in Nicholson et al. (2001), Usman and Reason (2004) and Edossa et al. (2014). The rest of the intervention years are either immediately before or after a given El Niño or La Niña event.

#### **4.2.2 Mann-Kendall (MK) trend analysis and percentage change**

As discussed in Chapter 2, more than one statistical test is required for trend detection. In this research, the MK test and Sen’s slope estimator was used. After the classification of the stations from the homogeneity tests, for stations that were denoted as suspect, only data after the indicated year of intervention has been used in the trend analysis. Results for the Trend statistics are presented for rainfall, maximum and minimum temperature in Tables 4-4, 4-5 and 4-6.

##### **4.2.2.1 Rainfall trends and percentage changes**

###### *Trends in Annual rainfall*

Results from the MK trends and Sen’s Slope estimator have been presented in Table 4-4. Both increasing and decreasing trends are experienced over the study area with significantly decreasing trends ( $\alpha=0.05$ ) registered at Kasane and Pandamatenga all located in the northeast. Increasing trends are only observed at Francistown and Ghanzi though not significant. The highest percentage reduction in rainfall during the study period was 41% at Pandamatenga.



86% of the stations recorded decreasing trends in annual rainfall totals. The regionalised annual percentage change over the study area indicates a 14.6% decrease in rainfall. This demonstrates an overall rainfall decrease across the study area during the period of analysis.

**Table 4-4.** MK trend and Sen's Slope estimator results for rainfall

Station	Rainfall-Annual				Period of trend analysis
	p-value	MK-Z	Sen-S	%change	
Francistown	0.53	0.63	0.74	8.67	1960/61-2015/16
Ghanzi	0.90	0.12	0.16	2.03	1960/61-2015/16
Jwaneng	0.24	-1.17	-4.43	-29.19	1988/89-2015/16
Kasane	0.02*	-2.37	-3.63	-29.30	1968/69-2015/16
Letlhakane	0.25	-1.16	-4.10	-24.49	1993/94-2015/16
Mahalapye	0.93	-0.09	-0.14	-1.80	1960/61-2015/16
Maun	0.53	-0.63	-0.87	-10.76	1960/61-2015/16
Pandamatenga	0.04*	-2.05	-11.30	-40.67	1998/99-2015/16
Selibe-Phikwe	0.50	-0.68	-3.45	-16.40	1998/99-2015/16
Shakawe	0.35	-0.94	-1.17	-12.71	1960/61-2015/16
SSKA	0.31	-1.02	-3.39	-22.36	1985/86-2015/16
Sowa Pan	0.86	-0.17	-1.40	-7.52	1992/93-2015/16
Tsabong	0.86	-0.18	-0.26	-4.78	1960/61-2015/16
Tshane	0.37	-0.89	-1.01	-16.50	1960/61-2015/16

$\alpha = 0.05$ , \* Significant trends

Spatial distribution of annual rainfall presented in Figure 4-1 show decreasing trends in the north, central and southern locations with a northeast to south decreasing gradient. There is marginally increasing trends in the east at Francistown.

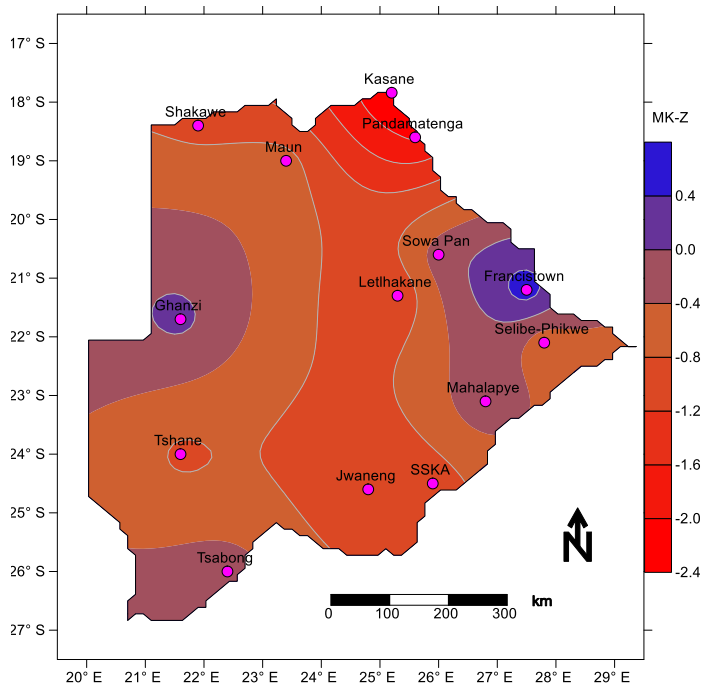


**Fig. 4-1.** Annual rainfall MK-Z trends

Results have indicated decreasing trends in annual rainfall across the study area. Declining rainfall totals could pose a threat to Botswana's water and agricultural resources. This is envisaged because most of the negative trends are reported in Shakawe, Maun and Kasane located in the Okavango basin, a Ramsar heritage site that moderates local climate (Byakatonda et al., 2016). The other locations SSKA, and Selibe-Phikwe lies in the Limpopo basin that hosts majority of surface dams that supplies most of the water needs for both industrial and irrigation. Further still Kasane and Pandamatenga which also showed significantly decreasing trends hosts most of the commercial farms responsible for domestic food supply. Spatial trends in rainfall indicate decreasing amounts from northeast at Kasane to central around Lethakane progressing southward to SSKA. Overall there is a regionalised decrease in rainfall amounts over the study area of 14.7%.

#### **4.2.2.2 Trends in maximum temperature and percentage changes**

Results showing trends in maximum temperature are presented in Table 4-5. Results from annual maximum temperature time series show decreasing trends at some locations such as

Kasane, Lethakane and SSKA. None of the identified decreasing trends were significant at  $\alpha = 0.05$  with the highest percentage decrease of 1.8% recorded at Kasane. At 86% of the stations, increasing trends were recorded with significant trends at Mahalapye and a percentage increase of 4.4%. Regionalised trends indicate that annual maximum temperature has increased by 1.2% over the period of analysis.

**Table 4-5.** MK trend and Sen's Slope estimator results for maximum temperature

Station	p-value	MK-Z	Sen-S	%change	Period of trend analysis
Francistown	0.13	1.53	0.02	2.34	1980/81-2015/16
Ghanzi	0.07	1.80	0.01	2.26	1961/62-2015/16
Jwaneng	0.11	1.58	0.02	2.29	1989/90-2015/16
Kasane	0.19	-1.32	-0.02	-1.82	1983/84-2015/16
Lethakane	0.59	-0.54	-0.01	-0.88	1994/95-2015/16
Mahalapye	0.01*	2.64	0.03	4.44	1971/72-2015/16
Maun	0.99	0.01	0.00	0.06	1980/81-2015/16
Pandamatenga	0.23	1.21	0.04	2.62	1998/99-2015/16
Selibe-Phikwe	0.56	0.59	0.03	1.60	2000/01-2015/16
Shakawe	1.00	0.00	0.00	0.21	1988/89-2015/16
SSKA	0.56	-0.58	-0.01	-1.46	1985/86-2015/16
Sowa Pan	0.41	0.82	0.02	1.45	1992/93-2015/16
Tsabong	0.06	1.91	0.01	2.23	1961/62-2015/16
Tshane	0.09	1.69	0.01	1.85	1961/62-2015/16

$\alpha = 0.05$ , \* Significant trends

Spatial analysis in Figure 4-2 indicates that, western locations progressing to southwest are experiencing warming trends. Cooling trends are observed in the northeast, central and south around SSKA. A northeast to southwest warming gradient is evident from the spatial patterns.

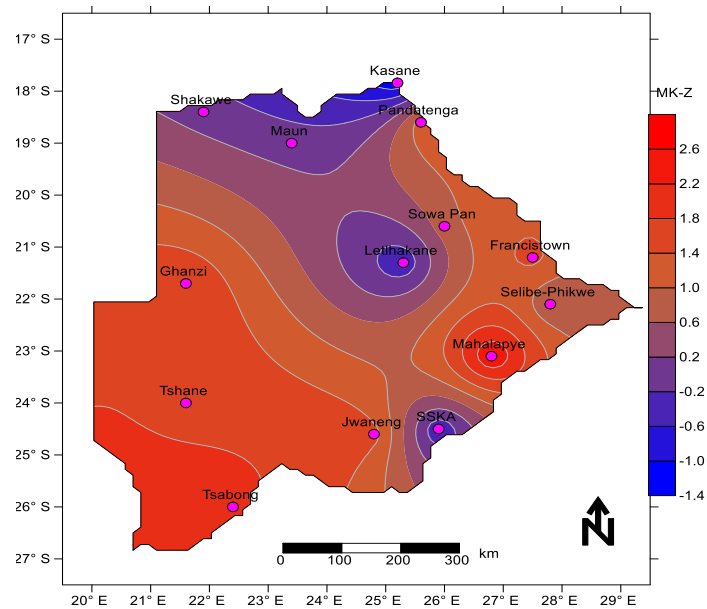


**Fig. 4-2.** Maximum temperature MK-Z trends

Annual trends indicate that locations bordering Kalahari Desert such as Shakawe, Ghanzi, Tshane and Tsabong are experiencing warming trends. This could be evidence of increasing desertification. The northern locations of Maun, Kasane and Pandamatenga are showing cooling trends which could favor agricultural activities in these locations due to reduced evapotranspiration rates. Mahalapye in the Limpopo basin is experiencing significantly warming trends which could increase the atmospheric evaporative demand hence affecting surface water storage. Overall there is a regionalised increase in maximum temperature of 1.2%.

#### **4.2.2.3 Trends in minimum temperature and percentage changes**

Results from investigations of long term trends in annual minimum temperature are presented in Table 4-6. Similarly both increasing and decreasing trends are reported in minimum temperature time series at annual scale over the study area. Decreasing trends are observed at Kasane, Mahalapye, Shakawe and SSKA though none is significant. The highest decrease of 4.4% is recorded at Shakawe. 71.4% of the stations recorded increasing trends with significant trends registered at Ghanzi, Maun, Sowa Pan and Tsabong. The highest increase of 9.6% is

recorded at Tsabong. Regionalised trend indicate an overall increase in annual minimum temperature of 2.0% across the study area during the period of analysis.

**Table 4-6.** MK trend and Sen’s Slope estimator results for minimum temperature

Station	p-value	Z	Sen S	%change	Period of trend analysis
Francistown	0.76	0.30	0.00	0.64	1960/61-2015/16
Ghanzi	0.03*	2.22	0.02	5.38	1984/85-2015/16
Jwaneng	1.00	0.00	0.00	-0.08	1989/90-2015/16
Kasane	0.59	-0.54	-0.01	-1.90	1991/92-2015/16
Letlhakane	0.08	1.75	0.04	5.34	1994/95-2015/16
Mahalapye	0.17	-1.38	-0.02	-4.14	1981/82-2015/16
Maun	0.03*	2.15	0.03	5.29	1991/92-2015/16
Pandamatenga	0.36	0.91	0.02	2.55	1998/99-2015/16
Selibe-Phikwe	0.32	0.99	0.03	3.22	2000/01-2015/16
Shakawe	0.09	-1.68	-0.01	-4.35	1965/66-2015/16
SSKA	0.48	-0.71	-0.01	-2.87	1985/86-2013/14
Sowa Pan	0.00*	3.20	0.05	8.63	1992/93-2015/16
Tsabong	0.01*	2.45	0.06	9.59	1997/98-2015/16
Tshane	0.79	0.26	0.01	1.15	1990/91-2015/16

$\alpha = 0.05$ , \* Significant trends

Spatial presentation in Figure 4-3 indicates warming trends across the study area except for locations in the northeast and northwest. Southeastern locations of SSKA, Jwaneng and Mahalapye are also showing cooling tendencies. Central, east to west and southwest are showing increasing trends in minimum temperature. There are warming gradients observed at three fronts, a gradient is observed from southeast towards the west. Another gradient originates from the northeast progresses southwards to the west. The final gradient originates from the north progressing southwest.

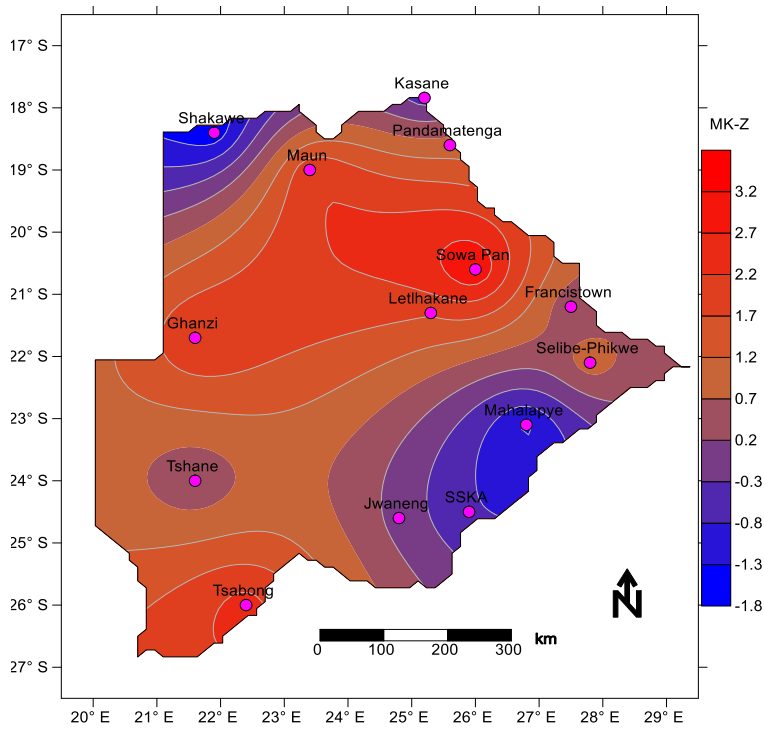


**Fig. 4-3.** Minimum temperature MK-Z trends

Minimum temperature patterns showed decreasing trends in the northern locations. Locations near the Kalahari desert progressing to central through to northeast at Pandamatenga are all experiencing warming trends. There is a generally warming climate over the study area with a change of 2.0%. Warming gradients are predominantly inclined towards the Kalahari Desert. These warming trends could be an indicator that effects of global warming reported in Pachauri and Reisinger (2008) and Stocker et al. (2013) are already being felt across the study area.

#### **4.2.3 Detection of serial correlation in meteorological variables**

As indicated in Chapter 3, meteorological time series that are serially correlated may record significant trend even when there is no trend. In view of this, it was therefore necessary to test for any effect of serial correlation for all the three meteorological variables used in this research such that any dataset with significant serial correlation can then be corrected. Results from tests for persistence in meteorological variables are presented in this subsection. At all stations, it was observed that, rainfall series were serially independent and random at 95%

confidence level. Positive correlations are observed at Jwaneng, Mahalapye, Selibe-Phikwe and Tsabong as shown in Figure 4-4. For maximum temperature, positive serial correlations were predominant with only Pandamatenga and Selibe-Phikwe showing negative correlations. Most stations showed non significant lag-1 correlations in maximum temperature except at Shakawe as shown in Figure 4-5a. Minimum temperature recorded positive correlations at all stations except Pandamatenga. Most of the lag-1 correlations were significant at 95% confidence level except for Pandamatenga, Selibe-Phikwe, Jwaneng, Ghanzi and Sowa Pan. The distribution of these stations along with their respective lag-1 serial correlation coefficient have been shown in Figure 4-5b.

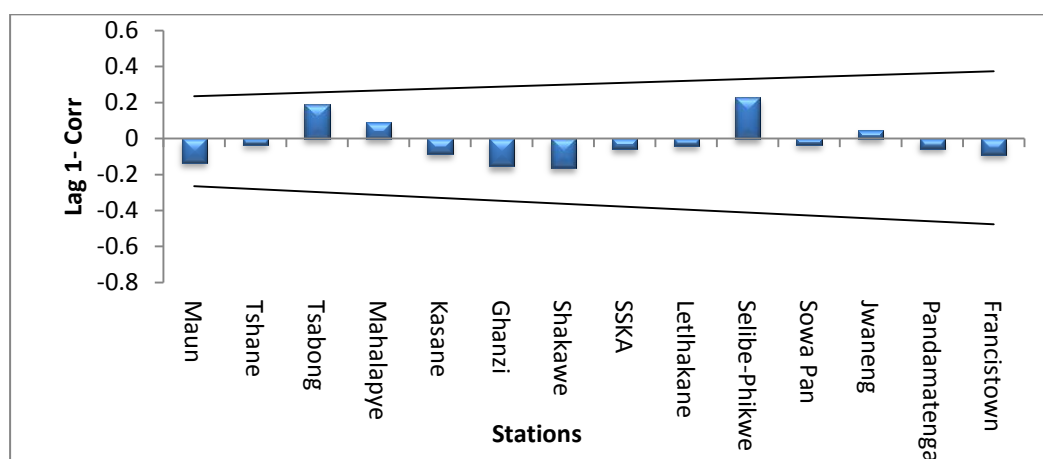


**Fig. 4-4.** Serial correlation effect on annual rainfall time series

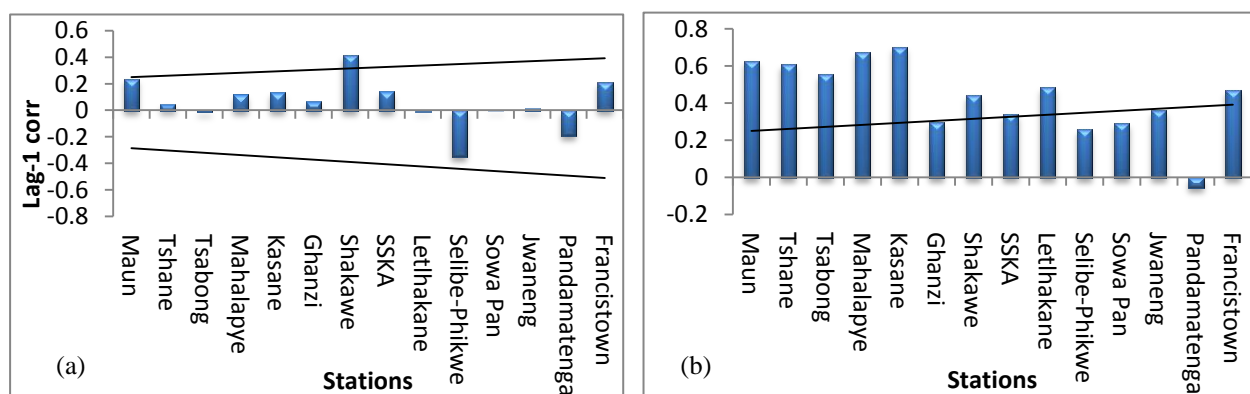


**Fig. 4-5.** Serial correlation effect on annual (a) Maximum (b) Minimum temperature series

Rainfall time series which were reported to be homogenous also appears to be independent. The maximum temperature series are also independent except at Shakawe. Minimum

temperature shows a number of stations with significantly dependent time series. The distribution of the stations in the study area has no specific spatial pattern. Those stations whose series were found not independent, the effective sample size technique was applied to adjust the Z-statistic obtained from the MK trend analysis.

#### **4.2.4 Influence of ENSO on local climatic variables**

Previous studies have shown that southern Africa's climate is influenced by ENSO, this subsection attempts to quantify the degree of association between local climate of the study area and ENSO. The analysis showed that positive correlations resulted from analysis of rainfall and southern oscillation index (SOI) for annual time series. Significant correlations at annual scale were recorded at 50% of the stations. Correlations between rainfall and sea surface temperatures (SSTs) were negative. Significant negative correlations are reported in 43% of the stations. Correlations between maximum temperature and SOI were negative at all the stations used in this study with 86% of the stations recording significant correlations. Correlations between maximum temperature and SSTs returned positive correlations. Significant correlations are registered at 78.5% of the stations.

Correlations between minimum temperature and SOI over the study area reveal weakly negative associations at annual time scale. The annual minimum temperature associations with SOI are significant at Francistown, Jwaneng and Mahalapye. Investigations of association between minimum temperature and SSTs reveal significant association at 36% of the stations



at annual scale. Distribution of stations with significant correlations is presented in Figure 4-6.

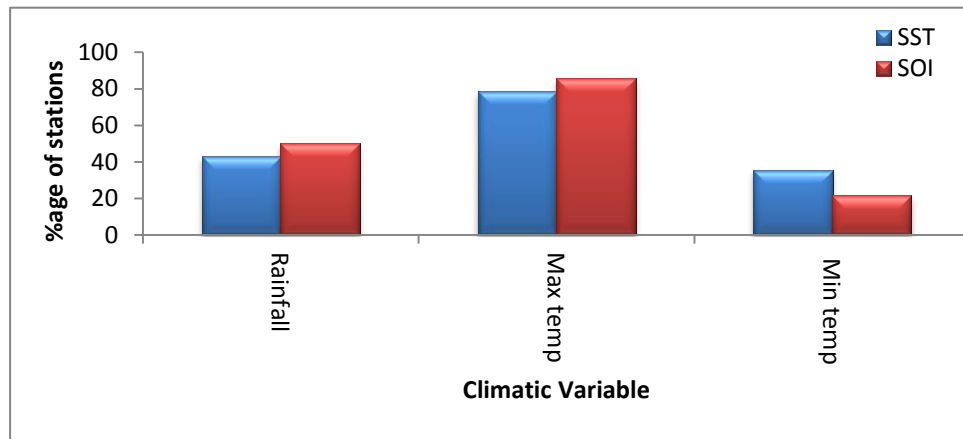


**Fig. 4-6.** Proportions of stations with significant correlation between ENSO and local climatic variables

To further illustrate the influence of ENSO on the local climate, relationships between maximum temperature anomalies and SST from Nino 3.4 are presented in Figure 4-7 for Mahalapye. The relations are found to be strongest particularly during the years of 1972/73, 1982/83, 1997/98, 2007/08 and 2015/16.

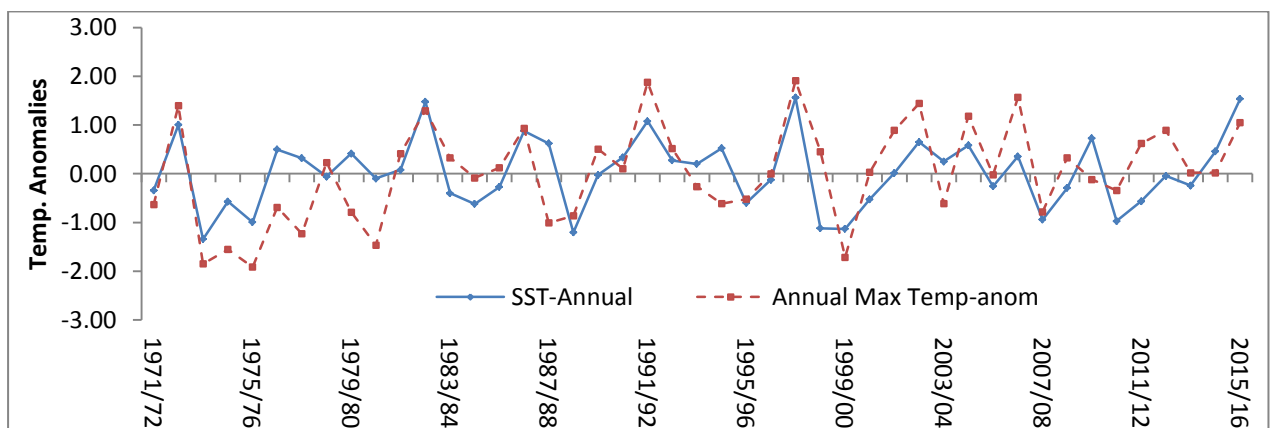


**Fig. 4-7.** Annual maximum temperature normalised at Mahalapye and Nino 3.4 SST time series

Significant positive correlations between rainfall and SOI and negative correlations between rainfall and SSTs demonstrate the association of local rainfall with ENSO events. Earlier studies by Kenabatho et al. (2012) had indicated negative correlations between rainfall and

local temperature. Coupled with highly positive correlations between local temperature and SSTs, it is evident that ENSO events influence rainfall patterns over the study area. Similar studies on the influences of ENSO on local climate in other semiarid environments such as Iran reported similar order of magnitudes in correlations with opposite signs (Nazemosadat et al., 2006; Tabari and Talaei, 2011). This could be attributed to the location of Iran in northern hemisphere as compared to Botswana.

Temperature time series shows negative correlations with SOI and positive with SSTs, a similar association between SSTs and SOI. Correlations were higher with maximum temperature as compared to minimum temperature. This could imply that maximum temperature has more influence on local climate than minimum temperature. In this case maximum temperature can act as a potential indicator of ENSO impacts on local climate.

To further illustrate the close interaction between maximum temperature and ENSO signal, Figure 4-7 indicates that relationship between SSTs and maximum temperature got stronger during El Niño years of 1972/73, 1982/83, 1997/98, 2015/16 and La Niña year of 2007/08. During the El Niño years, positive anomalies which are responsible for droughts conditions over southern Africa are evident. Likewise, during La Niña years negative anomalies are observed on the plot accounting for wet conditions over the region.

#### **4.2.5 Summary**

The monotonic trends and abrupt changes in meteorological time series for a period of 1960-2016 were investigated to ascertain the influence of climate variability and change on local climate. Four absolute homogeneity tests were used to check for possible nonhomogeneities and abrupt changes in the time series. The Mann-Kendall and Sen's Slope estimator were used to detect trends and absolute changes over the period of study. The association of local climatic variables with ENSO was also investigated through multivariate correlation analysis. The following summary is deduced from the study:

1. The rainfall time series were fully homogenous during the study period at all the stations. 78.6% of the stations for maximum temperature and 43% of the stations for minimum temperature were also homogeneous and are classified as 'useful'. Due to absence of metadata, it was not possible to conclude if the presence of homogeneous time series or lack of was as a result of nonhomogeneities or normal climate regime shift. Most of the years of intervention identified also either coincide with El Niño/La Niña or closely followed and at times preceded ENSO episodes.
2. Trends in rainfall indicated a general decrease of 14.7% at annual scale across the study area. Of particular interest, are the drying trends in the Okavango basin at Shakawe, Maun and Kasane. Similar drying trends were also recorded in the Limpopo basin at SSKA and Selibe-Phikwe. These two basins are responsible for the majority of the water resources supply in Botswana. There was a regionalised warming trend in annual maximum temperature of 1.2%. Minimum temperature also reported warming trends of 2.0% in annual series across the study area.
3. The rainfall time series were completely random with only temperature series showing some persistence at some stations. Maximum temperature time series are found to be random except at Shakawe. 57% of the stations showed persistence tendencies in minimum temperature. The effective sample size technique was used to adjust the Z-statistic for the MK trend analysis in stations with persistence.
4. Positive correlations existed between rainfall and SOI, at the same time rainfall was negatively associated with SSTs. More significant positive associations were identified between SST and maximum temperature. However, close association between local climatic variables and ENSO during El Niño years of 1972/73, 1982/83, 1997/98, 2015/16 and La Niña years of 2007/08 were noticed, indicating that during El Niño years the study area observed high temperatures and rainfall largely suppressed.

### **4.3 ONSET, CESSATION OF RAINFALL AND DRY SPELL FREQUENCY**

#### **ANALYSIS**

In order to understand rainfall behavior over the study area, seasonal characteristics that comprised of average rainfall, rain onset dates, cessation of rain dates, length of the rain season and dry spell frequency were investigated. Also their coefficients of variation (CV) were analysed to understand the degree of their variability. Rainfall characteristics were considered for the summer season (October-April). The selection of this period is premised on the fact that studies by Byakatonda et al. (2018d) have indicated that more than 90% of Botswana's rainfall is experienced during summer season. This is further confirmed in Figure 1-3. Results of the seasonal rainfall characteristics are presented in Table 4-7. Long term changes in these characteristics were also investigated using MK trend test statistic and Sen's Slope estimator, their results are also presented in Table 4-8.

#### **4.3.1 Seasonal rainfall totals**

Results for seasonal rainfall, indicate that the maximum seasonal average rainfall of 540 mm is recorded at Kasane in the northeast. A minimum rainfall of 226 mm is also observed at Tsabong in the southwest of the study area. Seasonal rainfall increases from southwest to northeast. Generally the CV in seasonal rainfall at all stations is greater than 20%. The highest variability of 51% is recorded at Tsabong. The lowest CV of 28% is recorded at Kasane a location with the highest seasonal rainfall. Locations from west to east presented with high CVs of more than 40% as is the case at Ghanzi, Letlhakane, Sowa Pan, Francistown and Maun.

**Table 4-7. Seasonal rainfall characteristics**

Station	Seasonal rainfall (mm)		Rainy days		Onset date		Cessation date		Length of rain season		Dry spell frequency	
	Avg.	CV(%)	Avg.	CV(%)	Avg.	CV(%)	Avg.	CV(%)	Avg.	CV(%)	Avg.	CV(%)
Francistown	404.9	41.9	32	30.3	30-Nov	18.8	9-Mar	13.2	100	34.5	18	19.2
Ghanzi	366.3	44.5	34	27.2	15-Dec	26.7	15-Mar	16.8	90	48.4	17	19.2
Jwaneng	344.5	33.0	34	22.7	15-Dec	22.4	20-Mar	11.9	95	44.5	16	16.1
Kasane	539.1	28.3	46	20.8	2-Dec	12.5	18-Mar	8.7	106	24.2	13	26.5
Letlhakane	342.7	41.2	29	29.3	3-Jan	18.5	17-Mar	12.1	73	37.4	18	14.4
Mahalapye	388.6	38.5	29	30.0	3-Dec	20.8	3-Mar	15.6	90	44.2	18	16.8
Maun	402.7	40.5	37	29.4	17-Dec	15.5	9-Mar	14.0	82	41.8	15	24.6
Pandamatenga	454.6	33.2	39	29.9	1-Dec	15.1	28-Mar	7.8	117	19.2	14	22.0
Selibe-Phikwe	284.6	38.8	24	28.8	11-Dec	29.5	12-Mar	19.3	91	50.3	20	11.9
Shakawe	470.5	38.9	42	26.2	9-Dec	16.5	31-Mar	9.4	112	28.7	14	26.5
SSKA	369.5	39.1	32	24.0	4-Dec	20.9	8-Mar	16.1	95	39.5	19	14.7
Sowa Pan	387.4	45.0	32	34.0	7-Dec	20.5	13-Mar	8.1	96	36.1	17	20.5
Tsabong	226.2	51.1	23	33.9	11-Jan	27.6	25-Feb	22.7	45	55.5	21	16.9
Tshane	273.3	48.6	27	26.0	28-Dec	23.3	23-Feb	22.0	56	59.8	19	14.8

The spatial presentation of seasonal rainfall is shown in Figure 4-8 together with the values of CVs at respective locations. From this presentation, a southwest to northeastern increasing gradient of seasonal rainfall is evident. Locations in the southwest presents with higher CVs compared to northern and eastern areas. The gradients of rainfall totals and their CVs are similar but opposite in direction.

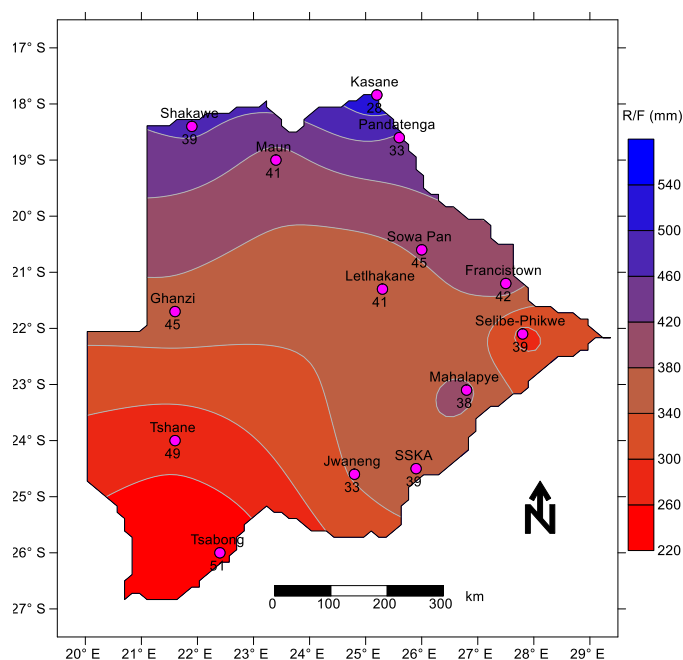


**Fig. 4-8. Seasonal rainfall totals with coefficient of variation at each station**

Results from the MK trend Z-statistic and Sen Slope estimator are presented in Table 4-8. These results indicate a reduction in seasonal rainfall at 78% of the stations though none of them is significant at 95% confidence interval. The highest decrease in trend is recorded at Pandamatenga of 6 mm/season and 4 mm/season at Selibe-Phikwe. The results further reveal that there is an increase in seasonal rainfall at some stations such as Francistown, Kasane and Tsabong though non significant.

The high rainfall areas are situated in the northeast declining towards the northwest with seasonal totals above 450 mm. The southwestern locations receive the lowest of less than 300 mm. This confirms the southwest to northeast rain season progression which was reported earlier by Batisani and Yarnal (2010) while analysing annual rainfall totals from six meteorological stations across Botswana. The agreement in rainfall gradient could be attributed to the fact that 90% of Botswana's annual rainfall is received in austral summer which was also reported in Byakatonda et al. (2018d). High coefficients of variation (30-50%) in seasonal rainfall recorded are a sign of erratic rains rendering rainfed farming a more risky venture across Botswana. This high variability however, are in line with other semiarid locations such as the Mediterranean areas of Iran (Modarres and da Silva, 2007).

The trends generally indicate decreasing rainfall at more than 70% of the stations which agrees with findings of Parida and Moalafhi (2008) who reported trends in the same direction since 1980 over the study area. An IPCC report by Pachauri and Reisinger (2008) projects a reduction in global rainfall but further indicates that this reduction will be more severe in already drier arid and semiarid locations. Interestingly Tsabong which is the driest location shows increasing rainfall trends although not significant. This however could be true in the short term, calling for periodic monitoring of trends in seasonal rainfall to inform policy direction on rain water management.

### **4.3.2 Number of rainy days**

The mean number of rainy days are presented in Table 4-7 with the highest number of rainy days registered over northeast at Kasane of 46 days and 42 days in the northwest at Shakawe. The lowest number of rainy days was recorded at Tsabong of 23 days per season. Their variability indicates high levels exceeding the threshold of 20% as suggested by Nsubuga et al. (2014). The highest variability of 34% is recorded at Sowa Pan and the lowest of 20.8% recorded at Kasane. Results show that locations with higher number of rainy days have lower CVs.

Results from the MK Z-statistic in Table 4-8 indicate that all the stations used in this study are experiencing reducing number in rainy days. Significant reduction is recorded at Ghanzi, Pandamatenga and Shakawe at a rate of 2.2, 2.9 and 3.3 days/season respectively.

The number of rainy days shows lower variability compared to seasonal rainfall totals. This is an indication of more stability in the number of rainy days. From the results, high rainfall areas in the north (Shakawe and Pandamatenga), which are more suitable for rainfed farming are facing significantly decreasing trends in number of rainy days. The rest of the locations are also experiencing decreasing trends though not significant. This revelation may put rainfed farming at more risk across Botswana especially in the north and northeast where majority of the farms are located. Spatial pattern still show progression from southwest to northeast as is the case with seasonal rainfall totals.

### **4.3.3 Onset and cessation of rain dates**

Table 4-7 presents the mean dates for onset and cessation of rain for the 14 synoptic stations. It can be seen that the onset dates in general start from the final week of November and at some stations starts as late as the second week of January, while the cessation dates vary between the last week of February and last week of March. For example, the earliest onset is recorded at Francistown on 30<sup>th</sup>-November and Pandamatenga on 1<sup>st</sup>-December while late dates of onset

have been recorded at Tsabong on 11<sup>th</sup>-January. Similarly, early cessations are recorded on 23<sup>rd</sup> and 25<sup>th</sup>-February at Tshane and Tsabong respectively while Pandamatenga and Shakawe recorded the latest cessation on 28<sup>th</sup> and 31<sup>st</sup>-March respectively. From a further scrutiny of the CVs, stations that recorded early onset mostly showed lower CVs such as 19% and 15% observed at Francistown and Pandamatenga respectively. Stations with late onset generally show high CVs as is the case of Tsabong with CV of 28%. Similarly stations with early cessation such as Tsabong and Tshane showed higher CVs of 23% and 22% respectively. Pandamatenga and Sowa Pan showed the lowest CVs in cessation of 8% at both the stations. At all the stations, onset dates exhibited higher CVs compared to cessation. This can also be evidenced by the fact that onset is spread over three months of November, December and January while cessation dates covers only the months of February and March.

The trends in rain onset dates indicate no major changes except at Jwaneng where onset is significantly getting late at a rate which is slightly more than 2 days/season. The rest of the stations recorded marginal changes with 71% of the stations showing that rain onset dates are getting later. Onset is only getting earlier at Kasane, Maun, Shakawe and Tsabong. Earlier onset tendencies are statistically significant at Tsabong at a rate of 2 days/season. Trends in cessation do indicate that rains at Kasane are significantly getting later at a rate of 2 days/season. The results also do indicate that rains are terminating earlier at 64% of the stations though the trend is not significant. To determine the degree of association between onset and cessation of rain, a Pearson correlation analysis has been undertaken at which seemingly weak negative correlation of  $R=-0.45$  results between these rainfall characteristics.



**Table 4-8.** MK trends Z-statistic and Sen's Slope estimator for rainfall characteristics

Station	Seasonal rainfall (mm)		Rainy days		Onset date		Cessation date		Length of rain season		Dry spell frequency	
	MK-Z	Sen-S	MK-Z	Sen-S	MK-Z	Sen-S	MK-Z	Sen-S	MK-Z	Sen-S	MK-Z	Sen-S
Francistown	1.15	1.306	-0.31	0.000	0.34	0.043	1.42	0.417	0.70	0.238	-0.77	-0.111
Ghanzi	-0.45	-0.650	-2.15*	-0.156	0.60	0.262	0.75	0.320	0.45	0.136	1.71	0.250
Jwaneng	-0.42	-1.756	-0.40	-0.111	2.15*	2.333	-0.96	-0.417	-2.06*	-2.500	0.19	0.050
Kasane	0.05	0.208	-0.16	0.000	-0.40	-0.160	2.00*	0.966	1.94	0.866	-1.58	-0.519
Letlhakane	-0.93	-3.321	-1.92	-0.375	0.56	0.722	-0.14	-0.385	-0.79	-0.846	0.79	0.500
Mahalapye	-1.09	-2.345	-1.79	-0.200	0.45	0.150	-0.38	-0.226	-1.09	-0.517	2.55*	0.473
Maun	-0.10	-0.177	-1.02	-0.125	-1.27	-0.364	-0.18	-0.074	0.46	0.188	0.85	0.176
Pandamatenga	-1.29	-6.054	-2.89*	-1.500	0.15	0.167	-0.27	-0.375	-0.53	-0.600	2.73*	2.222
Selibe-Phikwe	-0.95	-3.800	-0.36	-0.155	0.84	1.875	0.40	1.286	0.40	1.000	-1.04	-0.690
Shakawe	-1.04	-1.654	-3.25*	-0.308	-0.07	-0.027	-1.53	-0.308	-1.19	-0.361	3.37*	0.630
SSKA	-1.12	-2.565	-1.69	-0.280	0.66	0.353	-0.10	-0.133	-0.22	-0.222	1.60	0.462
Sowa Pan	-0.32	-2.001	-0.62	-0.240	0.53	0.750	-0.82	-0.636	-0.66	-0.944	0.72	0.481
Tsabong	0.36	0.264	-1.11	-0.063	-2.09*	-1.113	-1.81	-0.733	1.36	0.273	0.46	0.071
Tshane	-0.71	-0.684	-1.30	-0.060	0.02	0.022	0.50	0.269	0.97	0.200	-0.07	0.000

\*significant trend at 95% confidence level

Spatial representation of onset and cessation of rain trends together with dates are presented in Figure 4-9a and Figure 4-9b. The patterns indicate that onset is earliest in the east to northeast with westerly progression and latest in the southern drier locations. Spatial trends in rain onset dates indicate that in the north, northeast and southwest, the onset of rains is getting earlier. Figure 4-9a further shows that, the central and eastern locations are exhibiting marginal changes in onset dates.

Cessation is earliest in the south with a northerly progression, drier locations bordering the Kalahari desert show early cessation of rains. At most location as shown in Figure 4-9b, rains are terminating earlier except at Kasane in the northeast and Francistown in the east.

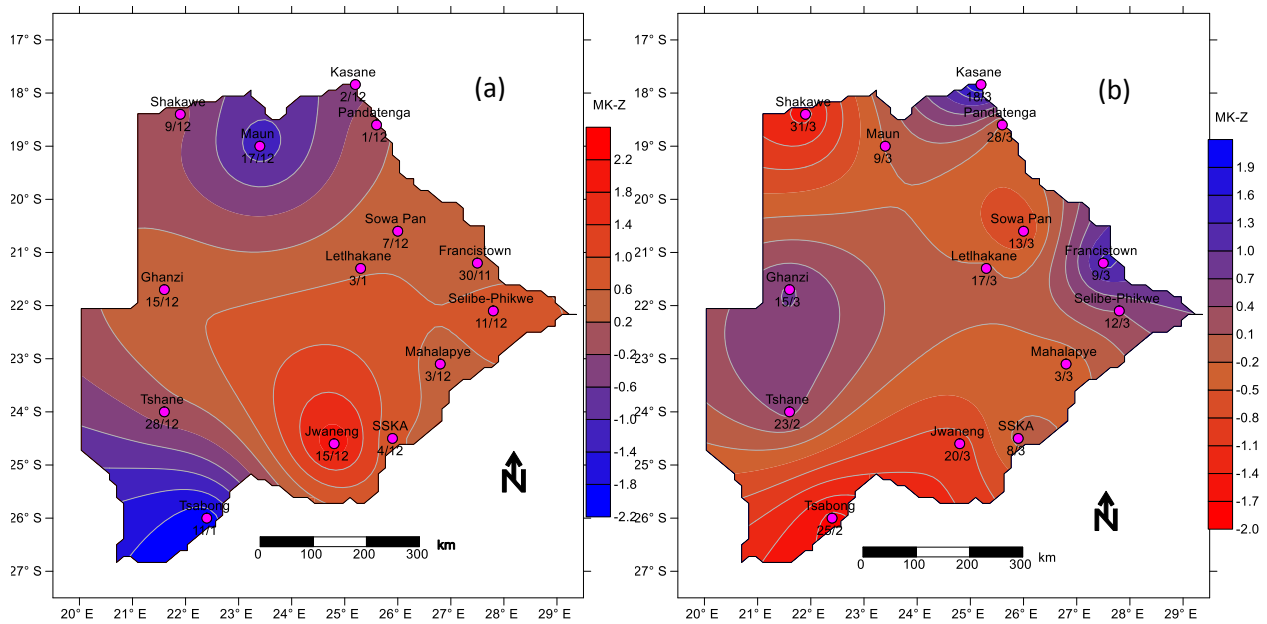


**Fig. 4-9.** MK trends and dates for (a) Rain onset and (b) Rain cessation

Rain onset dates are spread over November through to January while cessation dates covers February to March. The onset dates exhibit higher variability compared to cessation dates pointing to increased risks associated with insufficient and unrealistic moisture at the start of the planting season and for kick starting surface and ground water replenishments. The variability in onset is in agreement with findings of Moeletsi and Walker (2012) who reported a similar scenario in South Africa which is in the same climatic zone as most locations in the study area. Early onset of rain in November in the northeast which is a high rainfall area in Botswana could be associated with the presence of the ITCZ during November in northern Botswana. The ITCZ approaches latitudes of 15-20° S covering northern Botswana in November triggering onset and retreating in March northwards leading to cessation in that month (Usman and Reason, 2004).

Negative correlation between onset and cessation though weak, confirms the inverse relationship between early onset and late cessation of rain over the country. This means that delayed onset of rains weakly brings early cessation of the rains which could shorten the rain season. Therefore onset dates may give an indication of the length of rain season. The

southwestern dry areas manifest with late onset and early cessation of rain. This could be influenced by the weather patterns in the neighbouring Kalahari desert.

#### **4.3.4 Length of the rain season (LRS)**

Mean length of the rain season presented in Table 4-7 indicate that the longest duration of rain is recorded at Pandamatenga in the northeast of 117 days and the least of 45 days at Tsabong southwest of the study area. The eastern to northeastern locations which showed earlier onset dates are experiencing longer rains as compared to the southern locations that have relatively late onset dates. The resulting CVs from the analysis indicate that the length of the rain season is highly variable at locations with short rains such as Tsabong and Tshane with CVs of 56% and 60% respectively. Pandamatenga which has the longest rains shows the lowest CV of 19%.

Trends in the length of rain season (LRS) in Table 4-8 indicate that Jwaneng where rains are getting later is having significant reduction in the LRS at a rate of 2.5 days/season. For purposes of evaluating the effect of onset and cessation on the LRS, Pearson correlation was also used. The results show a strong negative correlation of -0.9 between onset and the LRS. Similarly for cessation of rain and LRS, a strong positive correlation of 0.8 resulted. Spatial presentation in Figure 4-10 indicates progression of the LRS from southwest to east with LRS getting longer in the northeastern areas. Locations such as Tsabong, Tshane and Ghanzi that borders the Kalahari desert and traditionally dry, are showing increasing trends in LRS though not significant. The east to northeastern locations are also showing increasing trends. The central region is generally showing marginal changes. Jwaneng and Mahalapye in the south, Shakawe northwest of the study area shows reduction in LRS.

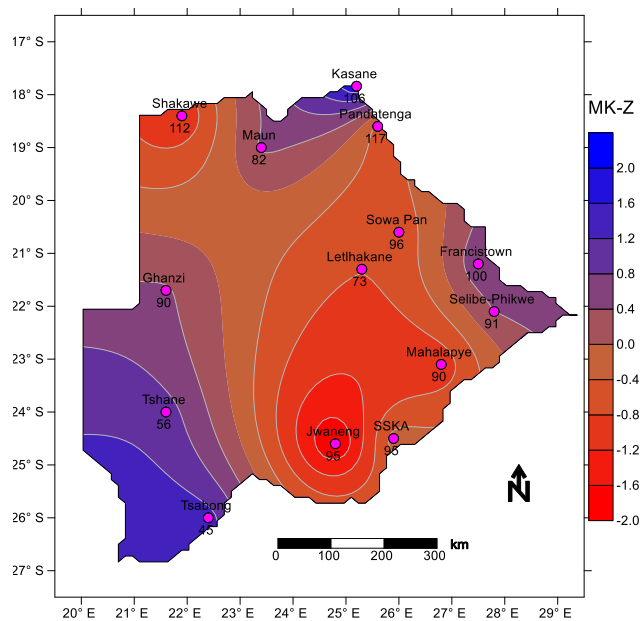


**Fig. 4-10.** Spatial trends of length of rain season (LRS) and values of LRS

The southwestern locations show highly variable LRS signaling high risks to rainfed farming with Tsabong and Tshane posting 45 and 56 days respectively. Spatial analysis shows two progressions in the LRS. The first arm progresses from southwest to north through Ghanzi ending at Shakawe while the second is from southwest to east ending up northeast. Only four locations are identified with LRS of more than 100 days. These locations are Kasane, Pandamatenga, Francistown and Shakawe. Based on the criteria of LRS only, these stations are able to support short to medium season maize varieties as reported by Moeletsi and Walker (2012). In Kenya the medium season varieties are recommended for LRS not exceeding 140 days (Mugalavai et al., 2008). The same variety however may not mature at the same time in different locations due to varying heat flux conditions that affect the phenological processes of maize (Neog et al., 2008; Moeletsi and Walker, 2012).

High negative correlations between LRS and rain onset is an indication that early onset mostly results in long rains. This is in agreement with findings from similar studies in Kenya by Mugalavai et al. (2008) and Ngetich et al. (2014) who found correlations in the same order and direction. The strong degree of association implies that onset date can be used to predict the

LRS and hence the cessation date. The findings could be handy in advising farmers on the correct cultivar at the beginning of the growing season which coincides with rain onset. The high positive association between LRS and cessation is also an indication that late cessation corresponds to a long rain season and vice versa.

#### **4.3.5 Dry spell frequency (DSF) analysis**

Results from dry spell frequency analysis also in Table 4-7 show a high number of dry spells in the southwestern locations of the study area at Tsabong and Tshane of 21 and 19 episodes per season respectively. Pandamatenga and Kasane in the northeast show the lowest episodes of 14 and 13 respectively. Results also indicate that drier locations have lower CVs, an indication that dry spells are more persistent at these locations.

Trends in dry spells in Table 4-8 reveal increase in dry spells at 71% of the locations though only significant at Mahalapye, Pandamatenga and Shakawe. The remaining stations have dry spell frequency trends decreasing though none of them are significant. Spatial representation of the dry spells with their frequency values is shown in Figure 4-11. The map indicates a southwest to northeast decreasing gradient in dry spells, a similar pattern as the length of the rain season and seasonal rainfall totals. From Figure 4-11 the southwest which is already experiencing high DSF are showing decreasing trends though not significant. Similarly, the east to northeast is showing decreasing tendencies in DSF while the central region shows marginal changes in DSF. Mahalapye in the south and Shakawe in the northwest are two locations showing significant increase in DSF. Significantly increasing trends in DSF are mainly observed in the northwest.

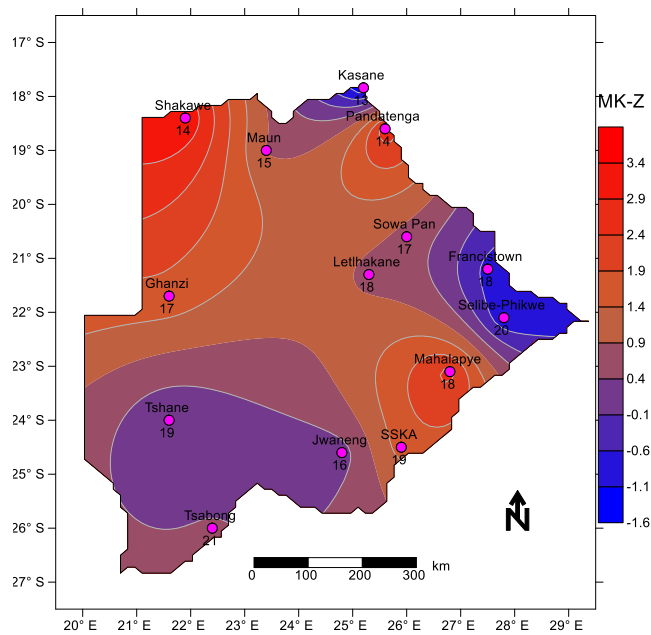


**Fig. 4-11.** Dry spell frequency (DSF) trends (Figures at the stations indicate DSF values) for October-April season

Dry spell analysis is another seasonal characteristic that directly relates to plant water stress. It measures reliability of seasonal rainfall. A season with good rains but higher than average number of dry spells will have plants suffering from water stress and hence poor yields (Usman and Reason, 2004). The low variability in dry spells is an indication that they are a common occurrence in the study area. A normal season for rainfed farming has been defined as one with at most average number of dry spells. A season in the austral summer is then required to have not more than 14 dry spells to be categorised as normal. From the LRS criteria, four stations were identified to be suitable for rainfed farming, combining the LRS criteria and DSF, only Kasane, Pandamatenga and Shakawe are suitable for rainfed agriculture in Botswana.

Trends in dry spell frequency indicate a significant increase at Pandamatenga and Shakawe which is rather a shortcoming in attempts to improve productivity of rainfed farming over the study area. On a positive note, the northern high rainfall locations are still registering the lowest number of dry spells, this could also be influenced by the ITCZ movement over these

locations. The southwestern locations still experience the highest number of dry spell which could be attributed to the fact that the ITCZ has little influence at latitudes greater than 20° S and mainly depend on westerlies for moisture supply (Nicholson et al., 2001; Usman and Reason, 2004).

#### **4.3.6 Summary**

Analysis of seasonal rainfall characteristics that included dry spell frequency, number of rainy days, onset and cessation of rain dates were investigated in this subsection. The variability and trends in these rainfall characteristics were also evaluated. Based on the results and discussions above, the following summary is deduced;

1. Seasonal rainfall totals are highly variable with coefficients of variation ranging between 30% and 50% from northeast to southwest. This high variability is an indicator of erratic seasonal rainfall, making rainfed farming more risky with uncertainties over the study area.
2. Number of rainy days exhibited more stability in their variability as compared to rainfall totals by recording lower coefficients of variation ranging from 20% to 35%. However rainy days showed decreasing trends at all the stations across Botswana with significant reduction at Ghanzi in the west, Pandamatenga and Shakawe situated in the high rainfall region of the north where most rainfed farming is practiced at a commercial scale.
3. The earliest onset was recorded in the east at Francistown on 30<sup>th</sup>-November while the latest on 11<sup>th</sup>-January in the southwest at Tsabong. The earliest cessation on 23<sup>rd</sup> -February was recorded at Tshane and the latest on 31<sup>st</sup> -March occurred at Shakawe. The onset dates were less stable with higher coefficients of variation as compared to cessation dates. This suggests that reliability of the rain season across Botswana is more related to onset of rain rather than cessation. A negative correlation exists between onset and cessation of rain across the study area.

4. The longest rainfall season over the study area was 117 days at Pandamatenga and shortest of 45 days at Tsabong. This research observed that only short to medium varieties of maize can successfully be grown at Kasane, Pandamatenga and Shakawe with LRS more than 100 days. A high negative correlation of  $R=-0.9$  exists between onset and length of the rain season, thus implying that early onset is associated with long rain season.
5. Kasane, Pandamatenga and Shakawe are observed to experience less than average number of dry spells during the rain season. Using dry spell frequencies as a measure of a normal agricultural season, these locations are identified as low risk areas for rainfed farming.



## **4.4 DROUGHT SEVERITY UNDER CLIMATE VARIABILITY AND ITS RELATIONSHIP WITH ENSO**

In an attempt to understand drought characteristics in Botswana, their evolution at timescales of 1-, 3-, 6-, 12-, 18-, and 24-months have been explored. Based on SPEI values, droughts have been categorised as extreme, severe and moderate, their spatial and temporal distribution are presented in this subsection. The influence of large scale climate predictors such as ENSO on drought severity is also explored here.

### **4.4.1 Drought occurrence and evolution**

A drought is registered when SPEI (Z-values) drop below zero whereas humid events are represented with positive Z-values. Drought/wet events are identified by their duration and magnitude. The duration of drought is the time taken when Z-values are continuously negative. The magnitude of drought is also defined as the accumulated Z-values during the period of moisture deficit. The temporal evolution of drought at each synoptic station has been determined and presented in Figures 4-12 and 4-13. Only plots of evolutions at 3-, 6-, 12-, and 24-months are presented since the temporal patterns at 1-month are similar to those of 3-months whereas the evolutions at 18-months are adequately represented by those at 24-months. From Figures 4-12 and 4-13, the temporal variations at lower timescales of 3- and 6-months exhibit more variations than those at higher timescales. At these lower timescales, it may not be easy to identify a pronounced dry/humid period. At higher timescales, dry/humid events are clearly pronounced. However regardless of the timescale, all evolutions report dry/humid periods concurrently. For illustration purposes, evolutions from 4 regions of the study area are used to present the spatial and temporal evolutions of drought episodes in Botswana. These locations include Francistown in the east, Ghanzi in the west, Tsabong in the south and Maun in the north. From the temporal patterns, all the locations recorded drought periods of 1963 to 1965 in the east and northern locations extending over the year in the west and southern locations. Another drought event that was recorded in the 1960s' was between 1968 and 1970

except in the eastern region where this drought was not pronounced. The longest drought episode recorded over the historical period was from 1980 to 1985 extending to 1987 in the west, south and northern locations. In the east, another dry spell between 1989 and 1994 is observed however the same spell was intermittent in other regions. Intermittent droughts are also recorded between 2001 and 2007 across the study area. During this period, only the north recorded a longer continuous dry spell between 2001 and 2004. The most recent drought of 2015/16 is also evident on the plots across the country. From these evolutions, it clearly shows that there are more frequent droughts during the period after 1980/81 to 2015/16 than in the 1960s and 1970s.

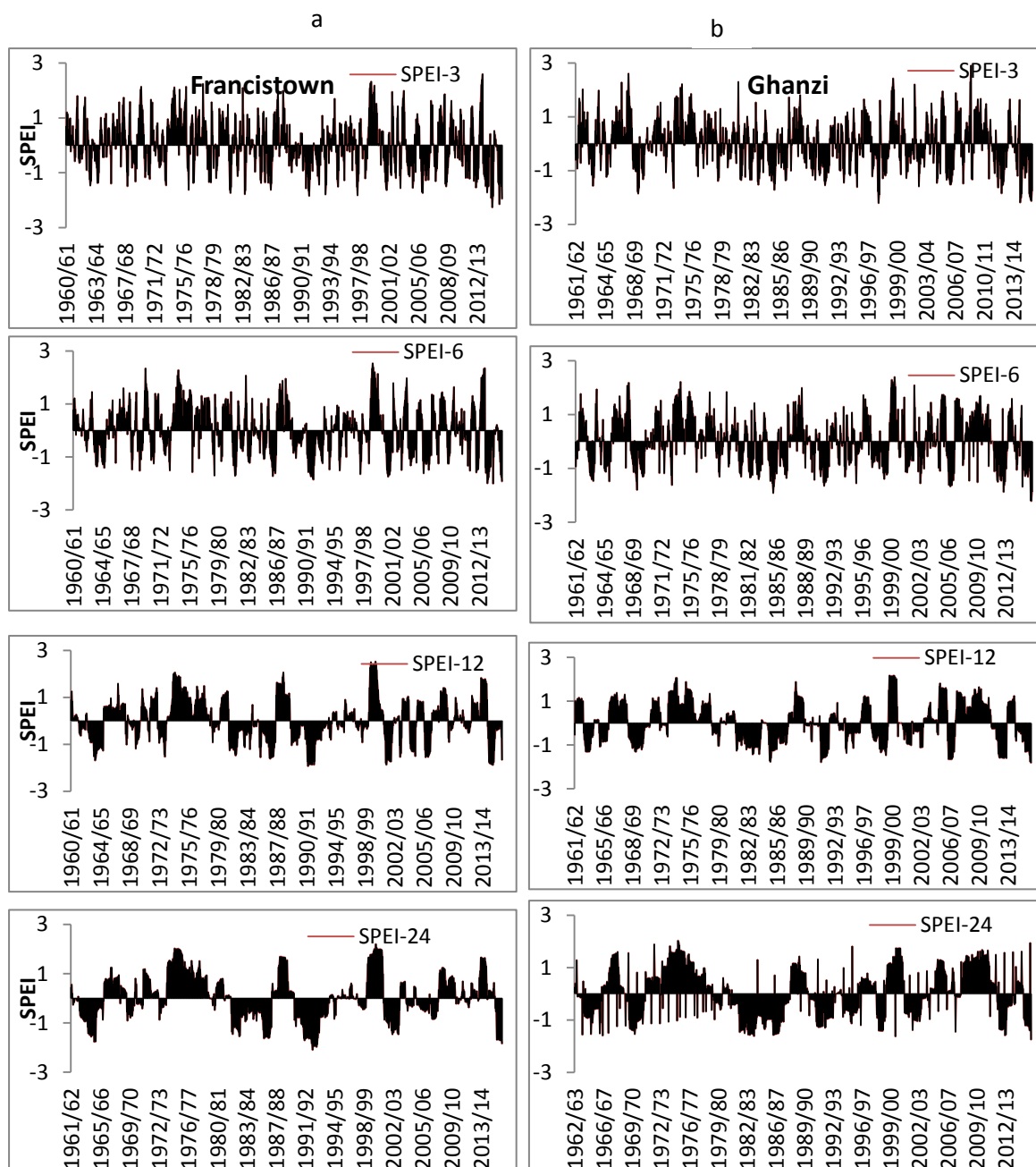


**Fig. 4-12.** Temporal evolution of SPEI of 3-, 6-, 12- and 24-month at a) Francistown and b) Ghanzi

Humid periods over the study area during the historical period were also recorded. The period of 1966 to 1968 was characterised with wet spells across all regions in Botswana. The longest humid spell during the historical period was recorded between 1973 and 1978 across Botswana. A short wet spell later followed from 1987 to 1989 which was evenly experienced across the study area. The most extreme wet spell was recorded in 1999/2000 in the east and

west. The same humid period was recorded in other regions but to a lesser extent. Another wet spell across Botswana is registered from 2009 to 2012. This period was more pronounced in the west, south and north compared to the east where it was predominantly intermittent.

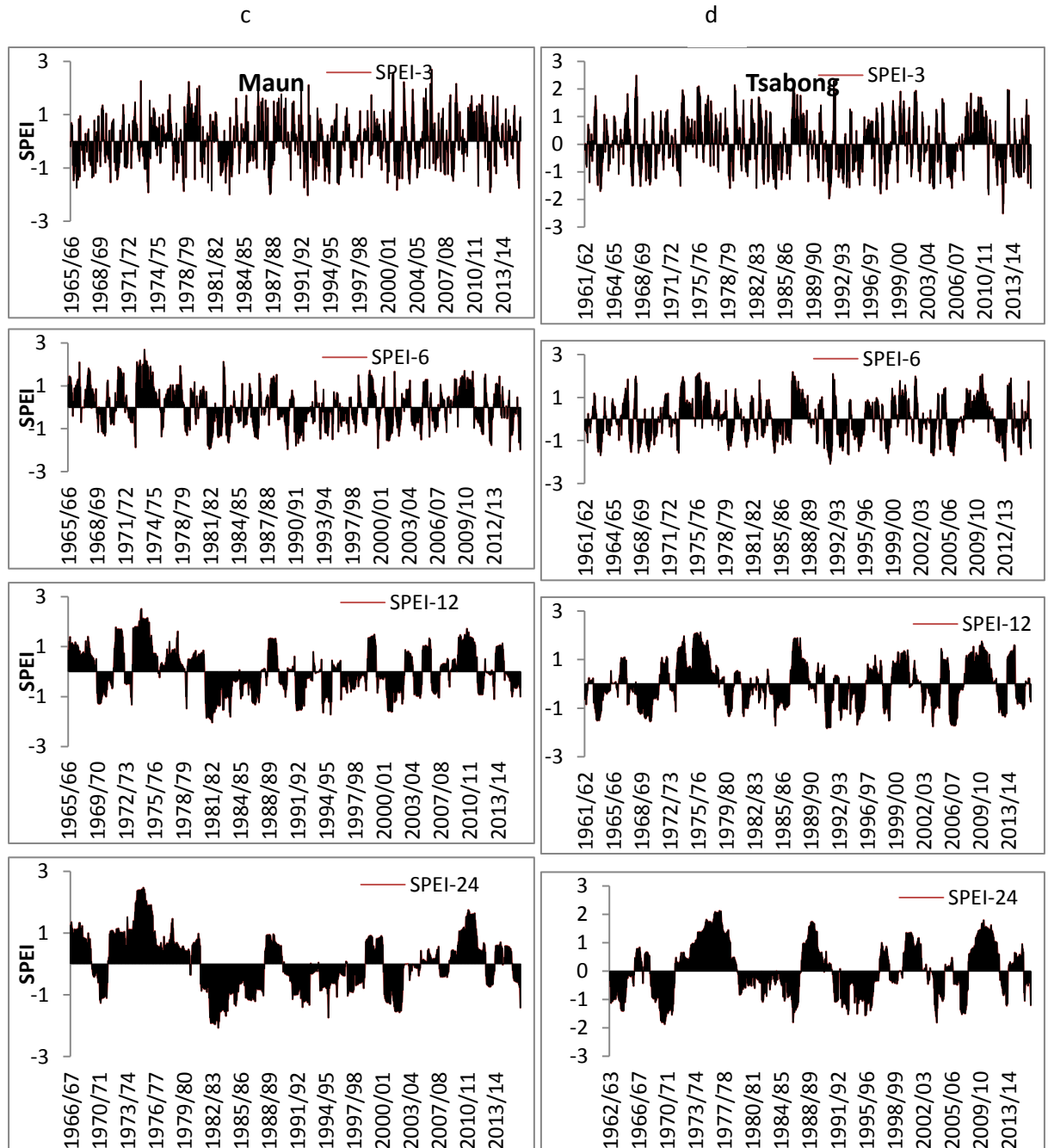


**Fig. 4-13.** Temporal evolution of SPEI of 3-, 6-, 12- and 24-month at c) Maun and d) Tsabong

The most severe drought events are shown in Table 4-9 for timescales of 6-, 12-, 18- and 24-months. They are presented in form of the longest duration and maximum severity during the

historical period. The results reveal that the longest drought events on record occurred from 1980 to 1987 and also between 2010 and 2016 mainly at Francistown, Ghanzi and Maun across timescales. The drought events that recorded the maximum drought severity were registered at Shakawe, Kasane and Tshane. The year 2015/16 was found to be the hottest on record for all the timescales. This year registered an extreme drought with maximum severity of -2.29 for the 6-months timescale at Shakawe in the northwest.

**Table 4- 9. Maximum drought severity (SPEI), duration and years of their occurrence**

Extreme drought events during the historical record																
Station	SPEI-6				SPEI-12				SPEI-18				SPEI-24			
	D <sub>max</sub> (M)	D <sub>max</sub> Period (Yrs)	S <sub>max</sub>	S <sub>max</sub> Yr	D <sub>max</sub> (M)	D <sub>max</sub> Period (Yrs)	S <sub>max</sub>	S <sub>max</sub> Yr	D <sub>max</sub> (M)	D <sub>max</sub> Period (Yrs)	S <sub>max</sub>	S <sub>max</sub> Yr	D <sub>max</sub> (M)	D <sub>max</sub> Period (Yrs)	S <sub>max</sub>	S <sub>max</sub> Yr
Francistown	49	1988/89-1992/93	-1.86	1991/92	59	1988/89-1993/94	-1.94	1991/92	70	1981/82-1987/88	-2.07	1991/92	61	1982/83-1987/88	-2.10	1992/93
Ghanzi	25	2011/12-2013/14	-2.23	2015/16	37	1981/82-1984/85	-1.82	2015/16	80	1981/82-1987/88	-2.04	2015/16	84	1981/82-1987/88	-1.76	2015/16
Jwaneng	27	2010/11-2012/13	-1.82	2015/16	24	2011/12-2012/13	-1.91	2015/16	42	2012/13-2015/16	-1.77	2015/16	53	2011/12-2015/16	-1.87	1999/00
Kasane	14	2000/01-2001/02	-2.14	2004/05	22	2000/01-2001/02	-2.18	2002/03	43	1993/94-1996/97	-2.11	2002/03	36	2000/01-2003/04	-2.15	1986/87
Lethakane	14	2000/01-2001/02	-2.14	2005/06	26	2000/01-2003/04	-2.05	1998/99	31	2001/02-2003/04	-1.97	1998/99	19	2002/03-2003/04	-1.94	1998/99
Mahalapye	22	2010/11-2012/13	-2.25	2001/02	35	2000/01-2003/04	-1.83	2001/02	32	1991/92-1993/94	-1.79	2001/02	19	2010/11-2011/12	-1.82	1989/90
Maun	24	1990/91-1992/93	-2.07	2014/15	75	1981/82-1987/88	-2.05	1981/82	29	1996/97-1998/99	-1.98	1991/92	83	1981/82-1987/88	-2.08	1983/84
Pandamatenga	14	2010/11-2011/12	-1.88	2015/16	53	2010/11-2015/16	-1.60	2013/14	62	2010/11-2015/16	-1.63	2011/12	62	2010/11-2015/16	-1.70	2011/12
Selibe-Phikwe	14	2005/06-2006/07	-1.72	2001/02	27	2010/11-2013/14	-1.68	2001/02	25	2011/12-2013/14	-2.00	2002/03	23	2011/12-2013/14	-1.85	2002/03
Shakakwe	33	1993/94-1996/97	-2.29	2015/16	36	1993/94-1996/97	-2.04	1994/95	67	1993/94-1999/00	-1.80	1998/99	63	1993/94-1999/00	-1.95	1995/96
SSKA	26	2010/11-2012/13	-1.81	2001/02	60	2011/12-2015/16	-1.78	2015/16	59	2011/12-2015/16	-1.75	2012/13	57	2011/12-2015/16	-1.78	1992/93
Sowa Pan	16	2003/04-2005/06	-1.82	2015/16	27	2000/01-2003/04	-1.87	1994/95	33	2000/01-2003/04	-1.72	2002/03	66	2001/02-2006/07	-1.76	2003/04
Tsabong	29	1984/85-1986/87	-2.10	1991/92	47	1966/67-1970/71	-1.84	1991/92	65	1991/92-1996/97	-1.91	1969/70	97	1979/80-1987/88	-1.88	1969/70
Tshane	31	1984/85-1986/87	-1.95	2004/05	45	1980/81-1983/84	-2.00	1963/64	74	1980/81-1986/87	-2.16	1964/65	72	1981/82-1986/87	-2.06	1964/65

- D<sub>max</sub> (M) = Longest drought duration on record in months  
D<sub>max</sub> Period (Yrs) = Period over which the longest duration occurred  
S<sub>max</sub> =Maximum drought severity (SPEI) on record  
S<sub>max</sub> Yr =Year of maximum SPEI

In this subsection, drought occurrence and evolution over the period of 1960-2016 has been analysed. The results indicate that droughts at each location show different temporal variations at different timescales. Temporal patterns at shorter timescale showed higher frequency compared to longer timescales. This is in agreement with findings by Yu et al. (2014), Vicente-Serrano et al. (2015) and Byakatonda et al. (2016) who found similar patterns in studies of drought occurrences using SPEI in China, Bolivia and Botswana respectively. Drought and humid periods were reported to occur at the same time across Botswana although with higher frequency in the east. This uniformity in drought occurrence across the study area could be attributed to the relatively flat topography of Botswana that facilitates uniform atmospheric circulation. Besides, studying drought evolution at various timescales gives insight on drought characteristics as they propagate from meteorological through agricultural at lower timescales of 1- and 3-months to hydrological and environmental droughts at higher timescales beyond 12-months (Nalbantis and Tsakiris, 2009; Lorenzo-Lacruz et al., 2010; Van Loon, 2013). Hence the temporal evolutions could be useful in drought monitoring and planning in an effort to mitigate impacts on various components of the hydrological cycle. The results also show that there were more frequent droughts after 1980/81 as compared to the previous period, this corroborates findings of Parida and Moalafhi (2008) who reported a sudden reduction in rainfall across Botswana during the same period. The periods of humid and dry spells indicated on the plots in most cases coincided with either La Niña for humid periods or El Niño for dry regimes. A case in point are the humid periods which coincided with La Niña years of 1967/68, 1973/74, 1999/2000 and 2010/11. Drought episodes also occurred during El Niño years of 1963/64, 1982/83, 1994/95, 2002/03, 2004/05, 2006/07 and the most recent of 2015/16. The year 2015/16 which was identified as the hottest during the historical period had also been identified by Hänsel et al. (2016) as the year that recorded the strongest El Niño in 100 years. This finding could also imply that large scale climate predictors are likely to have a direct influence on the local climate as earlier discussed in subsection 4.2.4. Nicholson et al.

(2001) and Usman and Reason (2004) had already reported earlier on the influence of ENSO on southern Africa's climate. Since these findings are in agreement, Botswana may be directly affected by climate variability as a result of ENSO activities in the Equatorial Pacific.

#### **4.4.2 Drought characteristics and their spatial patterns**

Droughts have been categorised according to Table 3-3 as extreme, severe and moderate droughts. Probabilities of occurrence of a drought event are determined from the frequency of drought per category as indicated in the classification. This is also taken as a degree of drought vulnerability towards that drought category. Results of these probabilities of occurrence are presented in Table 4-10. From these results, moderate followed by severe droughts are the most common across the study area. Extreme droughts are a rare occurrence with probabilities of less than 1.0% recorded at most stations except Letlhakane where probabilities of 1.1% and 1.5% were recorded at lower timescales of 1- and 3-months.



**Table 4-10.** Probabilities of occurrence of various drought categories

Probability of Drought occurrence (%)																		
Station	SPE1-1			SPE1-3			SPE1-6			SPE1-12			SPE1-18			SPE1-24		
	Extm.	Sev.	Mod.	Extm.	Sev.	Mod.	Extm.	Sev.	Mod.	Extm.	Sev.	Mod.	Extm.	Sev.	Mod.	Extm.	Sev.	Mod.
Francistown	0.6	4.5	10.3	0.3	4.5	11.5	0.3	5.2	11.7	0.0	7.3	7.9	0.5	5.3	9.6	0.2	7.2	6.3
Ghanzi	0.8	3.2	12.4	0.8	3.5	12.8	0.3	3.5	13.9	0.0	4.8	13.9	0.2	3.9	13.1	0.0	4.1	14.4
Jwaneng	0.6	3.1	12.3	0.3	4.7	9.6	0.0	5.0	11.6	0.0	3.8	13.7	0.0	5.9	13.7	0.0	7.0	9.3
Kasane	0.5	3.8	9.8	0.3	5.1	10.2	0.5	4.1	10.2	0.5	6.5	8.1	0.5	4.7	9.8	0.5	3.8	9.1
Letlhakane	1.1	3.4	11.0	1.5	3.4	12.2	0.4	3.5	14.3	0.4	4.3	11.5	0.0	4.9	10.5	0.0	4.6	10.8
Mahalapye	0.6	3.7	12.8	0.7	3.7	11.5	0.2	4.3	12.3	0.0	4.2	13.8	0.0	4.0	15.9	0.0	4.3	15.7
Maun	0.7	3.8	11.3	0.3	4.3	11.8	0.2	4.3	11.0	0.2	5.2	10.5	0.0	5.0	10.4	0.2	5.1	10.7
Pandamatenga	0.9	3.2	10.6	0.0	4.2	11.2	0.0	2.4	15.2	0.0	3.9	12.7	0.0	2.5	12.6	0.0	2.6	13.0
Selibe-Phikwe	0.5	2.6	12.0	0.0	2.1	12.6	0.0	2.1	13.4	0.0	5.0	12.2	0.0	5.7	12.0	0.0	6.5	9.5
Shakawe	0.5	4.2	11.8	0.5	4.6	12.6	0.2	2.5	16.0	0.2	2.8	18.6	0.0	5.0	14.1	0.0	5.9	12.9
SSKA	0.3	3.5	11.8	0.3	3.8	12.2	0.0	4.9	12.3	0.0	4.4	14.7	0.0	5.4	12.4	0.0	5.4	12.0
Sowa Pan	0.0	3.8	11.8	0.7	3.8	10.8	0.0	6.0	9.9	0.0	3.2	14.8	0.0	4.4	12.5	0.0	4.9	10.2
Tsabong	0.6	2.7	12.3	0.3	3.8	12.9	0.2	4.4	13.8	0.0	4.5	14.3	0.0	4.0	13.1	0.0	3.0	14.6
Tshane	0.6	2.9	13.2	0.2	4.7	12.3	0.0	4.4	11.9	0.0	6.8	9.7	0.6	4.7	9.8	1.4	3.6	9.1

Extm.= Extreme drought

Sev.= Severe drought

Mod.=Moderate drought

The highest probability of 18.6% for moderate drought was recorded at 12-months timescale at Shakawe in the northwest. Mahalapye and Pandamatenga are also showing high tendencies of vulnerability towards moderate droughts with probabilities close to 15%. For severe droughts, the highest probability of 7.3% is recorded at 12-months timescale at Francistown in the east. Kasane in the northeast and Jwaneng in the south are also showing higher vulnerability towards severe drought with probabilities of greater than 5%. The general pattern for all drought categories indicates that vulnerability to each drought category increases with timescale up to 12-months. The subsequent timescales have no particular trend. Figures 4-14 and 4-15 show spatial distribution patterns of various drought characteristics of severe and moderate droughts at all the timescales under consideration. Only severe and moderate droughts are presented since extreme droughts are a rare occurrence as mentioned earlier.

At 1-month timescale (Figure 4-14a), the north, northwest and eastern locations show tendencies of experiencing more severe droughts as compared to the rest of the country. Still at the same timescale, in Figure 4-14b, moderate drought vulnerability cover a considerable area of the southwest, south and northwest. These droughts show a southwest to northeast decreasing gradient. The northeast to eastern locations are less vulnerable towards this drought category.

At 3-months timescale (Figure 4-14c), severe droughts mostly affect the northeastern, eastern and southern locations. There is relatively lower vulnerability in the southeast cutting across to the western locations of Ghanzi. The moderate drought at this timescale (Figure 4-14d) shows a contrast from severe drought. The patterns indicate that the western axis from Shakawe through Ghanzi to Tsoabong on the fringes of the Kalahari desert are the most susceptible to this drought category. Southeastern locations are equally vulnerable around Selibe-Phikwe and Mahalapye. Spatial patterns however show that the northeastern to eastern and southern locations around Jwaneng are less vulnerable to this category of drought.

For the 6-months severe drought category (Figure 4-14e), the locations that are highly susceptible are the eastern and southern areas. Interestingly, the northwestern and southeastern locations that have been more vulnerable at lower timescales is less susceptible to this drought category. For moderate droughts (Figure 4-14f), the western axis bordering Kalahari desert are still showing higher tendencies of vulnerability towards this drought category. Areas in the northeast at Pandamatenga, in the central at Letlhakane and southeast at Selibe-Phikwe also show relatively higher vulnerability towards moderate drought at this timescale.

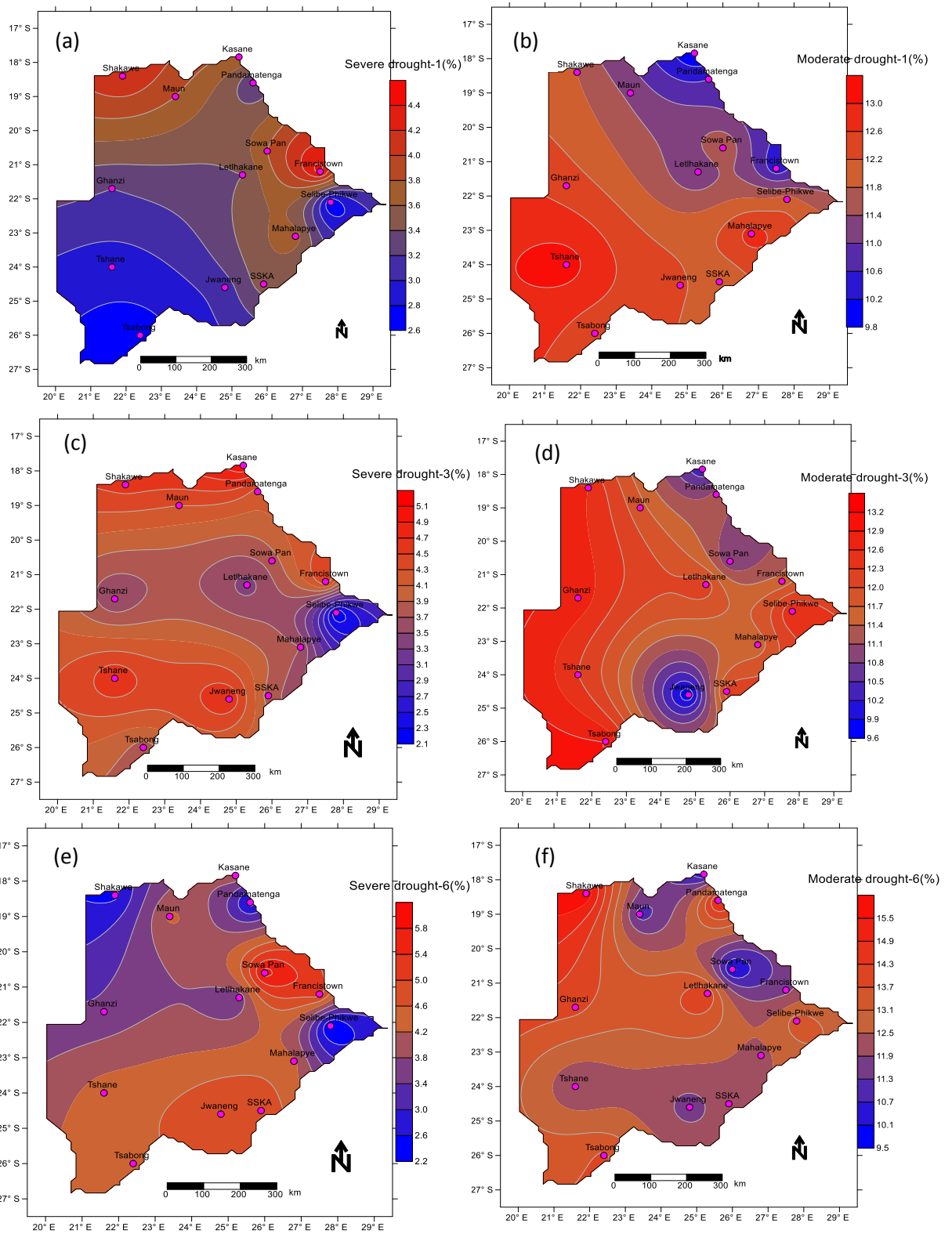


**Fig. 4-14.** Spatial patterns of vulnerability towards a) SPEI-1 severe drought, b) SPEI-1 moderate drought, c) SPEI-3 severe drought d) SPEI-3 moderate drought, e) SPEI-6 severe drought f) SPEI-6 moderate drought

At 12-months timescale, severe droughts (Figure 4-15a) show that majority of the country is less susceptible to this drought category. A few locations in the northeast at Kasane, southwest at Tshane and east at Francistown show tendencies of higher vulnerability. Moderate droughts at this timescale (Figure 4-15b) show a relatively larger area which is susceptible compared to severe droughts. Locations in the northwest, south to southeast are mostly susceptible to this drought category.

At 18-months timescale (Figure 4-15c), severe droughts show a northwest to southeast pattern of higher vulnerability towards this drought category. Interestingly, areas at the fringes of the Kalahari desert are showing less susceptibility towards this drought category. For the moderate droughts (Figure (4-15d), a southwest to northeast pattern shows the region as less susceptible towards this drought. The northwest and southeastern locations are the most vulnerable towards this drought category.

At 24-months timescale (Figure 4-15e), the severe drought category shows similar patterns as those of severe droughts at 18-months with a northwest to southeast pattern of vulnerability. Similarly the moderate drought at this timescale (Figure 4-15f) shows also similar behavior as those at 18-months timescale, although with a larger area but with similar degree of susceptibility. The northwest and southeast are the most affected locations with this drought category.

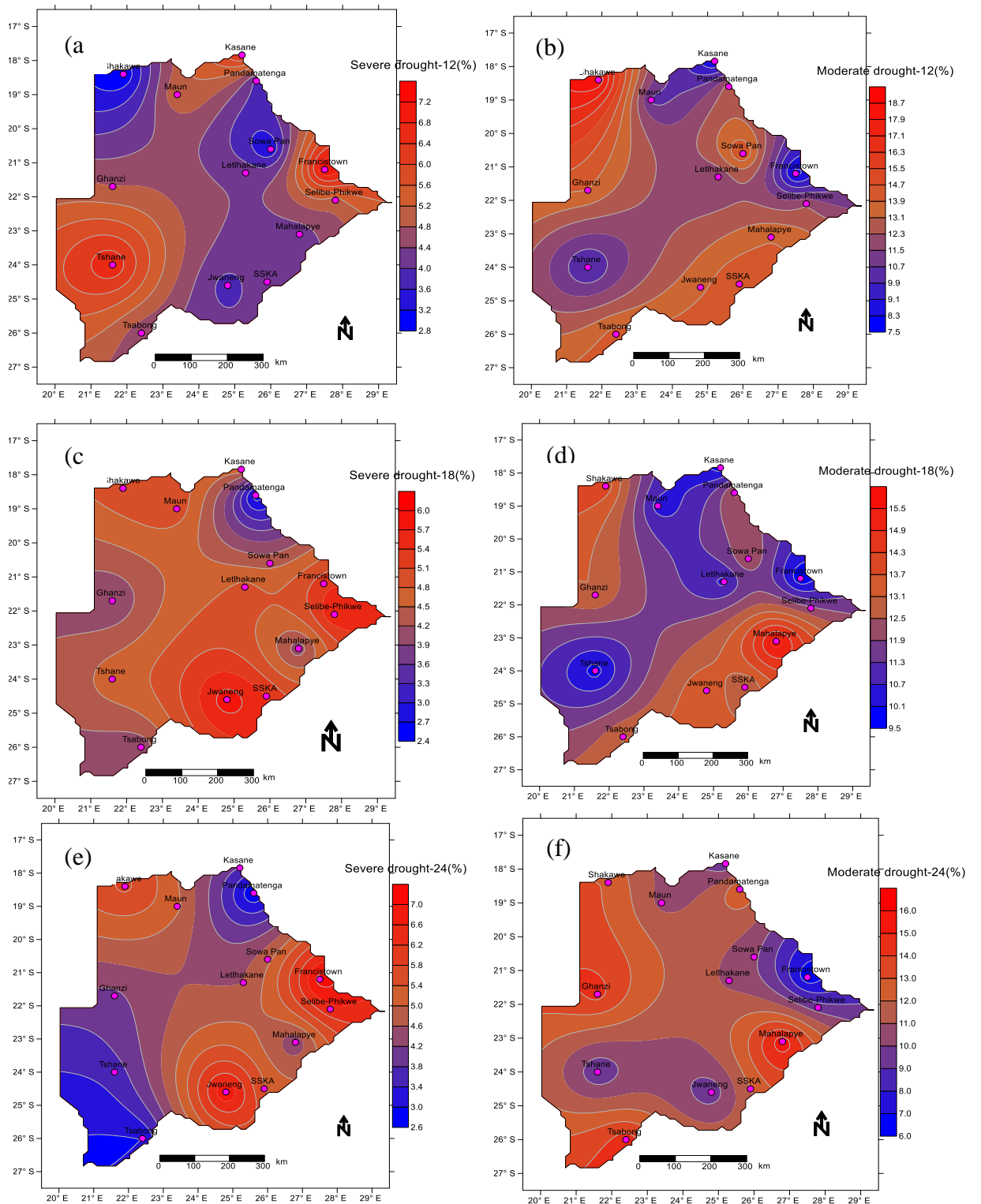


**Fig. 4-15.** Spatial patterns of vulnerability towards a) SPEI-12 severe drought, b) SPEI-12 moderate drought, c) SPEI-18 severe drought d) SPEI-18 moderate drought, e) SPEI-24 severe drought f) SPEI-24 moderate drought

Results indicated that the country is more vulnerable to moderate droughts than any other drought category. In earlier studies across Botswana on drought vulnerability assessment using SPI by Batisani (2011), they also reported similar results. This could imply that droughts in Botswana are more related to low or lack of rainfall than temperature rise as a result of ongoing global warming since SPEI incorporates both rainfall and  $ET_0$ . The northern locations of Shakawe, Pandamatenga and Sowa Pan are particularly identified to be highly vulnerable to this drought category. From Section 4.3, it was reported that Shakawe and Pandamatenga were potential areas for rainfed agriculture. Hence increased drought vulnerability in these locations poses a threat to efforts of improving the food security situation of Botswana. The results further revealed that vulnerability increased with timescale up to 12-months, thereafter the trend was not well defined. This could point to the fact that drought monitoring in Botswana can be managed within 12 months or slightly over the year timescales. This is further supported by the fact that drought vulnerability at 18- and 24-months show similar behavior. In this respect it may not be necessary to compute drought severity up to 24-months. The western axis from Shakawe through Ghanzi to Tsabong at the fringes of the Kalahari desert is generally showing the highest degree towards drought vulnerability than any other location for all the drought categories. Locations of Ghanzi and Tsabong are the driest locations in the study area. Since it has already been reported by Pachauri and Reisinger (2007) and Stocker et al. (2013) that with anticipated global temperature rise of 4 - 6 °C, there are likely to be changes in atmospheric circulation with drier areas progressing into arid and arid into hyper arid. This creates more uncertainties in locations such as Ghanzi, Tsabong and Jwaneng that lie on the fringes of the Kalahari desert.

#### **4.4.3 Association of ENSO with drought severity**

The influence of ENSO represented by SSTs and SOI are presented in the box and whisker plots of the Pearson's correlation coefficient between combinations of SPEI and SST on one hand and SPEI and SOI on the other hand. The results of the plots are presented in Figures 4-

16 and 4-17. From Figure 4-16, the correlations between SPEI and SST at all timescales used in this study showed mostly negative correlations. Correlations in January show a maximum correlation ranging from -0.7 at 1-month to -0.3 at 24-months, correlations during this month are mostly negative up to 12-months timescale. At 18- and 24-months, SSTs start to show no relationship with SPEI. For the months of February and March, the patterns are similar but with max correlations ranging from -0.6 to -0.3. For the month of April which marks the end of the rain season, correlations starts to drop and become non significant throughout the winter months of May, June, July and August characterised by dry spells. Correlations during this period are weak and in some cases for August and September, positive values were registered. This is an indicator of no relationship between SPEI and SSTs. Negative SPEI and positive SSTs are responsible for droughts in this region (Vicente-Serrano et al., 2011). For October which is the beginning of the summer rain season, weakly negative correlations start to dominate increasing in the subsequent months of November and December which also marks the onset of rain. The maximum correlation in November ranges from -0.5 to -0.35 at 1- and 24-months respectively whereas in December it ranges from -0.7 to -0.5 over the same timescales. It is further observed that correlations are negative until 12-months, at higher timescales they start to deviate from the general trend as the case of spatial patterns of vulnerability.



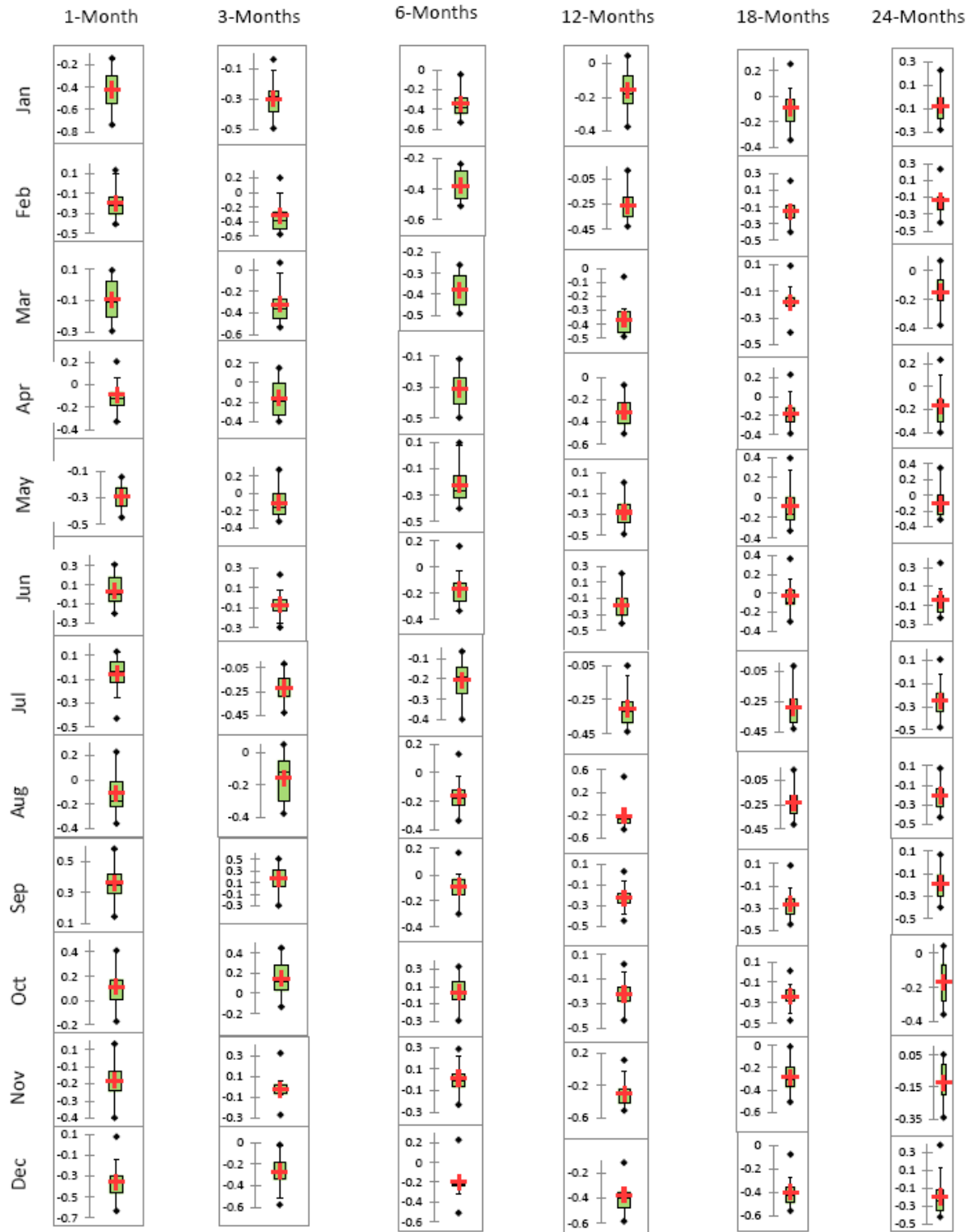


**Fig. 4-16.** Box and whisker plots of the Pearson's correlation coefficients between SPEI and SSTs

Correlations between SPEI and SOI in Figure 14-17 show similar trends as those between SPEI and SST although in this case they are mostly positive during the summer months.

January records the highest correlation of 0.7 at 1-month timescale and the lowest of 0.3 at 24-months. For the months of February and March, positive correlations range from 0.6 to 0.2 across timescales as the case for the association between SPEI and SST. Winter months of May through to August mostly returned weak correlations and in some cases negative values resulted. This is also an indication of no relationship with the local climate during the winter period. During the month of November when most rain onset occur across the study area, correlations are mainly positive and increasing significantly in December. In contrast, correlations between SOI and SPEI do not show any particular trend between timescales. December has maximum correlations ranging from 0.5 to 0.3 across timescales.

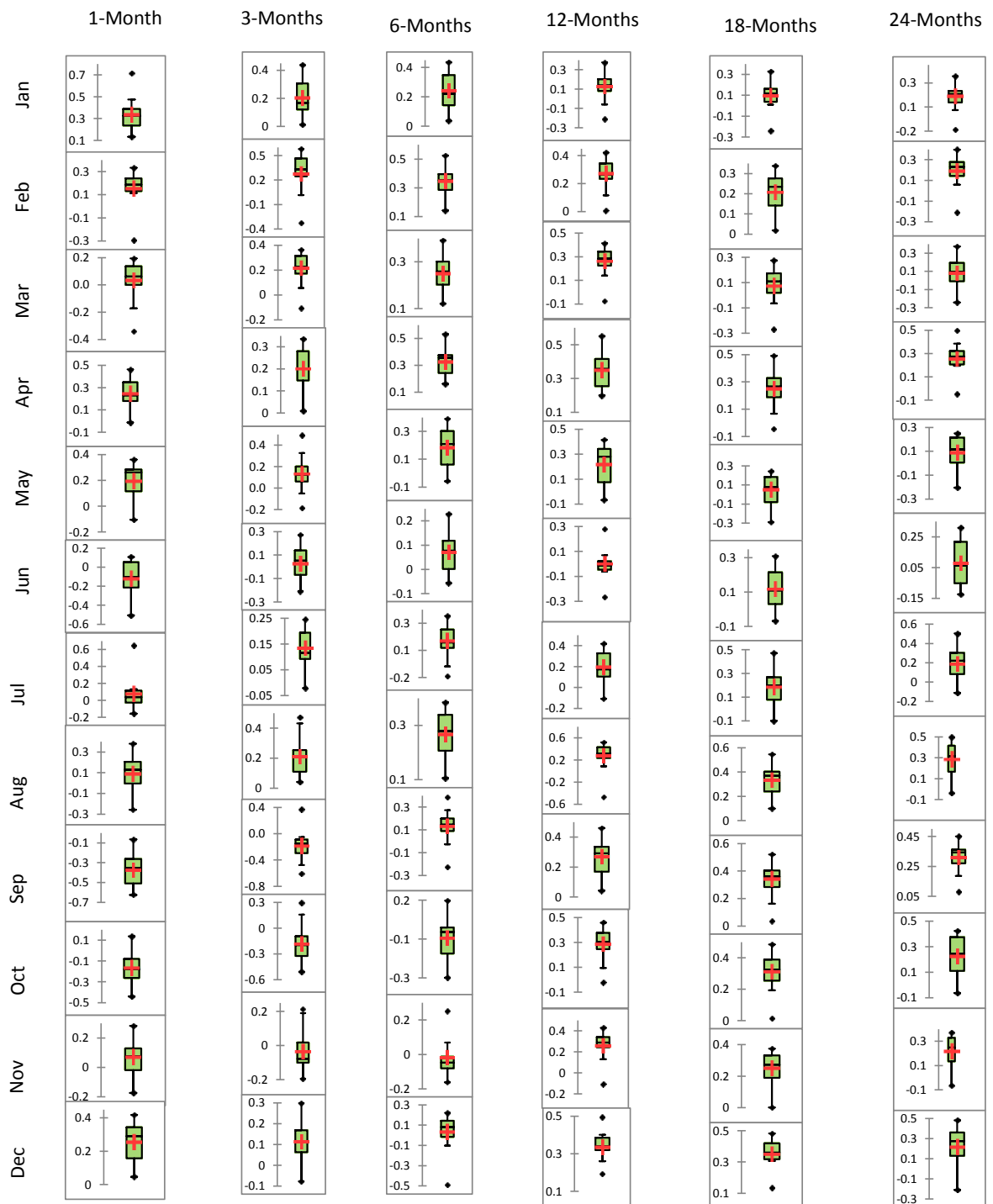


**Fig. 4-17.** Box and whisker plots of the Pearson's correlation coefficients between SPEI and SOI

Negative correlations between SPEI and SST is a clear manifestation that positive anomalies of SST which are responsible for the El Niño phenomenon corresponds to negative SPEI, a representation of drought episodes. Similarly positive correlations between SPEI and SOI,

demonstrates that positive anomalies of SOI responsible for La Niña conditions also correspond to positive SPEI representing humid spells. This further collaborates earlier studies by Nicholson et al. (2001), Jones et al. (2007) and Vicente-Serrano et al. (2011) who reported the ENSO influence on the southern Africa's climate while using gridded data.

The degree of associations returned significant values during summer which also coincides with the rain season. This may imply that rainfall totals and intensity during summer could be related to the Ocean Niño Index (ONI) of region 3.4 in the Equatorial Pacific. Correlations during winter did not show any relationship with ENSO across the study area, an indication that climatic patterns during winter season in Botswana can be explained by other atmospheric circulation mechanisms other than ENSO. Distribution of correlations across timescales shows a decreasing trend with increasing timescale up to 12-months. Correlations at higher timescales deviated from this trend just as the case of drought vulnerability. This may confirm the earlier assertion that timescales over the year may not take a central role in drought monitoring in Botswana.

#### **4.4.4 Summary**

Section 4.4 has quantified drought severity and its temporal and spatial variability using SPEI. The degree of vulnerability has been assessed through probabilities of occurrence and its extent presented to aid drought monitoring and planning. This study further reveals a close association between Botswana's summer climate and ENSO. Based on the results and discussion in subsection 4.4.3, the following summary is deduced.

1. The variation between wet and drought events was distinct across timescales of 1-, 3-, 6-, 12-, 18- and 24-months, with the lower timescales showing higher temporal variation. It is also observed that there were more drought episodes after 1980/81 with most of them coinciding with El Niño years.

2. Botswana is more vulnerable to moderate droughts in the north and also at locations on the fringes of the Kalahari desert exhibiting relatively high susceptibility. Vulnerabilities were observed to increase with timescale up to 12-months. Timescales greater than 18-months were found not useful in drought monitoring in Botswana.
3. ENSO has more influence on Botswana's climate during the summer rain season with the highest association resulting in December and January at the season's peak.

## **4.5 DROUGHT PROPAGATION AND ITS INFLUENCE ON WATER RESOURCES**

The drought propagation process was investigated in this Section to generate information that could be useful in water resources planning and drought monitoring. This was achieved through analysis of climatic and hydrological drought dynamics and determining their degree of association. A common timescale that can be used for drought monitoring across the two river basins of Limpopo and Okavango was also established. Rescaled range analysis was done at the identified common timescale to estimate the future behaviour of the hydrological droughts.

### **4.5.1 Dynamics of climatic and hydrological droughts**

Dynamics of climatic and hydrological droughts have been plotted on the same scale and presented in Figures 4-18 and 4-19 for the Limpopo and Okavango basins respectively. Climatic droughts were derived from Selibe-Phikwe, Mahalapye and SSKA synoptic stations located in the Limpopo basin while for the Okavango basin, Kasane, Maun and Shakawe were used. Both wet and dry spells have been recorded on the plots. The drought and humid events recorded by climatic dynamics correspond to those reported in Section 4.4. As is the case in section 4.4, dynamics at shorter timescales are more frequent than those at higher timescales. The dynamics of hydrological droughts show similar pattern though with a lag at both river basins. As earlier stated in Section 4.4, the behaviour of the dynamics after 12-months timescale deviates from an established trend between 1- and 12-months, for this reason, a 15-months timescale is introduced in this section to enable detailed analysis of dynamics at finer intervals. Just as the case of climatic droughts, negative standardised flow index (SFI) values signifies below average and positive SFI above average flow conditions usually occurring during wet spells.

In the Limpopo basin flow data was available for a period between 1997 and 2016, to facilitate comparison with climatic droughts, analysis is made over this period. In this basin as shown in Figure 4-18, a dry spell between 2000 and 2003 was recorded by climatic dynamics, during the

same period low flows were also recorded between 2002 and 2004 though with less severity. The next dry period recorded by the climatic dynamics is that between 2006 and 2007 with below average flows ensuing between 2008 and 2009. A period from 2011 to 2013 was also characterised by climatic droughts which was followed by low flows between 2012 and 2013. However the low flows during this period were of a shorter duration compared to climatic droughts. The last dry spell during the historical period is the most recent 2014 to 2016 with low flows recorded between 2015 and 2016.

Wet spells in the Limpopo basin were equally registered, the period between 1998 and 2000 is characterised by wet spells with above average flows registered during 1999/2000. The next wet spell on record was that between 2008 and 2009 with high flows following between 2009 and 2010. Another mild wet spell that has been recorded is between 2013 and 2014 which was followed by above average flows during the first half of 2014. From the dynamics, it is observed that at lower timescales both drought dynamics align together with lags more pronounced at higher timescales of 12-, 15- and 18-months. In the Limpopo basin, an average of 7 months lag between climatic and hydrological droughts is observed. This lag was confirmed through lag correlations between SPEI and SFI. This may be regarded as the time taken for meteorological drought to propagate to hydrological drought. Analysis of linear trends indicates increasing gradient towards drying conditions across the Limpopo basin with the drying gradient increasing at higher timescales. The drying gradients expressed as a percentage of Z-units were -0.08%, -0.07%, -0.13%, -0.24% and -0.29% at time scales of 3-, 6-, 12-, 15-, and 18-months respectively.

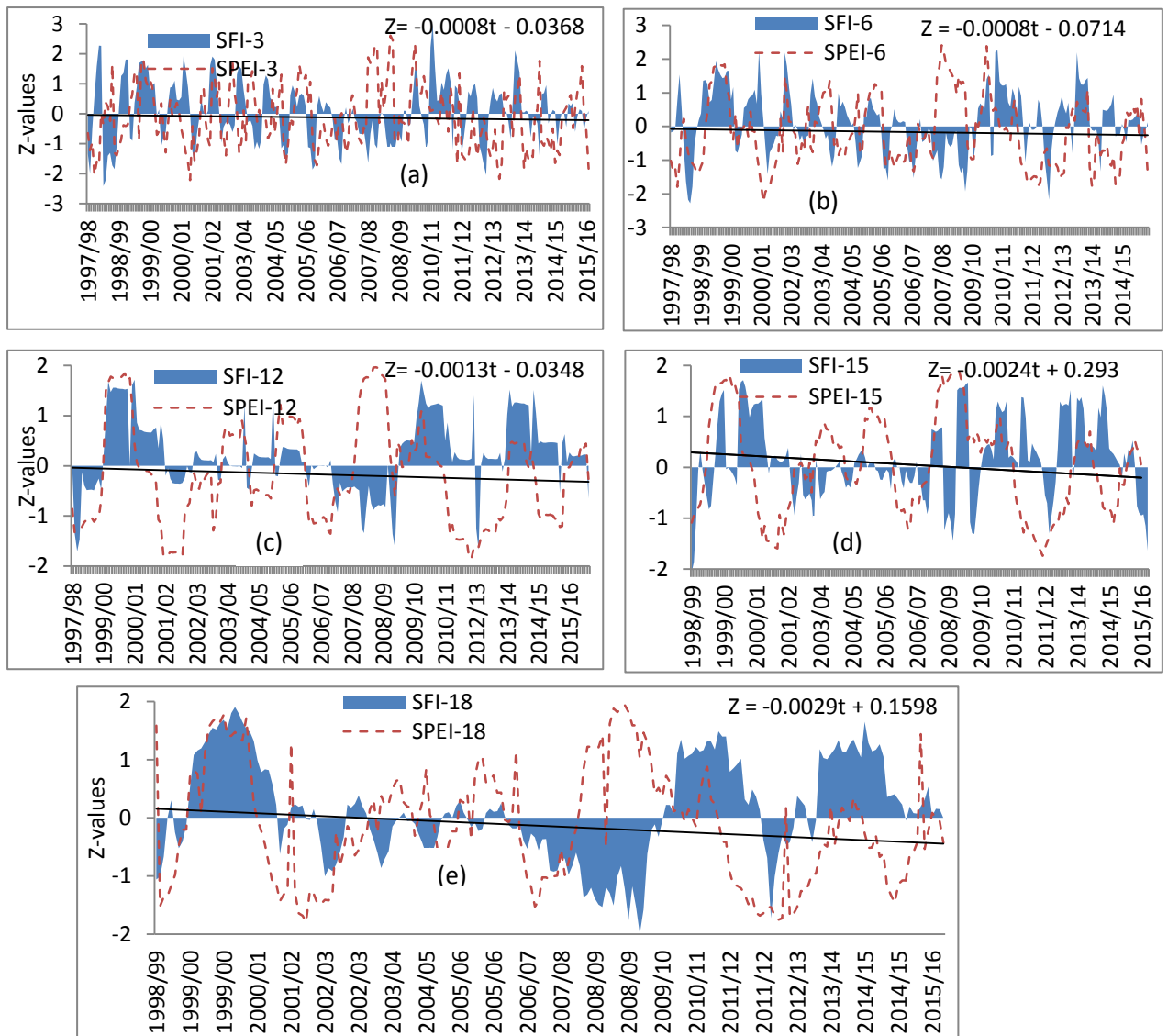


**Fig. 4-18.** Dynamics of climatic (red dotted line) and hydrological droughts (blue shaded area) in the Limpopo basin at timescales of a) 3-months, b) 6-months, c) 12-months, d) 15-months and e) 18-months

In the Okavango basin presented in Figure 4-19, also the general patterns of dry and wet spells recorded by dynamics of climatic drought were not different from those observed in the northern region in section 4.4. Flow data in the basin was available from 1975 to 2016. The dry spell from 1981 to 1984 that was recorded throughout the study area is also registered by the dynamics of droughts. The below average flows started earlier in 1980 as it emanated from another mild dry spell that had occurred during the period of 1979/80 season. These low flows normalised in 1983. Another dry spell recorded by the climatic dynamics is between 1990 and



1993 with hydrological drought closely following between 1992 and 1994. Further still between 1994 and 1996, climatic droughts recorded a dry spell together with low flows in the same year whose effects had accrued from the previous period but normalised in 1998. The subsequent dry spells registered by climatic drought were between 2002 and 2003 with a short punctuation but resumed shortly in 2004 until 2006. These dry spells did not result into significant flow reduction due to the wet spells that had been recorded between 2000 and 2002. The next dry spell that caused significant low flows occurred in the 2014/15 season.

Wet spells and above average flows in the Okavango basin were also registered by both climatic and hydrological droughts respectively. A wet spell which was registered between 1988 and 1990 did not generate high flows due to the prolonged drought in the previous period of 1981 to 1984. A wet period between 2009 and 2011 resulted into the highest flows recorded during the historical period from 2009 to 2013. As the case in the Limpopo basin, climatic and hydrological drought dynamics are found to align at lower timescales. At higher timescales of 12-, 15- and 18-months, it takes an average of 6 months for meteorological droughts to propagate to hydrological droughts in the Okavango basin. Linear trends indicate a constantly increasing gradient towards dry conditions of around -0.18%.

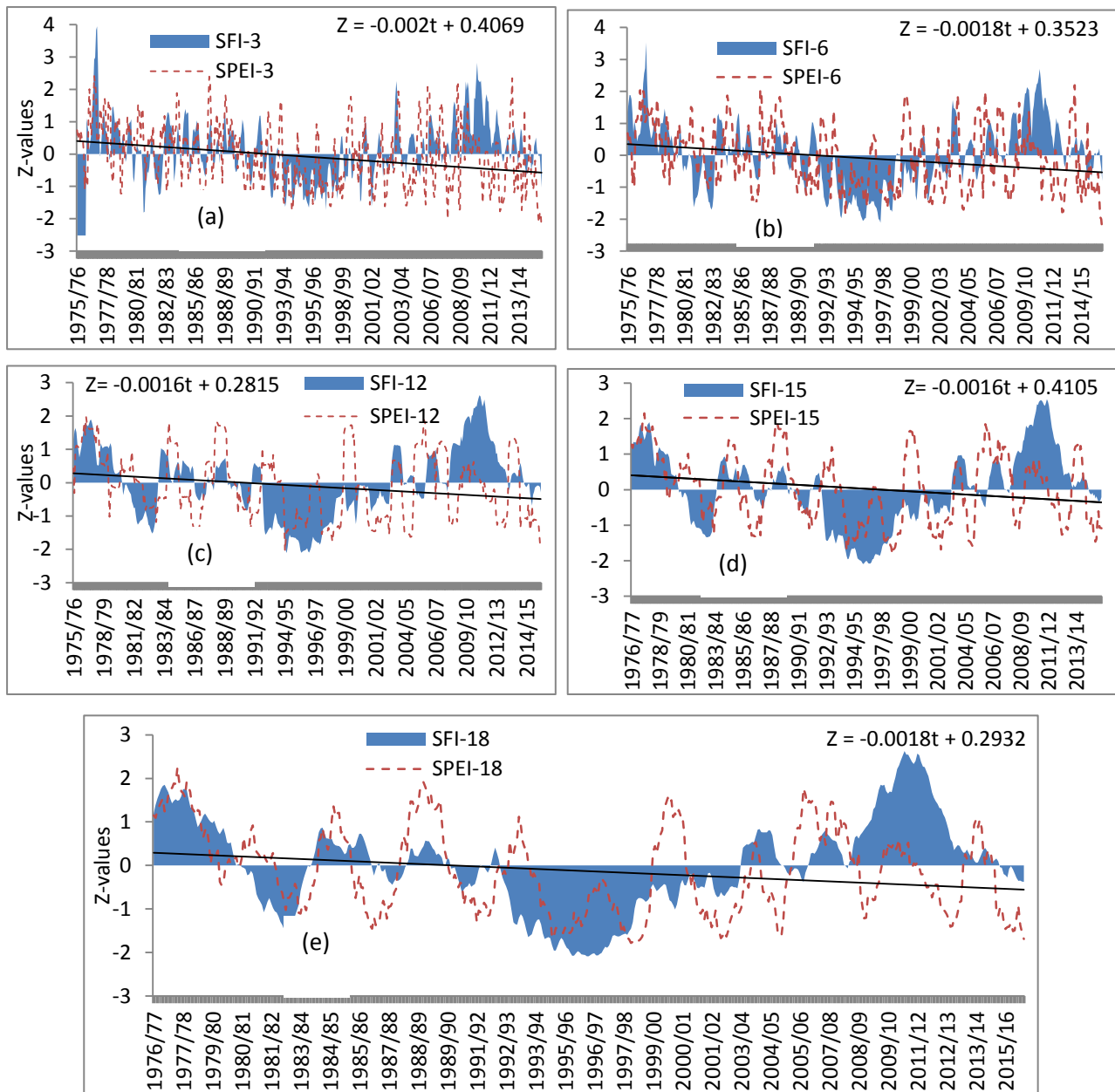


**Fig. 4-19.** Dynamics of climatic (red dotted line) and hydrological droughts (blue shaded area) in the Okavango basin at timescales of a) 3-months, b) 6-months, c) 12-months, d) 15-months and e) 18-months

This subsection investigated dynamics of climatic and hydrological droughts in the Limpopo and Okavango basins. The propagation of climatic drought to hydrological drought is also investigated. The duration of propagation was deduced from the relationship between climatic and hydrological droughts. This duration is useful in drought early warning and hence their mitigation. Several studies by Nalbantis and Tsakiris (2009), Vicente-Serrano et al. (2015) and

most recently Huang et al. (2017) have revealed the importance of studying drought propagation as part of basin wide planning. The closer alignment of dynamics of climatic and hydrological droughts at lower timescales could be attributed to the high frequency in variation between wet and dry episodes. This limits the time of expression of possible lags between these events. Besides, at lower timescales hydrological droughts are highly unlikely since at 3-months, agricultural droughts are the ones at play as demonstrated in a number of studies on drought propagation by Mishra and Singh (2010) and Van Loon (2013). The lags of 7 months and 6 months reported in the Limpopo and Okavango basins respectively between climatic and hydrological droughts are in the same order. This may be attributed to similar land use and relatively flat topography that aids a uniform atmospheric circulation. Drought trends reveal drying conditions which may threaten livelihood activities derived from these basins. These two river basins are the main source of water resources for Botswana. Okavango is a delta recognised as Ramsar site while Limpopo is host to majority of the surface dams that supply water for both domestic and industrial needs. Okavango basin equally hosts most of the commercial farms that supplies majority of the food demand. Therefore it is necessary to develop these early warning systems to assist in drought mitigation measures.

#### **4.5.2 Degree of association between climatic and hydrological droughts**

The degree of association has been analysed for both the combined and monthly series of climatic and hydrological drought indices. Results from this analysis are presented in Table 4-11. Analysis of monthly series is instrumental in understanding the seasonal behaviour of the drought dynamics.

In the Limpopo river basin, significant correlations are observed in March and April at 3-months timescale. At 6-months timescale, significant correlations occur in February, March, April, May, June and July. For the 12-months timescale, the only significant correlation is registered at the end of the summer rain season in March. The 15- and 18-months timescale shows no significant correlations across the entire period. The combined series show similar

trends as the monthly series. The degree of association for these series increases across timescale with a maximum of 0.25 occurring at 12-months and declining in the subsequent timescales. None of the correlations is significant at 95% confidence level for these series in the Limpopo basin.

**Table 4-11.** Correlation coefficient between climatic and hydrological droughts

Month	Timescale									
	Limpopo					Okavango				
	3	6	12	15	18	3	6	12	15	18
January	-0.09	0.01	0.20	0.02	-0.03	0.32	0.33	0.38*	0.45*	0.44*
February	-0.14	0.45*	0.26	0.15	0.14	0.26	0.31	0.47*	0.40*	0.42*
March	0.63*	0.62*	0.43*	0.32	0.07	0.01	0.22	0.36*	0.39*	0.41*
April	0.62*	0.50*	0.30	0.32	0.12	0.02	0.20	0.29	0.39*	0.42*
May	0.27	0.41*	0.33	0.18	0.10	0.28	0.19	0.29	0.41*	0.39*
June	-0.07	0.39*	0.29	0.15	0.17	0.35*	0.22	0.30	0.40*	0.42*
July	-0.18	0.41*	0.30	-0.02	0.05	0.28	0.27	0.31	0.36*	0.42*
August	-0.15	0.03	0.31	0.07	0.10	0.37*	0.45*	0.33	0.35*	0.45*
September	-0.06	-0.12	0.30	0.09	0.08	0.34*	0.45*	0.33	0.34*	0.43*
October	-0.04	0.06	0.25	0.17	0.18	0.36*	0.35*	0.35	0.36*	0.40*
November	-0.21	-0.01	0.11	0.18	0.13	0.47*	0.36*	0.33	0.39*	0.41*
December	-0.20	-0.22	-0.05	0.11	0.05	0.31	0.33	0.33	0.41*	0.41*
Combined series	0.02	0.18	0.25	0.16	0.07	0.27	0.31	0.34*	0.39*	0.42*

\*Significant at 95% confidence level

Correlations from the Okavango basin also presented in Table 4-11 indicate significant correlations in June, July, August, September, October and November at 3-months timescale. At 6-months, significant correlations were recorded in August, September, October and November. 12-months timescale had January, February, March, October and December also registering significant correlations. At higher timescales of 15- and 18-months, all correlations across the entire period were positive and significant. For the combined series, correlations increased across timescale with the lowest of 0.27 and a highest of 0.42 recorded at 3- and 18-months respectively in the Okavango basin. Generally the Okavango basin is significantly affected by droughts at higher timescales compared to the Limpopo basin.

This study has shown a clear relationship between climatic and hydrological droughts over the study area at different timescales. In the Limpopo river basin, longer timescales were found not useful in monitoring droughts. Higher responses were found at lower timescale in agreement with similar studies carried out in Greece by Nalbantis and Tsakiris (2009) and Spain by Vicente-Serrano and López-Moreno (2005). The short timescale response in the Limpopo river basin could be attributed to arenosols with limited moisture storage capacity that dominate the study area (FAO, 2001). At long dry periods, the soils do not have sufficient storage to contribute to stream flow hence the poor response at longer timescales. Comparing Limpopo and Okavango river basins in terms of response, the latter case can be treated as storage whereas the earlier as normal river flow system.

There was observed seasonal variations in response for the Limpopo river basin with significant correlations registered in the months of February, March and April at 3-months timescale. This time period coincides with Botswana's summer rain season. 3-months SPEI in March is an accumulation of moisture deficit for January, February and March, which period covers majority of the rain season. The high correlations are due to the fact that during the months of March and April there is adequate moisture available for atmospheric circulation. The SPEI-6 is also an accumulation of moisture over the six month period which is a summation of the entire summer rain season. Due to the same reasons as for SPEI-3, significant correlations were observed during the months of February, March, April, May, June and July. The same reason is also advanced to the significant correlation in March at 12-months timescale.

In the Okavango basin it was evident that hydrological responses increased at higher timescales. This may be explained by the fact that the Okavango river basin is a delta and as such it acts as storage of river discharge over long periods of time. Lorenzo-Lacruz et al. (2010) in their study found greater responses at higher timescales in Spain for reservoir storage as compared to inflows which showed higher response at shorter scales as in the case of

Limpopo basin. Drought in storage mediums depends on amounts previously impounded, implying existing drought conditions are a result of a combined effect of earlier conditions (either wet or dry years).

#### **4.5.3 Timescale for drought monitoring across Limpopo and Okavango river basins**

To enable drought monitoring and mitigation across the two river basins, a common timescale is required to guide operational hydrologists and users of water resources within these basins. Drought monitoring is directly linked to the degree and extent of vulnerability. Since Botswana has been identified in Section 4.4 to be more vulnerable to moderate droughts than any other drought category, this study uses moderate drought probabilities across the two basins to establish that common timescale that can be used in monitoring. To achieve this, the probability of occurrence of this drought category is plotted against timescale for both basins on the same axis as shown in Figure 4-20. The results indicate that, vulnerability increases with timescale in the Limpopo basin. In the Okavango basin the plot indicates that vulnerability increases steadily reaching the peak at 12-months timescale. These results further reveal that the Okavango basin is more vulnerable to moderate droughts than the Limpopo basin up to 15-months timescale. A common timescale established from this analysis across the two basins lies between 15- and 16-months. This study takes 15-months timescale as one recommended for joint drought monitoring. The hydrological behaviour at this common timescale needs to further be investigated to reveal possible future changes that may affect water resources in these basins.

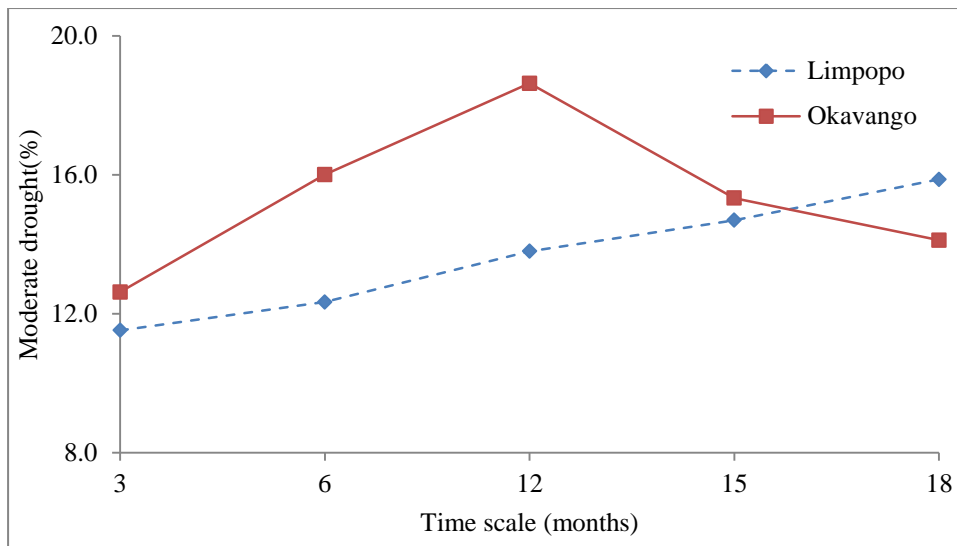


**Fig. 4-20.** Moderate drought probability across timescales

#### 4.5.4 Rescaled range analysis at 15-months timescale

Standardised flow indices (SFI) combined time series at timescale of 15-months are further analysed for the two basins. This is to establish if the prevailing historical conditions will be maintained or reversed in the near future using the Hurst coefficient as a measure. Results of the relationship between rescaled range and rescaled sample size are presented in Figure 4-21. These results reveal H-coefficients of 0.18 and 0.11 in the Limpopo and the Okavango basins respectively. These coefficients being significantly less than 0.5, indicates a possible reversion in the dynamics in the near future. The low values of the H-coefficients are also an indication of high variability in the dynamics. The rescaled range analysis only provides future direction of dynamics but does not give the magnitude of the change that is required for operational purposes. For this reason it is necessary to perform forecasts that will provide this magnitude over a given planning horizon.

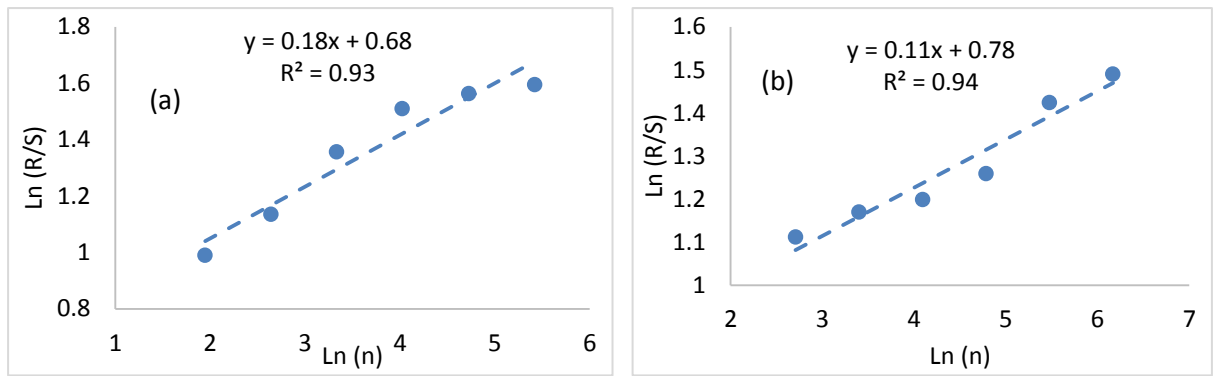


**Fig. 4-21.** H-Coefficient for the two river basins (a) Limpopo (b) Okavango

Rescaled range analysis with wide application in hydrological studies and financial time series analysis revealed a reversion tendency in the flow dynamics expressed through the H-coefficient. The use of rescaled range analysis in the study of capital markets has proposed other modifications for calculating the H-coefficient (Granero et al., 2008). This was necessary for testing randomness in the capital market returns. However in this case where the H-coefficient significantly smaller than 0.5, the possibility of having random flow dynamics is very minimal over the study area and hence the original method proposed by Hurst (1951) was sufficient in forecasting flow dynamics in this study. The low H-coefficient could also signify high climate variability which is a common feature in semiarid areas that has also been reported in numerous studies in the region (Richard et al., 2000; Batisani, 2012; Moalafhi et al., 2012; Moeletsi and Walker, 2012). Stream flow is highly linked to atmospheric circulation through evaporation which is influenced by climate variability that has already been reported to be high in the study area.

#### 4.5.5 Summary

This subsection has focused mainly on identifying the propagation period of climatic drought to hydrological drought. A common timescale for drought monitoring has been identified for Botswana as part of drought mitigation strategy. This research was also able to establish drought trends and their possible reversion or persistence in the near future. From the foregoing analysis and discussion, the following summary is deduced;



1. The dynamics of droughts show increasing trends in both Limpopo and Okavango basins. Climatic droughts were found to take 7 months to propagate to hydrological droughts in the Limpopo basin and the same process takes 6 months in the Okavango basin.
2. Correlations between climatic and hydrological droughts are mainly significant in March and April reaching the peak at 12-months timescale in the Limpopo basin. The same correlations were found to increase across timescale for the Okavango basin. A common timescale of 15-months was identified to be suitable for drought monitoring in Botswana. This common timescale will be useful during design of water storage reservoirs by using over the year storage concept (15-months) as hydrological measures to overcome the impacts of droughts.
3. The rescaled range analysis resulted in H-coefficients of 0.18 and 0.11 in the Limpopo and Okavango basin respectively. This reveals high variability and a likelihood of reversion in the existing drought dynamics due to the H-coefficient being significantly less than 0.5.

## **4.6 INFLUENCE OF CLIMATIC INDICES, LENGTH OF THE RAIN SEASON AND ENSO ON CEREAL YIELDS**

To understand the implications of climate variability on agriculture, the degree of association between cereal yields and climatic indices is investigated in this Section. Since it has been demonstrated in Sections 4.2 and 4.4 that large scale atmospheric circulation in the form of ENSO is also closely associated with local climate, its degree of association with cereal yields is also addressed. The climatic indices considered includes Standardised Precipitation and Evapotranspiration Index (SPEI) and Aridity Index (AI) at timescales of 1-, 3-, 6- and 12-months. The influence of the length of the rain season which takes care of onset and cessation of rain is also considered.

### **4.6.1 Crop yield data smoothing**

The double exponential smoothing technique has demonstrated its ability to detrend crop yield data as shown in Figure 4-22. The detrended cereal yields of maize and sorghum are those analysed and reported. The bivariate correlation analysis was used to investigate influences of climatic indices on crop yield from November to May (the growing season). The analysis was done for each month of the growing season to identify the period that may critically affect cereal yields.

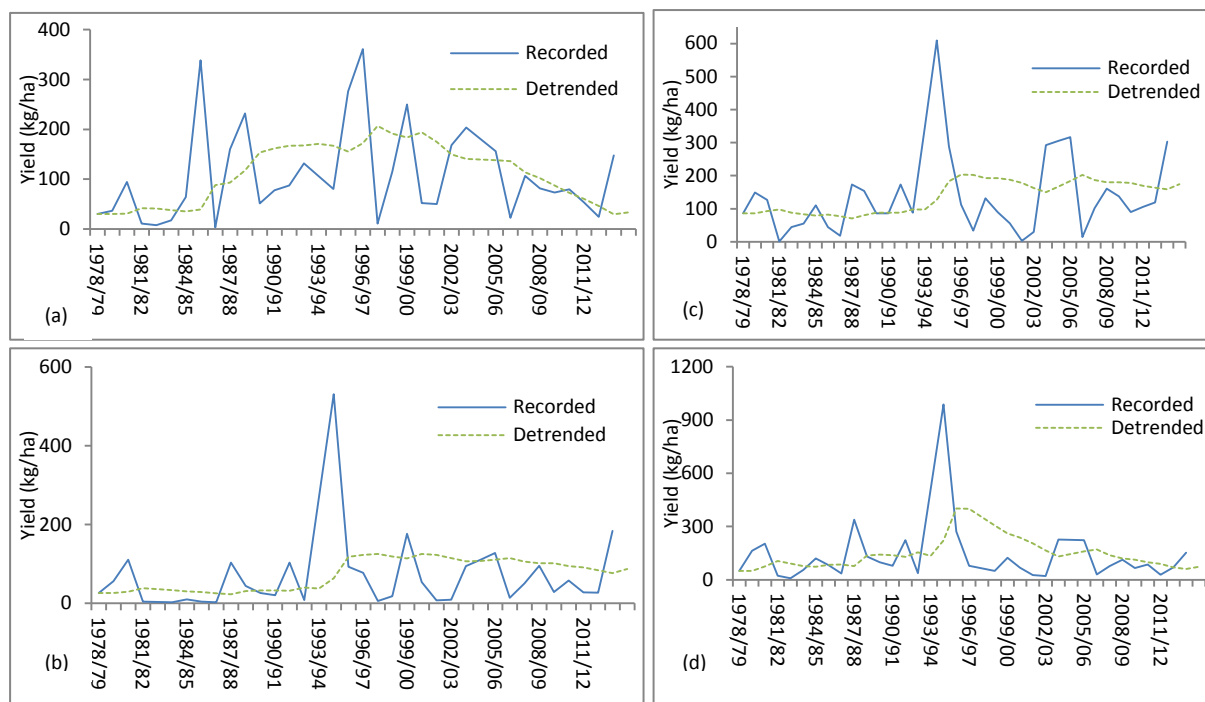


**Fig. 4-22.** Maize and sorghum yields (recorded and detrended) in selected regions (a) maize-northern, (b) maize-central, (c) sorghum-eastern, (d) sorghum-central

#### 4.6.2 Associations between cereal yields and aridity index (AI) at 1-month timescale

Results from correlation analysis between maize yield and AI original series are presented in Table 4-12. These results indicate that, in the southern region, AI accounts highly for variability in maize yield with significant correlations throughout the growing season. The months of December and January recorded the highest correlations of 0.78 and 0.77 respectively. This period also coincides with kernel and pollen shed development for maize grown in the study area. A correlation of 0.73 was also recorded for the entire growing season in this region. In the central region, only months of December and May showed significant correlations. This implies that yields are likely to be affected if moisture deficit is recorded at kernel development and grain filling stages during the maize growth cycle. Similarly in the eastern region, only January and May together with the growing season had significant correlations. The highest correlation in this region was 0.47 registered for the entire growing season. The northern region recorded a significant correlation of 0.41 in February. Months of January, March, April and May together with growing season correlations showed significant

associations for the western region. The highest correlation of 0.47 was recorded for the entire growing season in this region.

From the correlations between AI original series and sorghum yield (Table 4-12), each month of the growing season recorded significant correlations in the southern region. December recorded the strongest correlation of 0.79 while for the entire season it was 0.64. AI accounted for at least 60% in sorghum yields variation in all the months of the growing season in the southern region. AI also accounted for the highest variation of 50% in sorghum yield in the month of May for the central region. The rest of the cropping season recorded non significant correlations in this region. The eastern region had significant correlations in December, January and for the entire growing season which recorded the highest correlation of 0.52. Northern region registered a highest correlation of 0.62 in December with 0.34 recorded for the growing season. The western locations registered their strongest association of 0.48 in March and a crop season's correlation of 0.43.

**Table 4-12.** Maize and sorghum yield correlations (r) with climatic indices at 1-month timescale

Location	Climatic indices	1-Month timescale-Maize							
		Nov	Dec	Jan	Feb	Mar	Apr	May	Crop Season
Southern	AI-1	*0.68	*0.78	*0.77	*0.65	*0.66	*0.69	*0.66	*0.73
	SPEI-1	*0.65	*0.76	*0.76	*0.62	*0.65	*0.70	*0.67	*0.72
	SOI	*0.86	*0.82	*0.82	*0.80	*0.80	*0.83	*0.73	*0.85
	LRS								*0.50
Central	AI-1	0.20	*0.34	0.25	0.07	0.02	0.09	*0.56	0.32
	SPEI-1	0.14	0.32	0.24	0.10	0.05	0.13	*0.46	*0.34
	SOI	0.25	0.21	0.24	0.31	*0.35	0.16	-0.12	0.24
	LRS								0.16
Eastern	AI-1	0.06	0.13	*0.46	-0.01	0.11	0.21	*0.34	*0.47
	SPEI-1	0.00	0.19	*0.44	0.04	0.15	0.21	0.06	*0.38
	SOI	*0.37	0.31	0.32	0.30	0.28	*0.34	0.05	*0.38
	LRS								0.05
Northern	AI-1	0.30	0.04	0.32	*0.41	0.30	0.24	0.28	0.21
	SPEI-1	0.23	0.21	*0.34	*0.47	*0.33	*0.33	0.31	0.25
	SOI	0.25	0.30	0.29	*0.37	0.27	0.18	0.20	0.24
	LRS								0.22

**Table 4-12 continued**

Western	AI-1	0.25	0.32	*0.45	0.18	*0.44	*0.37	*0.42	*0.47
	SPEI-1	0.26	*0.35	*0.50	0.19	*0.47	*0.35	*0.40	*0.47
	SOI	*0.39	*0.40	*0.39	*0.39	*0.47	*0.43	0.09	*0.38
	LRS								*0.58
<b>1-month timescale-sorghum</b>									
Southern	AI-1	*0.60	*0.79	*0.69	*0.60	*0.66	*0.63	*0.76	*0.64
	SPEI-1	*0.58	*0.78	*0.67	*0.58	*0.64	*0.61	*0.73	*0.65
	SOI	*0.80	*0.72	*0.74	*0.75	*0.77	*0.72	*0.70	*0.78
	LRS								*0.62
Central	AI-1	0.14	0.27	0.22	0.27	0.21	0.11	*0.50	*0.40
	SPEI-1	0.12	0.28	0.24	0.32	0.23	0.16	*0.46	*0.43
	SOI	0.07	0.08	0.14	0.15	0.17	0.02	-0.15	0.05
	LRS								0.02
Eastern	AI-1	0.22	*0.35	*0.36	0.11	0.30	-0.17	0.30	*0.52
	SPEI-1	0.18	*0.33	*0.38	0.14	*0.33	-0.10	0.08	*0.45
	SOI	0.19	0.21	0.26	0.24	0.31	0.17	-0.19	0.24
	LRS								0.28
Northern	AI-1	*0.54	*0.62	*0.52	0.28	0.26	0.29	*0.33	*0.34
	SPEI-1	*0.56	*0.58	*0.62	0.27	*0.45	0.26	0.26	*0.50
	SOI	*0.42	*0.44	*0.46	0.30	*0.38	*0.43	*0.48	*0.42
	LRS								*0.54
Western	AI-1	0.15	0.28	*0.40	0.18	*0.48	0.29	*0.35	*0.43
	SPEI-1	0.17	0.32	*0.45	0.18	*0.51	0.30	0.32	*0.41
	SOI	0.32	*0.36	*0.33	*0.37	*0.36	0.31	0.02	0.30
	LRS								*0.60

\*significant at 95% confidence interval and LRS=length of the rain season

#### **4.6.3 Associations between cereal yields and aridity index (AI) at timescales of 3-, 6- and 12-months timescale**

Results of the correlation analysis between AI at 3-months timescale and maize yield are presented in Table 4-13. They do not show much departure from the results of correlations with AI original series presented in Table 4-12. The strongest association of 0.75 was recorded in January for the southern region. During kernel, pollen shed and silk formation period for the maize crop occurring in the months of January, February and March, AI was found to account for more than 70% of the variations in maize yield in the southern region. At the same time, a significant correlation of 0.74 was registered for the entire growing season. Similarly, all the months of the growing season recorded significant correlations in the southern region.

However the central region only registered a significant correlation of 0.36 during January. The eastern region registered significant correlations in January and for the entire growing season of 0.37 and 0.38 respectively. There were no significant correlations observed in the northern region at this timescale. However in the western region, significant correlations were registered in January, February, March, May and for the entire season with the highest correlation of 0.38 registered in January. This implies significant correlations were registered during kernel development, flowering through to full kernel capacity and full maturity.

The results between 3-months timescale AI correlations and sorghum yield are presented in Table 4-13. From these results, the southern region still showed significant correlations for the entire growing season. The strongest association of 0.70 was recorded in January while the entire growing season registered 0.64 in this region. In the central region, a significant correlation of 0.35 was observed in February a period of half bloom for the sorghum crop across the study area. Significant correlations at 3-months moving average were only observed in January and for the entire crop season of 0.35 and 0.40 respectively in the eastern region. The northern region experienced the strongest association of 0.56 in January. A correlation of 0.33 was also registered for the entire growing season. The western region recorded significant correlations during months of February, March and May, a period of pinnacle development, flowering and grain filling. The strongest correlation of 0.40 was recorded for both March and May towards full maturity of sorghum in this region.

Results from analysis of 6-months timescale AI correlations with maize yield are also presented in Table 4-13. From these results, the southern region recorded significant correlations throughout the growing season just as is the case at lower time scales. The highest correlation of 0.77 was registered in May. The central region correlations were mainly weak with none of them significant. The eastern region equally recorded weak correlations with significant values only observed in April and for the cropping season of 0.34 and 0.37 respectively. The northern region experienced significant correlations in November, December,

January, April and for the entire growing season. The strongest association of 0.43 was registered in November at tillering stage. The western region also had significant correlations during the months of February, March, April, May and the entire growing season.

At 6-months timescale AI correlations with sorghum yield (Table 4-13), the southern region indicated significant correlations for the whole season with AI accounting for more than 60% in sorghum yield variation. The strongest association of 0.68 was registered in May together with a correlation of 0.64 for the entire growing season. However the central region only registered a significant correlation of 0.34 in February. The eastern locations showed no significant correlations during the period of study. In contrast, the northern region registered significant correlation of 0.36 in March, 0.37 for both April and May. The western region had only April and May with significant correlations of 0.35 and 0.44 respectively.

Results from the 12-months timescale AI correlations with maize yield (Table 4-13) indicate that up to 70% in yield variation is accounted for by AI during the months of November, December, January, May and for the entire growing season in the southern region. The strongest association of 0.72 was recorded during the months of December and May for this region. None of the months registered a significant correlation in the central region. In contrast, the eastern and western regions registered significant correlations throughout the growing season. The strongest correlations in these regions were 0.50 and 0.42 for eastern and western regions respectively, recorded in December. Equally the northern region registered significant correlations throughout the growing season except in the month of November.

At 12-months timescale AI correlations with sorghum yield (Table 4-13), the southern region showed similar patterns to the ones at lower timescales. AI still accounted for more than 60% in sorghum yield variations in the southern region. The central and northern regions did not show any significant correlation during the growing season. However, the eastern region exhibited significant correlations of 0.45 and 0.35 in December and January respectively.

Similarly the western region showed significant correlations during the months of December and March.

Associations between aridity index and maize yield have been analysed at four (4) timescales of 1-, 3-, 6- and 12-months. The order in magnitude of correlations is observed not to vary substantially with increasing timescale. This could be attributed to the fact that during the summer growing season, evapotranspiration (ET) rates are relatively high limiting moisture storage that would be of importance at higher timescales. Evapotranspiration rates have been reported to be 4 times higher than rainfall during summer period (Byakatonda et al., 2016). This revelation could imply that monthly aridity index (AI) series is sufficient in describing maize yield variability in Botswana. This also corroborates findings by Bannayan et al. (2010) who found zero lags of AI to be sufficient in predicting wheat and barley yields in other semiarid areas of Iran. From the results presented in subsection 4.6.2 and 4.6.3, significant correlations between maize yield and AI are observed throughout the growing season mainly in the southern region. In the central and eastern regions, significant correlations occur mainly during the months of December, January and May. During the period of December-January, maize crop in Botswana undergoes silk formation, kernel and pollen shed development while during the month of May grain filling takes place. During the same period, the sorghum crop undergoes panicle development and flowering. These are critical phenological stages where plant moisture stress causes yield loss (Darby and Lauer, 2004). This implies that for better yields in the southern and western regions, sustained adequate moisture supply is paramount for the entire growing season. This makes it unfeasible to maintain high yields in these locations. From Figure 1-2 and Figure 3-2, these regions are observed to be occupying low rainfall areas of Botswana and highly variable with coefficient of variation greater than 40%. Hulme (1992) and Nsubuga et al. (2014) in their studies reported that CVs greater than 20% is an indicator of unreliable rainfall posing high risk to rainfed farming. This may explain low cereal yields in these locations compared to the central, eastern and northern regions.



As the case with maize yield, correlations between sorghum yield and AI are performed at 4 timescales. The patterns of correlations across regions are similar to those of maize yield and AI with the southern region showing significant correlations. Crop season's correlations of sorghum yields returned weaker associations as compared to those of maize yield at all the 4 moving average windows. This could be in support of Critchley et al. (1991) who in their studies established that sorghum's crop water requirement is 500 mm/season compared to 600 mm/season for maize. Further still Gerik et al. (2003) indicates that during tillering and vegetative development stages, sorghum is more tolerant to moisture stress in comparison with maize. This may explain the lower association of sorghum with climatic indices which makes it a better option for the southern locations than maize as a drought resistant crop. Comparing correlations between timescales shows no substantial changes in the degree of association. This demonstrates that also monthly AI series can adequately be used to monitor sorghum yield across Botswana.

#### **4.6.4 Associations between cereal yields and Standardised Precipitation**

##### **Evapotranspiration Index (SPEI) at 1-month timescale**

Results of the analysis at 1-month SPEI (SPEI-1) with maize yield in Table 4-12 revealed that, the strongest association between SPEI and maize yield in the southern region is 0.76. This association was registered for both December and January, a period of kernel and brace roots development for the maize crop in Botswana. SPEI accounts for more than 60% of yield variation in the southern region. The entire growing season recorded a correlation of 0.72 in this region. In the central region, correlations were generally weak with highest of 0.46 and 0.34 only observed in May and for the growing season respectively. The eastern region exhibited significant correlations of 0.44 and 0.38 in January and for the entire growing season respectively. The northern region recorded significant correlations in January, February, March and April with a highest correlation of 0.47 realised in February. The western region had

significant correlations throughout the growing season with only November and February showing non significant correlations. The strongest association of 0.50 was recorded in January for this region.

Results of correlation between sorghum yield and SPEI-1 (Table 4-12) presents the southern region with the strongest correlation of 0.78 recorded in December and crop season's association of 0.65. Significant correlations were again observed throughout the growing season. Conversely, for the central region only correlations in May and for the entire season were significant amounting to 0.46 and 0.43 respectively. In the eastern region, significant correlations were observed in December, January, March and for the entire season. The strongest degree of association in this region was 0.45 registered for the entire growing season. In the northern region, the strongest association of 0.62 was registered in January and the crop season's correlation of 0.50 was also realised. In the western region, significant correlations were observed in January, March and for the entire growing season of 0.45, 0.51 and 0.41 respectively.

#### **4.6.5 Associations between cereal yields and Standardised Precipitation**

##### **Evapotranspiration Index (SPEI) at 3-, 6- and 12-months timescale**

Results from analysis of 3-months SPEI (SPEI-3) with maize yield presented in Table 4-13 show that the southern region still exhibits significant correlations throughout the growing season. These results also reveal that SPEI-3 accounts for more than 60% in maize yield variation in this region. The strongest correlation of 0.74 was recorded in January while the crop season's correlation was 0.70. The only significant correlation in the central region was 0.37 registered in January. Eastern region showed similar patterns as the central region with the only significant correlations of 0.39 and 0.36 registered in January and the entire growing season respectively. In the northern region, a significant correlation of 0.41 was registered for both March and April. The western region showed mostly significant correlations except for

November. The strongest correlation of 0.47 was registered in January and February in the western region.

Results from analysis between SPEI-3 and sorghum yield (Table 4-13) showed the highest correlation in the southern region of 0.67 registered in January. A crop season's correlation of 0.59 was also realised with significant correlations throughout the growing season as the case for SPEI-1. However in the central region, only February showed significant correlation of 0.35. The eastern region registered significant associations in January, March and entire crop season amounting to 0.35, 0.34 and 0.40 respectively. Correlations in the northern region were mainly significant except for the months of November, April and May. The strongest correlation of 0.56 was recorded in January for this region. In the western region, significant correlations were recorded throughout the growing season except at the beginning of the season in November and December. The highest correlation of 0.46 was recorded in March for the western region.

**Table 4-13.** Maize and sorghum yield correlations (r) with climatic indices at timescales of 3-, 6- and 12-months

Location	Climatic indices	3-Months timescale-Maize							
		Nov	Dec	Jan	Feb	Mar	Apr	May	Crop season
Southern	AI-3	*0.62	*0.67	*0.75	*0.72	*0.71	*0.65	*0.65	*0.74
	SPEI-3	*0.57	*0.64	*0.74	*0.72	*0.68	*0.67	*0.68	*0.70
Central	AI-3	-0.04	0.28	*0.36	0.24	0.13	0.07	0.10	0.22
	SPEI-3	-0.10	0.23	*0.37	0.25	0.15	0.09	0.13	0.22
Eastern	AI-3	-0.10	-0.01	*0.37	0.30	0.26	0.13	0.21	*0.38
	SPEI-3	-0.20	-0.05	*0.39	0.29	0.27	0.15	0.19	*0.36
Northern	AI-3	0.30	0.15	0.20	0.23	0.31	0.27	0.26	0.23
	SPEI-3	0.22	0.02	0.21	0.32	*0.41	*0.41	0.32	0.20
Western	AI-3	0.17	0.31	*0.38	*0.37	*0.40	0.30	*0.41	*0.36
	SPEI-3	0.18	*0.34	*0.47	*0.47	*0.45	*0.38	*0.43	*0.40
<b>6-Months timescale-Maize</b>									
Southern	AI-6	*0.64	*0.64	*0.69	*0.68	*0.69	*0.75	*0.77	*0.73
	SPEI-6	*0.58	*0.60	*0.67	*0.64	*0.66	*0.69	*0.95	*0.73
Central	AI-6	-0.08	0.19	0.20	0.26	0.21	0.25	0.19	0.20
	SPEI-6	-0.13	0.14	0.26	0.26	0.20	0.23	0.19	0.21
Eastern	AI-6	-0.03	0.01	0.30	0.24	0.25	*0.34	0.32	*0.37
	SPEI-6	-0.19	-0.06	0.23	0.21	0.23	*0.35	0.31	0.25
Northern	AI-6	*0.43	*0.38	*0.35	0.28	0.26	*0.33	0.31	*0.33
	SPEI-6	0.23	0.06	0.20	0.27	0.23	0.22	0.26	0.15
Western	AI-6	0.17	0.18	0.30	*0.35	*0.34	*0.35	*0.41	*0.36
	SPEI-6	0.13	0.19	*0.40	*0.41	*0.45	*0.43	*0.47	*0.39
<b>12-Months timescale –Maize</b>									
Southern	AI-12	*0.71	*0.72	*0.69	*0.68	*0.68	*0.68	*0.72	*0.70
	SPEI-12	*0.70	*0.71	*0.69	*0.66	*0.69	*0.68	*0.67	*0.70
Central	AI-12	0.16	0.23	0.21	0.24	0.20	0.21	0.22	0.21
	SPEI-12	0.14	0.22	0.24	0.23	0.18	0.22	0.21	0.21
Eastern	AI-12	*0.33	*0.50	*0.46	*0.33	*0.33	*0.40	*0.40	*0.40
	SPEI-12	0.32	*0.42	*0.44	0.29	0.27	*0.33	0.32	*0.37
Northern	AI-12	0.32	*0.33	*0.41	*0.43	*0.43	*0.40	*0.43	*0.40
	SPEI-12	0.27	0.28	0.26	0.24	0.28	0.26	0.26	0.26
Western	AI-12	*0.37	*0.42	*0.34	0.31	*0.39	*0.36	*0.39	*0.37
	SPEI-12	*0.40	*0.46	*0.40	*0.38	*0.42	*0.41	*0.44	*0.39

**Table 4-13 continued**

<b>3-Months timescale-Sorghum</b>									
Southern	AI-3	*0.58	*0.66	*0.70	*0.65	*0.66	*0.61	*0.67	*0.64
	SPEI-3	*0.57	*0.63	*0.67	*0.60	*0.63	*0.58	*0.64	*0.59
Central	AI-3	-0.16	0.16	0.27	*0.35	0.27	0.20	0.15	0.26
	SPEI-3	-0.13	0.15	0.31	*0.35	0.30	0.25	0.21	0.28
Eastern	AI-3	-0.05	0.14	*0.33	0.25	0.29	0.13	0.17	*0.38
	SPEI-3	-0.14	0.09	*0.35	0.25	*0.34	0.17	0.19	*0.40
Northern	AI-3	0.24	*0.44	*0.56	*0.49	*0.35	0.25	0.26	*0.33
	SPEI-3	0.24	*0.44	*0.56	*0.49	*0.36	0.25	0.26	*0.33
Western	AI-3	0.08	0.21	0.31	*0.35	*0.40	0.32	*0.40	*0.33
	SPEI-3	0.14	0.30	*0.41	*0.41	*0.46	*0.39	*0.42	*0.38
<b>6-Months timescale-Sorghum</b>									
Southern	AI-6	*0.58	*0.64	*0.65	*0.63	*0.63	*0.66	*0.68	*0.64
	SPEI-6	*0.57	*0.64	*0.64	*0.60	*0.60	*0.59	*0.74	*0.60
Central	AI-6	-0.23	0.09	0.17	*0.34	0.31	0.28	0.29	0.24
	SPEI-6	-0.16	0.11	0.28	*0.36	0.32	0.31	0.30	0.28
Eastern	AI-6	0.00	0.17	0.17	0.13	0.22	0.28	0.27	0.28
	SPEI-6	-0.15	0.09	0.16	0.15	0.25	0.31	0.31	0.25
Northern	AI-6	0.13	0.20	0.29	0.32	*0.36	*0.37	*0.37	0.24
	SPEI-6	*0.40	*0.61	*0.70	*0.59	*0.58	*0.56	*0.48	*0.64
Western	AI-6	0.08	0.10	0.20	0.28	0.32	*0.35	*0.44	0.30
	SPEI-6	0.13	0.18	0.31	*0.38	*0.44	*0.43	*0.50	*0.37
<b>12-Months timescale –Sorghum</b>									
Southern	AI-12	*0.63	*0.63	*0.61	*0.61	*0.62	*0.60	*0.61	*0.61
	SPEI-12	*0.60	*0.61	*0.61	*0.60	*0.61	*0.57	*0.58	*0.61
Central	AI-12	0.19	0.26	0.23	0.31	0.24	0.26	0.27	0.25
	SPEI-12	0.23	0.31	0.30	*0.34	0.26	0.29	0.29	0.31
Eastern	AI-12	0.18	*0.45	*0.35	0.22	0.18	0.23	0.23	0.26
	SPEI-12	0.28	*0.46	*0.35	0.23	0.22	0.27	0.25	0.30
Northern	AI-12	0.17	0.18	0.21	0.19	0.22	0.21	0.20	0.17
	SPEI-12	*0.52	*0.55	*0.63	*0.60	*0.56	*0.55	*0.52	*0.57
Western	AI-12	0.32	*0.38	0.25	0.25	*0.35	0.29	0.32	0.29
	SPEI-12	*0.39	*0.44	*0.37	*0.34	*0.41	*0.38	*0.41	*0.36

\*significant at 95% confidence interval

Results from 6-months SPEI (SPEI-6) with maize yield are shown in Table 4-13. The strongest correlation of 0.95 was recorded in May for the southern region. Significant correlations are recorded throughout the growing season with crop season's correlation of 0.73. The central region showed weak correlations throughout the season while the eastern region registered the only significant correlation in April of 0.35. The northern region generally shows weak correlations for all the months with none of them being significant. The western region mostly

registered significant correlations except at the beginning of the cropping season in November and December. The region's strongest correlation was 0.47 realised in May while the entire season it was 0.39.

Results from analysis between SPEI-6 and sorghum yield (Table 4-13) also showed significant correlations in the southern region for all the months in the growing season. The strongest correlation of 0.74 was observed in May while 0.60 was recorded for the entire growing season. In the central region, only February showed significant correlation of 0.36. In the east, correlations were mainly weak with none of the months showing significant correlations for the entire season. Significant correlations in the northern region were observed for the entire season. The highest variation in sorghum yield that could be accounted for by SPEI-6 was 70% occurring in January in the northern region. The western region showed also significant correlations in February, March, April, May and for the entire growing season.

Results of 12-months SPEI (SPEI-12) with maize yield are also presented in Table 4-13. These results revealed similar patterns in the southern region as those at lower timescales. The highest correlation of 0.71 in the region was registered in December. A significant crop season's correlation of 0.70 was also realised for the entire growing season. The central region still showed weak correlations with none of them significant. Eastern region showed significant correlations in December, January, April and for the entire growing season. The highest correlation of 0.44 was registered in January in this region. In the northern region non significant correlations were registered for all the months in the growing season. In the western region, all the months including crop season correlations were significant with a highest of 0.46 registered in December.

Results from analysis of correlations between SPEI-12 and sorghum yield (Table 4-13) indicates that SPEI accounts for 60% in sorghum yield variations for most of the season in the southern region. In contrast, the central region only registered a significant correlation of 0.34

in February. Also in the eastern region, the only significant correlations of 0.46 and 0.35 were registered in December and January respectively. Conversely, the northern region registered significant correlations for the entire season. The strongest correlation in this region of 0.63 was registered in January and 0.57 for the entire growing season. Similarly the western region recorded significant correlations for the whole season with the strongest being 0.44 realised in December.

The influence of SPEI on maize yield in this study is also investigated at 4 timescales described in subsection 4.6.4 and 4.6.5. The patterns of correlations between SPEI and maize yield are similar to those between AI and maize yield. The southern region still show significant correlations for the entire growing season implying that any negative SPEI experienced during the season could result in maize yield reduction. The central and eastern regions only showed significant correlations in January and May respectively while the northern and western from January to May for SPEI-1 meaning that moisture deficits occurring in these months would lead to yield loss. These periods of significant associations are linked to critical crop growth stages. This may explain low cereal yields across Botswana compared to the continental average.

Since correlation for both AI and SPEI with maize yield are in the same order across the study area, it could imply that both AI and SPEI are important in monitoring and/or predicting maize yield with equal accuracy. This could be attributed to the fact that in the computation of both AI and SPEI, rainfall and temperature are the main variables. Association of SPI and maize yield have been previously conducted in Botswana by Batisani (2012). Their study also found significant relationships in the south pointing to the fact that, rainfall rather than temperature may be the most influencing factor of yield since rainfall is the only variable in SPI.

Similarly correlations between SPEI and sorghum yield are investigated at 4 timescales. Significant correlations are observed across the study area for the entire growing season. This

could be attributed to significant associations registered at critical phenological stages that occur in December, January and May. Further still, SPEI is an aggregation of temperature and rainfall which are known climatic factors that affect cereal yields. These factors (temperature and rainfall) have been identified to be influenced by events of global warming (Costa and Soares, 2009b; Hänsel et al., 2016). Studies by Rowhani et al. (2011) in Tanzania revealed that variations in rainfall and temperature are injurious to yields of maize and sorghum. From correlations between sorghum yield and SPEI, this study reveals minor variations in correlations at different timescales. This makes SPEI-1 adequate in monitoring sorghum yield across the study area. Since SPEI is a measure of drought severity of a given location, its close association with cereal yields goes a long way in describing how drought is impacting on the food security situation of that location. From drought monitoring strategies, projections of sorghum yield can be made to aid planning.

#### **4.6.6 Association between Southern Oscillation Index (SOI) and cereal yields at 1-month timescale**

Results for analysis of the influence of large climatic predictors represented by SOI on maize yield are shown in Table 4-12. The SOI accounted for the highest variation in maize yield over the study area. The highest correlation of 0.86 was recorded in November in the southern region with crop season's correlation of 0.85 also realised. All correlations were significant for the entire growing season in the southern region. In the central region, the only significant correlation of 0.35 was registered in March while in the eastern region significant correlations were registered in November, April and for the entire growing season. The influence of SOI on maize yield in the northern region was not statistically significant except for the month of February which realised a correlation of 0.37. In the western region, significant correlations were observed for the entire growing season except May. The strongest association of 0.47 was registered in March with crop season's correlation being 0.38.



Results of correlations between SOI and sorghum yields are also presented in Table 4-12. These results reveal that in the southern region SOI accounted for up to 80% in sorghum yield variation occurring in November. SOI accounted for 78% of sorghum yield variations for the entire growing season in this region. However in the central and eastern regions, no significant correlations were registered. In the northern region, significant correlations were observed throughout the season except for February. The strongest association in this region was 0.48 registered in May. Significant correlations are further observed in the west for the months of December, January, February and March.

SOI representing large scale climatic predictors has been observed to account for the biggest percentage of maize yield variations in the southern region. This implies that maize yield in regions with significant correlations can benefit from longterm SOI predictions currently ongoing. Based on forecasts of climatic indices such as North Atlantic Oscillation (NAO), Bannayan et al. (2011) demonstrated that barley and wheat yields could accurately be predicted. In Botswana, managers and policy makers in the agricultural sector could use this information to predict yields in these locations at the beginning of the growing season. The rest of the regions with non significant correlations can still benefit from other prediction mechanisms such as ANN used in this research.

Significant correlations between SOI and sorghum yield are also observed in southern region though lower than those of maize yields. Since it has been indicated that positive SOI are associated with high yields, it means that sorghum is likely to register higher yields than maize under moisture deficit conditions. With high degree of associations between sorghum and SOI, sorghum yield can also benefit from predictions of large scale predictors conducted by various agencies. However the high association between cereal yields and SOI in the region could be injurious to crop production.

#### **4.6.7 Association between Length of the rain season (LRS) and cereal yields**

Results from the investigation of the influence of LRS on maize yield are presented in Table 4-12. The results are aggregated for the entire growing season. The investigations reveal that, LRS only registered significant correlations in the southern and western regions of 0.50 and 0.58 respectively. For the rest of the study area, maize yield was not significantly associated with LRS.

Associations of LRS with sorghum yield are also presented in Table 4-12. The LRS accounts for 62% of sorghum yield in the southern region. The central, eastern and northern regions all showed non significant correlations while in the northern region LRS accounted for 54% in sorghum yield variations. In the western region, LRS accounts for 60% of sorghum yield variation.

Results from this analysis indicate a positive association between LRS and maize yield in all regions, however only significant in the southern and western regions. Association between LRS and sorghum yield were equally positive though only significant in the southern and western regions as well as in the north. This implies that sorghum yield is more affected by fluctuations in LRS across the study area compared to maize yield. These positive associations indicates that the longer the LRS the higher the yields are expected. Amekudzi et al. (2015) in their study found that climate variability has tendency of altering the onset and cessation of rain and hence the LRS. Further still semiarid areas have been identified to suffer from higher incidences of climate variability than any other region (Omoyo et al., 2015; Byakatonda et al., 2016; Khan et al., 2016). This makes areas in the south and west which are low rainfall areas in Botswana more vulnerable to fluctuations in LRS as a result of increased climate variability and hence low yielding areas. This may explain the high associations in these regions.

Correlations are mostly significant in the southern and western regions all located in low rainfall areas of Botswana with unreliable rainfall expressed through high CVs. This agrees

with studies by Modarres and da Silva (2007) who revealed that drier locations experiences higher rainfall uncertainties that in turn affect agricultural production. Yields in central and eastern regions are less influenced by fluctuations in LRS hence registering higher yields compared to southern and western locations.

#### **4.6.8 Spatial distribution of correlations ( $r$ ) between cereal yields and climatic indices**

Spatial representation of the influence of AI and SOI on maize yield in Figure 4-23(a) and 4-23(b) indicate that yields in the central and northern regions are not significantly influenced by these climatic indices as compared to the south, west and east of the study area. However correlations between AI and sorghum yield (Figure 4-24a) were significant in all the regions across the study area. Also the patterns of correlations between maize yield and SPEI-1 in Figure 4-23(c) reveal similar direction as those of maize yields and AI except that the central region exhibited a significant correlation. Significant correlations which are shown on the maps are mainly observed in the south, east and southeast. Spatial and temporal patterns of AI, SPEI and SOI influence on crop yield indicates a northwest to southeast increasing gradient.

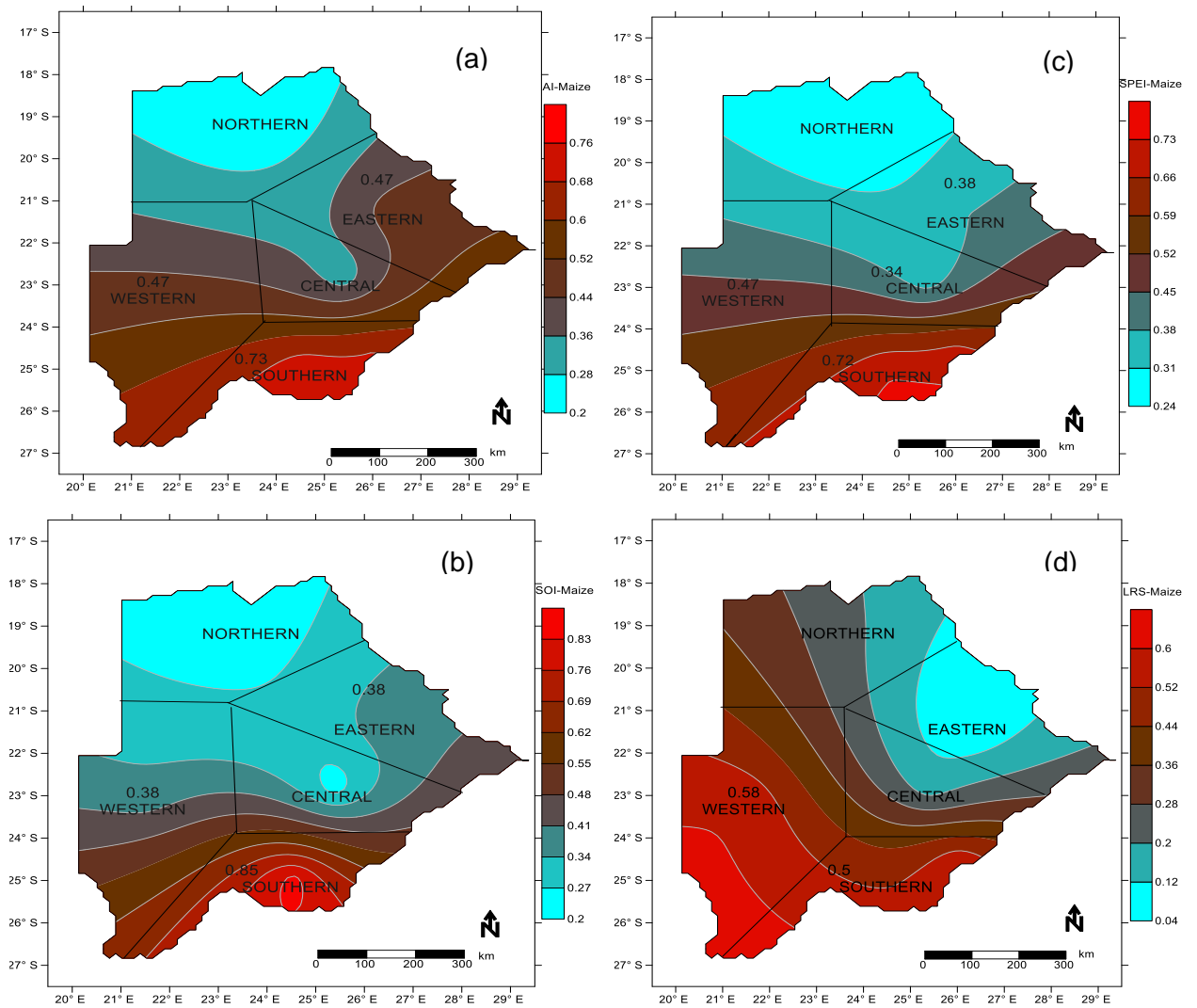


**Fig. 4-23.** Spatial distribution of correlations ( $r$ ) (significant values are shown) between maize yield and (a) Aridity Index (AI), (b) Southern oscillation index (SOI), (c) Standardised Precipitation Evapotranspiration Index (SPEI) and (d) Length of the rain season (LRS)

Spatial patterns of correlations between sorghum yields and SPEI-1 in Figure 4-24(c) revealed that yields across the study area are significantly associated with SPEI-1. There was no particular gradient observed to describe the pattern of correlations between regions. Presentation of correlations between sorghum yield and SOI at spatial and temporal scales is shown in Figure 4-24(b). The distribution show yields in the southern and northern locations being significantly associated with SOI. Sorghum yield in the western, central and eastern regions were not significantly associated with ENSO activities in the Equatorial Pacific.

Spatial representations of the influence of LRS on maize and sorghum yields are presented in Figure 4-23(d) and Figure 4-24(d) respectively. Patterns revealed that cereal yields in the southern and western regions were significantly affected by variability in LRS which could be attributed to high rainfall variability with CVs greater than 40% in these locations. Yields in the eastern and central regions were not significantly influenced by LRS except the northern locations for sorghum yield. Correlation patterns showed an east to southwest increasing gradient.

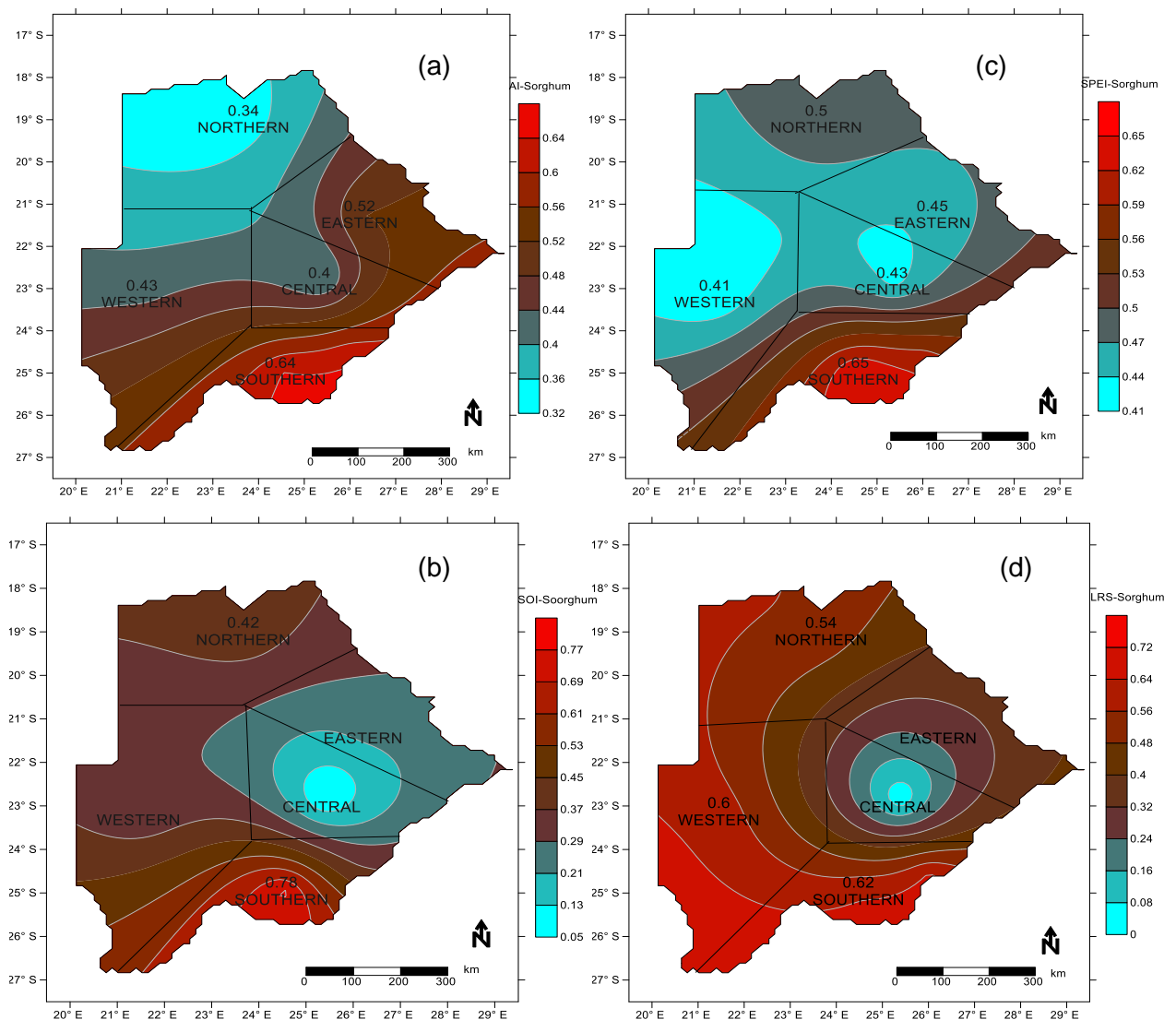


**Fig. 4-24.** Spatial distribution of correlations (r) (Significant values are shown) between sorghum yield and (a) Aridity Index (AI), (b) Southern oscillation index (SOI), (c) Standardised Precipitation Evapotranspiration Index (SPEI) and (d) Length of the rain season (LRS)

#### **4.6.9 Comparisons between climatic indices and crop yield trends**

Plots of detrended yield anomalies and climatic indices such as AI, SPEI, SOI and LRS are presented in Figure 4-25. The southern region, where significant correlations have been reported throughout the growing season, is used for illustration purposes. It is evident from the plots that the cereal yields followed the spatial and temporal patterns of the climatic indices. From Figure 4-25, it is observed that in the year 1995/96 when a yield jump was registered (Figure 4-22), a close match between the climatic indices and the yield anomalies was observed. Figure 4-25(a) indicates that positive anomalies of aridity index coincided with positive yield anomalies. Likewise in Figure 4-25(c) where positive SPEI signifies wet conditions, periods of positive yield anomalies matched with positive SPEI. Similarly positive SOI which is associated with rain seasons in the study area, are shown in Figure 4-25(b) to correspond with positive yield anomalies. Figure 4-25(d) also demonstrated how fluctuations in LRS could affect crop yield. The plot shows that the longer the LRS the higher the yield, as demonstrated by the alignment of positive anomalies of LRS and yield.

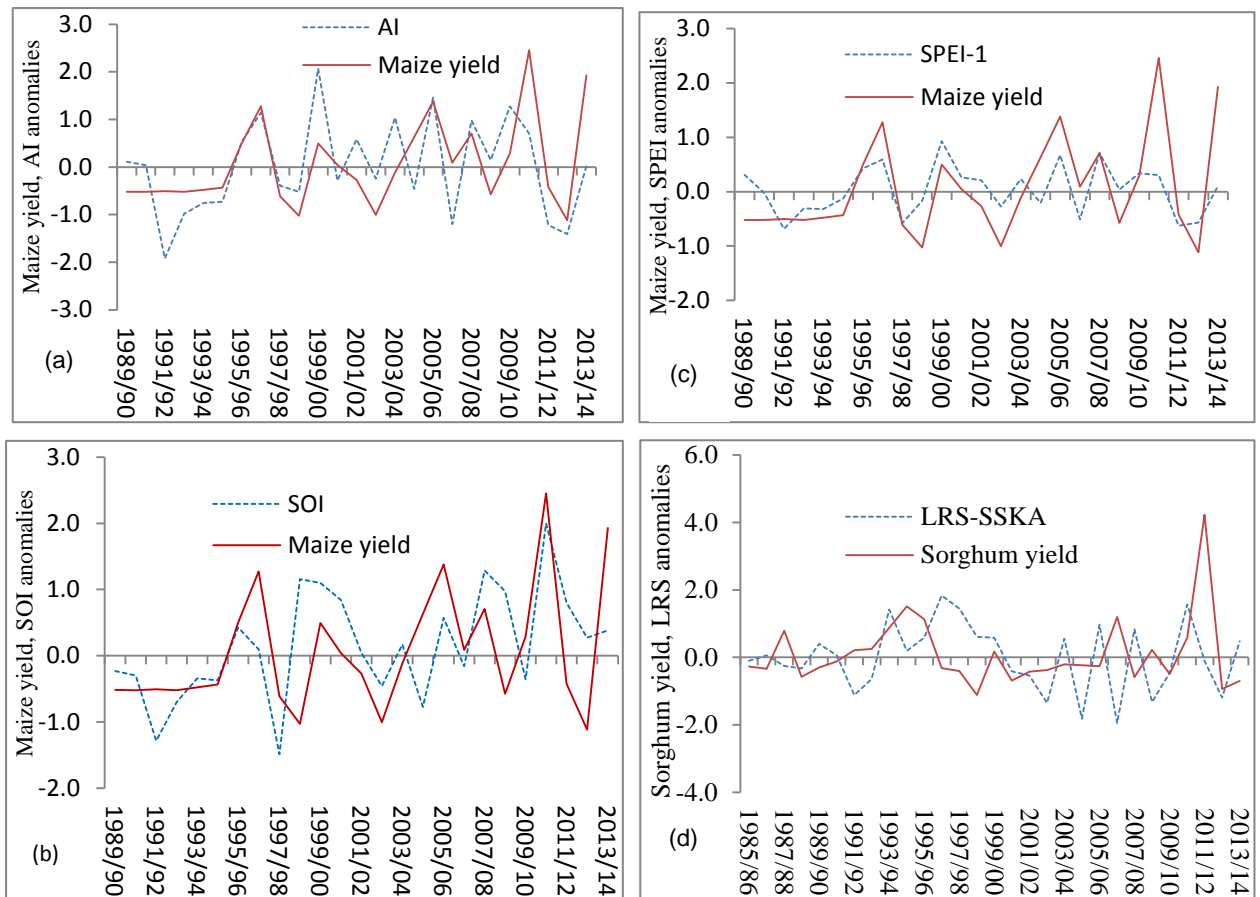


**Fig. 4-25.** Comparisons between time series of climatic indices and crop yield anomalies (a) AI and maize yield, (b) SOI and maize yield (c) SPEI and maize yield, (d) LRS and sorghum yield

#### 4.6.10 Summary

The influence of climatic indices such as Aridity Index, Standardised Precipitation Evapotranspiration Index, Southern Oscillation Index and Length of the Rain Season on cereal yields of maize and sorghum has been analysed. Investigations were performed through bivariate correlations between the climatic indices and maize yield on one hand and between climatic indices and sorghum yield on the other hand. From the results and discussions in subsection 4.6, the following summary is deduced from:

1. Maize yield is highly associated with climatic indices in the southern and western regions which are traditionally low rainfall areas. AI, SPEI, SOI and LRS accounts for a maximum of 73%, 72%, 85% and 50% of maize yield variations for the entire growing season in the

southern region respectively. This research also revealed that, the timescale of 1-month is adequate in monitoring maize yields in Botswana. It is also observed that SOI has the greatest influence on maize yield over other climatic indices further confirming the pronounced effect of ENSO on the local climate.

2. Significant associations between sorghum yield and climatic indices are predominant in the southern region. However, they were observed to be lower than those between climatic indices and maize yield. The strongest associations between AI, SPEI, SOI, LRS and sorghum yield for the crop season are 64%, 65%, 78% and 62% respectively. The lower correlations between climatic indices and sorghum yield compared to maize yield could mean that sorghum may yield better than maize under climate variability and change.



## **4.7 MODELING ONSET AND CESSATION OF RAIN, STREAM FLOW DROUGHT AND CEREAL YIELDS USING ARTIFICIAL NEURAL NETWORK**

To facilitate planning for water and agricultural resources in Botswana, predictions have been made using artificial neural network models. The models provide 5-years ahead predictions with the historical period ending in 2015/16. This Section provides predictions for onset and cessation of rain dates and hydrological flow index in the Okavango and Limpopo river basins. The Section further provides crop yield projections of maize and sorghum over the same time period. Nonlinear autoregressive with exogenous input (NARX) ANN model explained in subsection 3.3.6 is used to provide these predictions. Each model has a unique configuration specific to a particular variable being predicted. Sufficient neurons that can adequately learn the various interrelations between targets and inputs were selected for each of the predictions.

### **4.7.1 Prediction of rain onset and cessation dates**

The model used in the prediction of onset and cessation of rain dates comprised of an input regressor, one hidden layer and an output layer. The model architecture was made up of 9 neurons in the hidden layer with maximum delay of 4. The input vector comprised of seasonal rainfall totals, number of rainy days, dry spell frequency and length of the rain season. Results from the performance of ANNs and 5-years ahead predictions are presented in Table 4-14. Model performance is presented for both open loop (one step ahead prediction) and closed loop (multistep ahead prediction). From performance results, most of the stations used in this study show lower mean squared error (MSE) during open loop operations compared to closed loop. This is a clear manifestation that the network was able to learn well the predictors before the simulations were made. Coefficients of correlation ( $r$ ) were significantly high for all the stations which give credence to the predictions. The best performing network was recorded at Jwaneng with onset and cessation predictions returning 95% and 94% respectively.

**Table 4-14.** Artificial Neural Network (ANN) model performance together with onset and cessation of rain predictions

Station	Mean Squared Error (MSE)				Correlation (r) between targets and outputs		Historical mean date		Predicted 5-year mean date (2017-2021)	
	Open loop		Closed loop							
	Onset	Cessation	Onset	Cessation	Onset	Cessation	Onset	Cessation	Onset	Cessation
Francistown	0.05	0.19	0.45	0.26	0.77	0.67	30-Nov	9-Mar	28-Oct	7-Mar
Ghanzi	0.10	0.08	0.17	0.78	0.80	0.89	15-Dec	15-Mar	4-Jan	11-Apr
Jwaneng	0.03	0.05	0.68	0.34	0.95	0.94	15-Dec	20-Mar	7-Dec	13-Apr
Kasane	0.02	0.11	0.68	0.48	0.96	0.84	2-Dec	18-Mar	26-Nov	3-Mar
Lethlakane	0.10	0.03	0.31	0.17	0.89	0.95	3-Jan	17-Mar	2-Dec	26-Feb
Mahalapye	0.09	0.12	0.24	0.84	0.79	0.81	3-Dec	3-Mar	25-Nov	19-Feb
Maun	0.11	0.11	0.19	0.13	0.77	0.80	17-Dec	9-Mar	23-Nov	6-Mar
Pandamatenga	0.05	0.00	0.52	0.73	0.82	0.99	1-Dec	28-Mar	1-Jan	2-Apr
Selibe-Phikwe	0.08	0.02	0.16	0.11	0.90	0.94	11-Dec	12-Mar	31-Dec	6-Mar
Shakawe	0.04	0.07	0.21	0.56	0.89	0.86	9-Dec	31-Mar	5-Dec	13-Mar
SSKA	0.03	0.06	0.23	0.55	0.94	0.92	4-Dec	8-Mar	8-Nov	20-Feb
Sowa Pan	0.11	0.06	0.07	0.67	0.83	0.95	7-Dec	13-Mar	21-Dec	4-Mar
Tsabong	0.05	0.09	0.55	0.23	0.91	0.83	11-Jan	25-Feb	10-Jan	14-Mar
Tshane	0.08	0.07	0.22	0.33	0.83	0.84	28-Dec	23-Feb	26-Dec	16-Feb

ANN model performance is further demonstrated in Figure 4-26 through graphical representation of observed and predicted onset and cessation dates at various locations such as Kasane in the north, SSKA in the south and Ghanzi in the west. The plots reveal a nearly close fit between the observed and model outputs. This further demonstrates the NARX model's ability to provide accurate onset and cessation dates predictions. The results reveal that at 71.4% of the stations, onset and cessation of rain is coming earlier than during the historical period for between 2 to 4 weeks. This is an indication of a shift in the rainfall season across Botswana. These results also show that in addition to the shift in the rain season, the length of the season is likely to get shorter in the next 5 years at 50% of the stations. At Shakawe, Tsabong and Tshane rain onset dates are likely to remain the same with variations within a week. Cessation dates were also observed to remain the same at Francistown, Maun and Selibe-Phikwe.

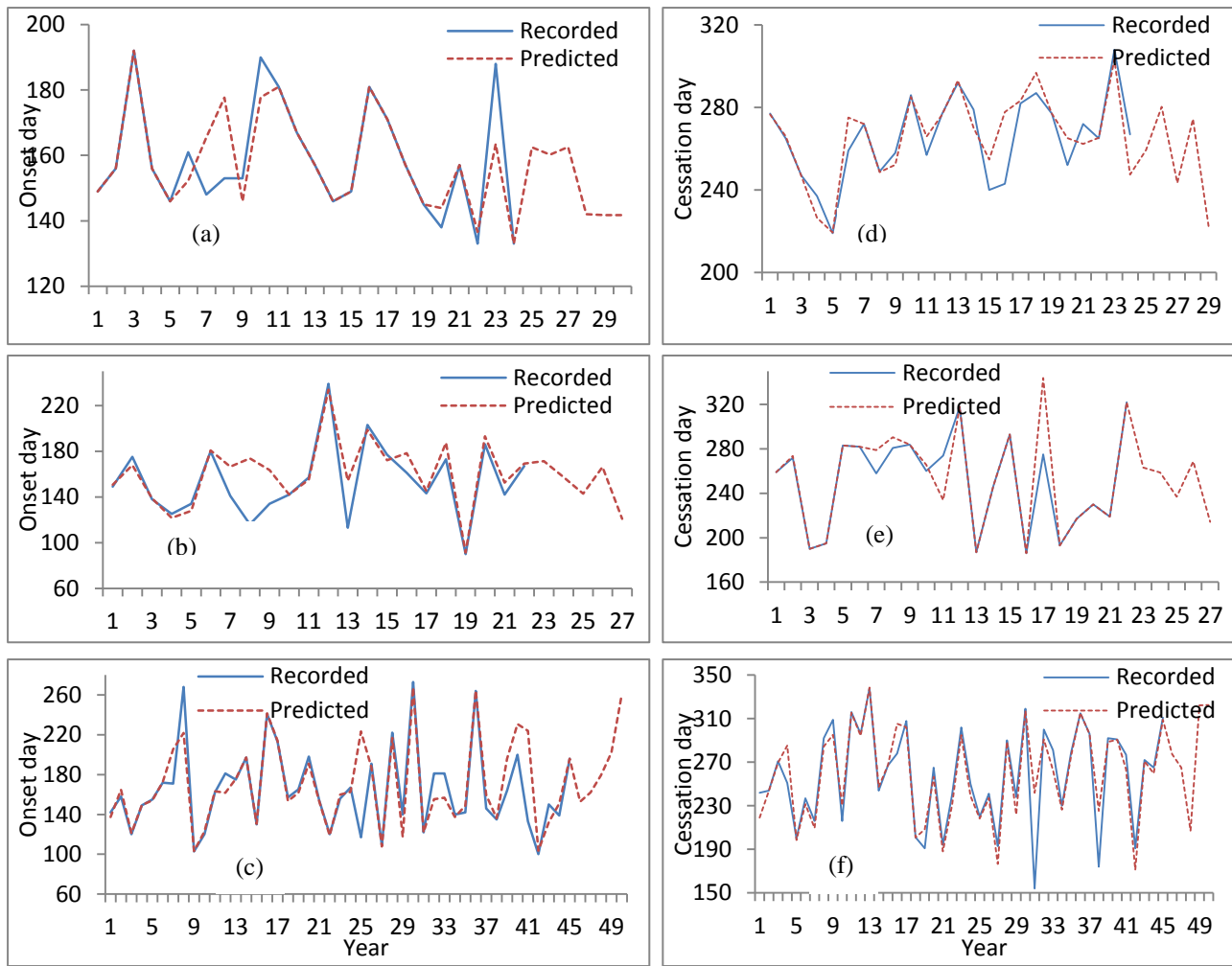


**Fig. 4-26.** Artificial Neural Network (ANN) model outputs and targets for onset and cessation dates at selected station. Onset dates predictions at (a) Kasane, (b) SSKA, (c) Ghanzi and cessation dates predictions at (d) Kasane, (e) SSKA, (f) Ghanzi

Realistic prediction of onset and cessation of rain dates are essential for successful rainfed farming. The NARX artificial neural network (ANN) model has demonstrated its capability to predict onset and cessation dates. High model performances as expressed through coefficient of correlation in the order of 95% are reported at Jwaneng and Sowa Pan. Predictions indicate that at 71.4% of the stations a shift in the rain season is likely in the next five years. At these stations, both early onset and cessation of rain is expected in the next five years (2017-2021) signaling a shift in the rain season. The shift in the rain season could be attributed to climate variability which is a prominent feature in semiarid areas. This is in agreement with studies

conducted by Omoyo et al. (2015) and Amekudzi et al. (2015) in Kenya and Ghana respectively. In their studies, they found out that high climate variability shifted the onset and cessation of rain at the same time shortening the length of the growing season. This likely shift in rain season in the near future could pose a threat to the food security situation of Botswana. The shortening of the rain season could also be part of the climate change cycle that has been projected by the IPCC scenarios to get worse in drier locations of the arid and semiarid locations (Pachauri and Reisinger, 2008; Stocker et al., 2013). This makes this research handy since information generated here could be useful in mitigating effects of climate change and variability if passed on to the various stakeholders in a timely manner.

#### **4.7.2 Predictions of Stream flow droughts**

A 15-months timescale was identified in Section 4.5 to adequately monitor drought dynamics in Botswana. Attempts were made to investigate futuristic behaviour of drought dynamics at this timescale through the Hurst coefficient. The results indicated a reversion and it was hence necessary to validate and quantify this behavior through predictions provided by the NARX neural network model. The model applied in this prediction comprised of 11 neurons in the hidden layer with a maximum delay of 4. The input vector for this model consisted of monthly rainfall, SPEI-15, minimum and maximum temperature. Predictions were made on a monthly basis for 60 months to guide water resources operations and planning in the Limpopo and Okavango basins. Results from the ANN model of future standardised flow dynamic conditions are presented in Figure 4-27. These results indicate that the NARX network is effective in learning the relationship between the inputs and the targets to produce an output that closely matched the actual targets. The model showed high performance with correlation coefficient of 0.88 in Limpopo basin and 0.99 in the Okavango. It is observed that, the NARX model performed better in the Okavango basin compared to the Limpopo.

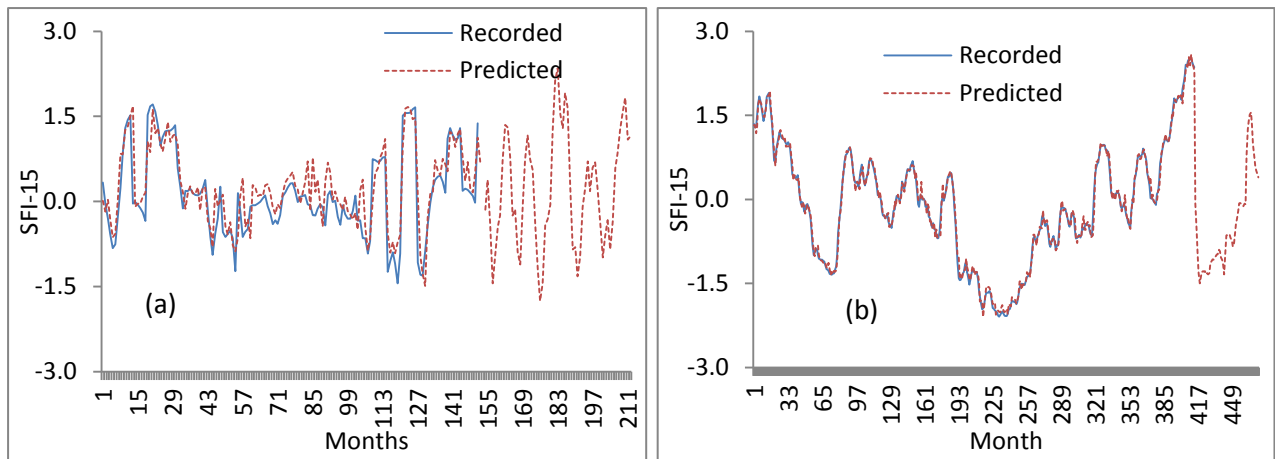


**Fig. 4-27.** Artificial Neural Network (ANN) model outputs and targets for standardised flow index (SFI) at the two river basins (a) Limpopo (b) Okavango

At the end of the historical period (June-2016 corresponding to month number 151 on the plot), the Limpopo basin (Figure 4-27a) was experiencing near normal wet conditions. A reversion as projected by the Hurst phenomenon in Section 4.5 is indeed observed with dynamics expected to change to near normal dry conditions at the beginning of the prediction period. These dry conditions are likely to continue for the next 8 months while the following 4 months may be characterised with wet spells. A high frequency between dry and wet spells is likely in the Limpopo basin in the next 60 months. Extreme wet conditions are expected during summer of 2018/19 corresponding to months number 187, 188, 189 and 190 on the plot (Figure 4-27a).

In the Okavango basin, equally a reversion from wet conditions at the end of the historical period (month number 409 on the plot) to moderate dry periods was observed as shown in Figure 4-27b. These moderate dry conditions are likely to continue for the next 24 months (until the end of 2017/18). The two years (2018/19 and 2019/20) following this period are expected to remain dry but under near normal conditions. The final year of the prediction period (2020/21) is likely to experience moderately wet conditions.

Equally the NARX model has demonstrated its ability to predict drought severity with help of appropriate exogenous inputs. This demonstration is based on the high performance levels exhibited by the model. The model confirmed the results of  $H < 0.5$  indicating a reversion of existing conditions at both river basins. The model performance being higher in the Okavango basin could be attributed to a longer record of flow data available in this basin compared to Limpopo. This gives more opportunity for the model to learn over a long period of time hence the closer fit. The results also showed more fluctuations of drought dynamics in the Limpopo basin with prolonged dry conditions only observed in the Okavango basin. In general terms dry conditions are expected until the final two years of the prediction period. The patterns of drought dynamics are different in the two basins with short intermittent dry and wet spells in the Limpopo as opposed to prolonged spells in the Okavango basin. This could be as a result of different rainfall formation mechanisms that influence climate over these locations. The Okavango basin in the north is mainly influenced by the Inter Tropical Convergence Zone (ITCZ) which has no influence at higher latitudes where the Limpopo basin is located (Byakatonda et al., 2018d). The atmospheric circulation mechanisms in the Limpopo are mainly influenced by easterlies (Nicholson et al., 2001; Usman and Reason, 2004). The agreement in results from rescaled range analysis and ANN shows the ability of combining the two techniques in generating predictions to facilitate better management of hydrological systems under climate change and variability. It has been demonstrated that this region's climate is highly influenced by ENSO, one limitation of ANN models is their inability to accurately predict El Niño conditions which could alter the predicted dynamics.

#### **4.7.3 Projections of cereal yields**

The ANN model developed for projection of cereal yields consisted of 8 neurons in the hidden layer and a delay of 2. The model's input vector comprised of onset and cessation dates, monthly aridity index, SPEI-1 and SOI representing ENSO influence. 1-month timescale of AI and SPEI were used because they had been identified to effectively describe crop yield

variability in Section 4.6. Results of 5 years ahead projections from the end of the historical period are presented in Table 4-15. The MSE results are presented for both open and closed loops.

For the maize yield projection model presented in Table 4-15, the coefficients of correlation are above 95% at all the locations used in the study. The best performance of 98% is realised in the central and western regions. Plots of the outputs and targets for the maize yield projection model in 3 selected regions are presented in Figure 4-28(a), (b) and (c). The plots reveal that the outputs closely fitted the target series, implying the model was in position to learn patterns of the historical inputs and targets to provide projections presented on the same plot. The projections reveal a possibility of a general yield decline from the end of the historical period. The maize yield projections indicates a likelihood of a decline in central and eastern regions for the next 5 years by 52 kg/ha and 21 kg/ha respectively. However the north is expected to have yield increase of 38 kg/ha over the same time period.

**Table 4-15.** Artificial Neural Network (ANN) model performance and crop yield projections

Location	Performance			Recorded yield (kg/ha)	Yield predictions (kg/ha)					
	R	Open loop (MSE)	Closed loop (MSE)	2015/16	Year 1	Year 2	Year 3	Year 4	Year 5	Mean
Maize yield projection ANN model										
Southern	0.97	0.012	0.150	175.1	169.0	197.1	168.5	192.7	193.4	184.1
Central	0.98	0.032	0.276	101.7	82.3	68.0	68.4	48.4	49.6	63.3
Eastern	0.97	0.540	0.054	90.3	59.9	68.5	80.5	68.6	69.6	69.4
Northern	0.96	0.014	0.064	72.8	133.0	122.5	92.7	105.8	110.8	112.9
Western	0.98	0.322	0.006	68.1	41.3	38.8	47.2	59.1	59.5	49.2
Sorghum yield projection ANN model										
Southern	0.90	0.023	0.672	213.0	215.8	227.1	201.5	202.0	174.8	204.2
Central	0.91	0.047	0.174	121.2	202.8	169.2	165.4	132.4	127.7	159.5
Eastern	0.99	0.054	0.157	180.5	141.9	141.0	102.2	63.5	54.5	100.6
Northern	0.95	0.087	0.432	229.9	124.9	119.3	148.6	134.2	184.8	142.3
Western	0.97	0.065	0.137	31.0	18.6	19.3	21.2	23.0	24.5	21.3

Results from the sorghum yield projection model performance are also presented in Table 4-15. These results reveal that the coefficients of correlation (r) for this model are 90% and

above with the best performance of 99% registered in the eastern region. Plots of the comparison between outputs and targets are presented in Figure 4-28(d), (e) and (f). As is the case for maize yield projection model, a close fit between the outputs and targets is observed for the selected regions. In all the selected regions, there is a possibility of sorghum yield decline from the historical period for the next 5 years. The projections reveal that, sorghum yield may decline by 126 kg/ha and 38 kg/ha in eastern and southern regions respectively over the projection period. Marginal changes are expected in the central and western regions.

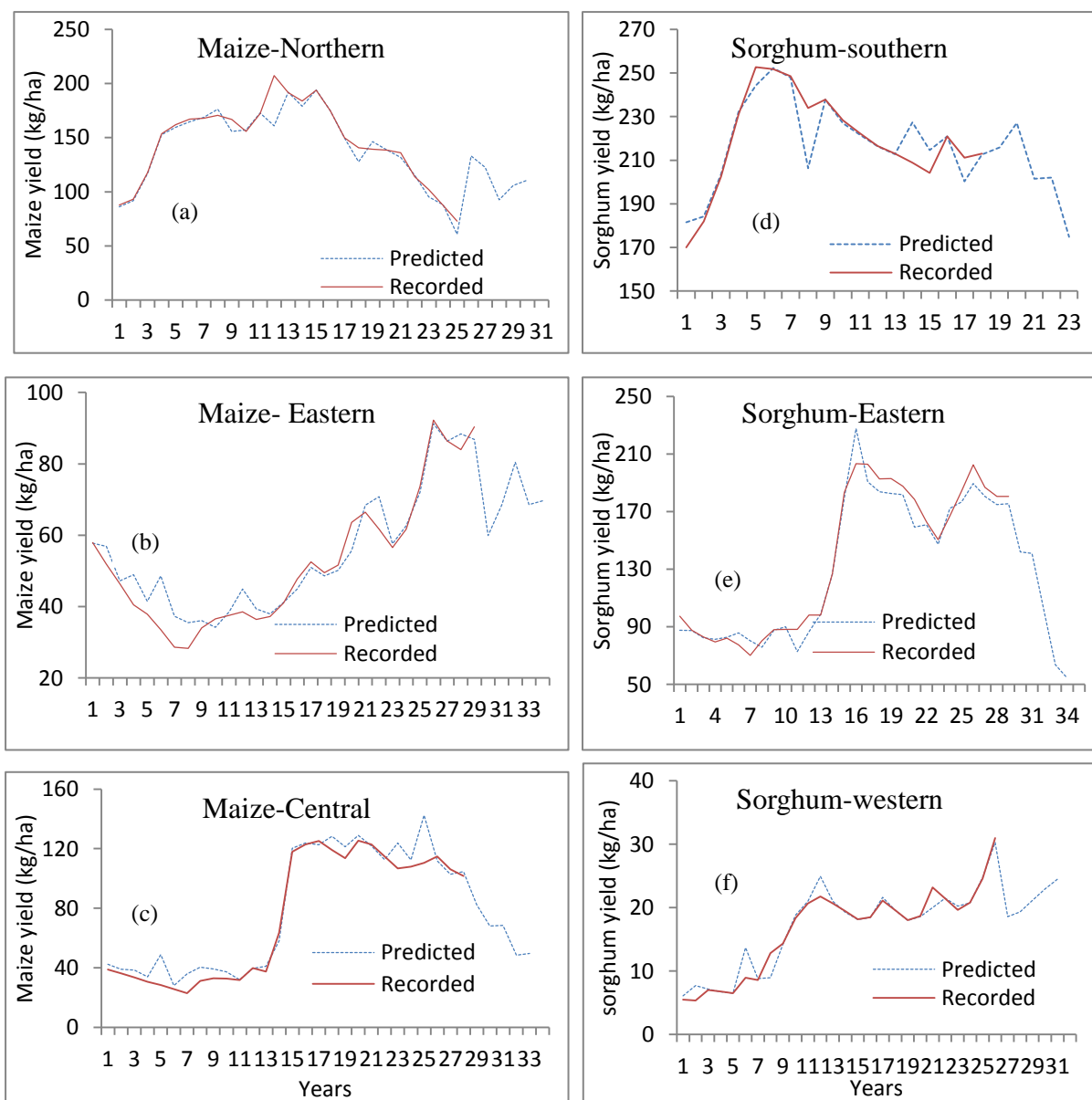


**Fig. 4-28.** Artificial Neural Network (ANN) crop yield projection model outputs and targets in selected regions (a) Maize yield-northern, (b) Maize yield-eastern, (c) Maize yield-central, (d) Sorghum yield-southern, (e) Sorghum yield-eastern and (f) Sorghum yield-western



The multistep ahead NARX model has again demonstrated its ability to learn the interrelations between associated inputs and target variables as represented by high  $r$  values and low MSE. Plots in Figure 4-28 further indicate a close fit between outputs and target series. This study is one of its kind where NARX model has demonstrated ability to project cereal yields. Previously NARX has been used to model water quality and flood heights (Menezes and Barreto, 2008; Chang et al., 2014; Chang et al., 2015). This high performance of NARX in open loop mode gives credence to the crop yield projections resulting from the trained model.

Maize yield projections reveal a likelihood of a yield decline in the central and eastern regions. These regions are among those reported with high yields during the historical period, which may equally pose a threat to food security in the near future. However the northern and southern regions are projected to have yield gains. But the southern locations may not be relied upon to alleviate the food security situation of Botswana since traditionally, they are low yield areas (Batisani, 2012).

Sorghum yield projections also reveal possibility of a yield decline in most locations except the central region which is expected to experience a marginal increase. The highest decline could be experienced in the east followed by the northern region. The models reveal that, there could be more declines in sorghum yield than maize. Results from these projections could aid planning and adaptive abilities for rural farmers to enable them cope with impacts of climate change and variability.

#### **4.7.4 Summary**

Predictions of hydrological flow dynamics, cereal yields, onset and cessation of rain have been made for the next five years (2016/17-2020/21) using a multistep ahead NARX ANN model. The models have demonstrated high performance in all occasions through high coefficient of correlation and low MSE. The graphical comparisons between model outputs and actual targets

have all demonstrated a close fit. Based on the results and discussion above, the following summary is arrived at;

1. Predictions of onset and cessation dates reveal a likely shift in the rain season at 71% of the stations in the next 5 years. In most of the cases the rain season is shifting with rainfall coming earlier at 71% of the stations. These predictions also indicate a possibility of a shorter length of the rain season over the same time period at 50% of the stations. The above findings from this study can facilitate better planning for rainfed agriculture in Botswana and improve on climate risk management.
2. The model predictions confirm a reversion reported by rescaled range analysis through the H-coefficient and further reveals intermittent droughts in the Limpopo basin. The Okavango basin is expected to be moderately dry until the year 2019/20.
3. The projections reveal a possibility of yield decline over the period of prediction with sorghum declining by 126 kg/ha over the next 5 years in the eastern region. Maize yields are also expected to decline by 52 kg/ha in the central region but also the model shows a likelihood of yield gains of 38 kg/ha in the northern region.

## **CHAPTER-5**

### **5. CONCLUSIONS AND RECOMMENDATIONS**

#### **5.1 INTRODUCTION**

In Chapter 4, a summary has been provided at the end of every Section to highlight specific conclusions to each of the objectives stated in Chapter 1. This section presents general remarks while summing up the conclusions, contributions to knowledge, limitations of the study and recommendations for further research.

In totality, this research has demonstrated that drier semiarid locations are experiencing significant association with climatic indices and hence likely to be more affected by events of increased incidences of climate variability. Effects of climate variability already exist as expressed through shortening of the rain season, low crop yields and dwindling water resources across the study area implying that conducting business as usual may exacerbate degeneration of the already fragile environment. Even stream flow and crop yield projections for the next five years have revealed intermittent conditions and crop yield decline. It has also been demonstrated, the rain season is becoming shorter. This calls for innovations in agricultural and water management practices to respond to future climate changes. This will require policies and robust institutional arrangements that resonate with these innovations. Policies that are aimed at economic development and poverty alleviation with necessary feedbacks to different levels of stakeholders will go a long way in mitigating impacts of increased incidences of climate variability on water resources and agriculture. In response to the objectives presented in Chapter 1, the following conclusions are hereby drawn.

#### **5.2 CONCLUSIONS**

The following conclusions resulting from the specific objectives in Chapter 1 are summed up as follows;

*Objective 1: To investigate the monotonic trends and abrupt changes in meteorological time series as a result of climate variability under ENSO influence.*

Explanatory data analysis was done for rainfall, minimum and maximum temperature data and their relationship with ENSO established. Through homogeneity and trend analysis, climatic shifts were established for each climatic variable during a period between 1960 and 2016. The following conclusions are deduced from the analysis under objective 1.

1. The identified years of intervention mainly coincided with either El Niño or La Niña years an indication of ENSO's influence on the local climate of the study area. Strong positive correlations were established between rainfall and SOI whereas negative correlations resulted with SSTs. During El Niño years of 1972/73, 1982/83, 1997/98 and 2015/16 positive temperature anomalies were registered and rainfall suppressed. This confirms the influence of ENSO on the local climate across the study area.
2. The analysis showed an overall decrease in rainfall by 15% and an increase in temperature by 2% over the period of analysis. Majority of the rainfall decrease was registered in the Limpopo and Okavango river basins which host most of the water resources for Botswana. This implies the current climatic trends are a threat to both agricultural and water resources across the study area. This necessitates interventions towards climate change resilience.

*Objective 2: To determine the dry spell frequency, onset and cessation of rainfall, their variability and trends.*

Seasonal rainfall characteristics were further explored to establish their behaviour and influence on agriculture in Botswana. The seasonal characteristics investigated were onset and cessation of rain, dry spell frequency and number of rainy days. From the analysis of these characteristics, the following conclusions addressing objective 2 are deduced;

1. Seasonal rainfall is highly erratic with coefficient of variation ranging from 30% to 50%.

Trends revealed that the number of rainy days was decreasing at all the synoptic stations

used in the analysis. More of concern is the significantly decreasing trends at Shakawe and Pandamatenga which are identified as suitable locations that could support rainfed agriculture.

2. The earliest onset was registered in the northeast, a high rainfall region while late onset was registered in the drier locations of southwest at Tsabong and Tshane. Equally, rain cessation was earliest in the southwest and latest in the northeast. The rain cessation dates exhibited lower coefficients of variation compared to onset dates implying that the uncertainty in rain could mainly be attributed to onset rather than cessation of rain.
3. Three locations of Shakawe, Pandamatenga and Kasane were found with rain season longer than 100 days making them the only locations suitable for medium maturing cereals. These locations were however found to exhibit significantly increasing trends in dry spells. This could be a bottleneck in efforts to alleviate the food security situation of Botswana.

In spite of this, information generated from this research is vital for effective planning in the agricultural sector as it can trigger other government sectors to act in order to minimise negative impacts as a result of climate variability and change.

*Objective 3: To determine drought severity using SPEI and its influence on hydrological systems under ENSO scenarios.*

The spatial and temporal variability of drought were explored culminating into drought vulnerability maps. The degree of association between ENSO and drought severity at timescales of 1-, 3-, 6-, 12-, 18- and 24-months was also established. Propagation of climatic droughts to hydrological droughts was determined together with a joint timescale for drought monitoring across the study area. The following conclusions were deduced from the study in response to objective 3.

1. It was established that there is higher temporal variability in drought at lower timescales of 1- and 3-months. At all the timescales, Botswana was found to be more vulnerable to moderate droughts. These droughts exhibited the strongest degree of association with

ENSO at the peak of the summer rain season in December and January. This implies quantities of summer rainfall received may be influenced by the ENSO events in the Equatorial Pacific with local teleconnections.

2. This research through objective 3 established that it takes 7 and 6 months for climatic droughts to propagate into hydrological droughts in the Limpopo and Okavango basins respectively. A common timescale of 15-months was found adequate in monitoring droughts across the two river basins. High variability of drought across the river basins was also demonstrated through H-coefficient being significantly less than 0.5.

*Objective 4: To determine the degree of association between climatic indices, length of the rain season and ENSO on cereal yield.*

The climatic characteristics that have been determined in objectives 2 and 3 have implications on agricultural systems since they affect moisture supply as part of the hydrological cycle. The influence of climatic indices, length of the rain season and ENSO on cereal yields was investigated under objective 4. Findings from the investigations are summarised below;

ENSO was found to have the greatest influence on cereal yield mainly in the southern region. It accounted for 85% and 78% variations in maize and sorghum yields respectively in this region. It was also established that sorghum was more tolerant to moisture deficit conditions compared to maize grown in the study area.

*Objective 5: To provide predictions of hydrological droughts, cereal yields, onset and cessation of rain dates across the study area.*

Artificial neural network (ANN) models for providing 5 years ahead predictions of rain onset and cessation dates, hydrological flow index and cereal yields were developed while addressing objective 5. Nonlinear autoregressive with exogenous input (NARX) ANN a class of dynamic recurrent neural network (DRNN) was used to develop these models that have been trained, tested and applied to provide predictions for a period between 2017 and 2021. It is anticipated that these models will facilitate planning for both agricultural and water

resources. The models provide predictions that could guide on different options available for climate change adaptation measures. Results from these models have revealed the following information for the next 5 years;

1. Predictions reveal a shift in the rain season across Botswana with both onset and cessation of rain coming earlier at 71% of the stations used in this research. This may lead to more uncertainty in rainfed agriculture as farmers are not certain when to sow. However if this information is passed on to the users in a timely manner, it could alleviate the uncertainty.
2. The models have also revealed high variability in hydrological indices with conditions remaining erratic until 2019. This may pose a threat to water resource availability and soil moisture supply necessary for supporting plant growth.
3. The model for crop yield projections reveals a general yield decline in both maize and sorghum. A yield decline in sorghum of 126 kg/ha is expected to occur in the eastern region over the next 5 years. The highest decline is expected in sorghum yield in spite of it being identified as more drought tolerant crop than maize.

### **5.3 CONTRIBUTIONS TO KNOWLEDGE AND RESEARCH OUTPUT**

The major contributions from this research include three avenues that could assist semiarid regions, Botswana in particular, to cope with impacts of climate change and increased incidences of climate variability. This high variability has been associated with frequent droughts that have ravaged agricultural and water resources in semiarid and arid locations. In the process of knowledge dissemination, various research outputs that resulted from the 5 objectives have been published in international peer reviewed journals. The contributions and research outputs are hereby presented below:

#### **5.3.1 Contribution to knowledge**

1. A criterion for determining onset and cessation of rainfall dates has been developed for locations with prolonged dry spells.

2. Drought early warning indicators such as rain onset, cessation and drought severity have been determined. These indices are major inputs in drought monitoring hence their analysis could support drought preparedness strategies in semiarid locations.
3. From this research, three 5-year ahead artificial neural network (ANN) prediction models have been developed using the nonlinear autoregressive with exogenous input (NARX) models, a category of dynamic recurrent neural network (DRNN) with tapped delay lines. These models have used ENSO as one of the predictors and have provided satisfactory results evidenced through high correlations and low MSE. This is the first attempt in which NARX has demonstrated ability to predict crop yields, rain onset and cessation dates under ENSO influence. These models can be replicated in regions whose climates are known to be influenced by ENSO.

### **5.3.2 Research outputs**

Peer reviewed journal and conference papers that have resulted from this research are listed below. The contents of these papers form a large part of this thesis with slight modifications.

#### **Journal papers**

1. Byakatonda J, Parida BP, Kenabatho PK (2018). Relating dynamics of climatological and hydrological drought in Semiarid Botswana; *Journal of Physics and Chemistry of the earth* 105C:12-24.
2. Byakatonda J, Parida BP, Kenabatho PK, Moalafhi DB (2018) Prediction of onset and cessation of austral summer rainfall and dry spell frequency analysis in semi-arid Botswana, *Theoretical and Applied Climatology*, 1–17.
3. Byakatonda J, Parida BP, Kenabatho PK, Moalafhi DB (2018) Influence of climate variability and length of rainy season on crop yields in semiarid Botswana. *Agricultural and Forest Meteorology* 248C:130–144.



4. Byakatonda J, Parida BP, Kenabatho PK, Moalafhi DB (2018) Analysis of rainfall and temperature time series to detect long-term climatic trends and variability over semiarid Botswana, *Journal of Earth Systems Science*, 127(25).
5. Byakatonda J, Parida BP, Kenabatho PK, Moalafhi DB (2016) Modelling dryness severity using artificial neural networks at the Okavango delta, Botswana, *GNEST* 18:463-481.
6. Byakatonda J, Parida BP, Kenabatho PK, Lesole D, Moalafhi DB (2018) Investigating Relationship Between Drought Severity in Botswana and ENSO, *Nat. Hazards journal* (under review).

### **Conference papers**

1. Byakatonda J, Parida BP, Kenabatho PK (2016). Aridity changes and its association with drought severity in Botswana; Preceding of the 5<sup>th</sup> African Higher Education Week and RUFORUM Biennial Conference, Cape Town, South Africa, 17-21 October, 2016.
2. Byakatonda J, Parida BP, Kenabatho PK (2015) Climate Variability and Trends in Meteorological Time Series in Semi-Arid Botswana, Preceding of the 10<sup>th</sup> Alexander von Humboldt International Conference Addis Ababa ,Ethiopia, 18 – 20 November 2015.

Objective 1 of this research is published in journal paper (4) and conference paper (2). A version of objective 2 is published in journal paper (2) while objective 3 appears in journal papers (1), (5) and (6). Objective 4 is covered in journal paper (3) and conference paper (1). The last objective is presented in Journal papers (1), (2), (3) and (5).

### **5.4 LIMITATIONS OF THE STUDY**

In the course of this research the following limitations were identified;

1. Synoptic stations are skewed to the east with sparse distribution to the west and central regions at the fringes of the Kalahari desert. This could affect the spatial interpolation of climate characteristics in these locations.

2. Only meteorological, agricultural and hydrological droughts are explored in this research. However, prolonged multiyear droughts may degenerate into social economical droughts which have not been addressed.
3. The absence of records at most synoptic stations on relative humidity, wind speed and solar radiation which are known factors that affects drought severity hindered the use of the recommended Penman-Monteith method of determining potential evapotranspiration.
4. Any observed climatic shifts during this study are mainly attributed to climate variability rather than change since some of the data length used in this study was less than the 30 years threshold recommended by the World Meteorological Organisation (WMO) for climate change studies.

## **5.5 RECOMMENDATIONS FOR FURTHER RESEARCH**

To further enrich the above research findings, the following recommendation for future studies are suggested.

1. Artificial neural networks are only able to provide short term predictions. This study recommends the use of re-analysis data to facilitate long term predictions.
2. Improvement on spatial density of synoptic stations in the west and central regions to enhance interpolated results over the study area is highly recommended.
3. Extend meteorological data measurement at all synoptic stations to wind speed, relative humidity and solar radiation, which are known factors that affect drought severity. The use of satellite data may be explored. Once these parameters are available, drought severity should be re-evaluated and compared with results obtained from this research.

## REFERENCES

- Abramowitz, M. and Stegun, I. A. (1964). *Handbook of mathematical functions: with formulas, graphs, and mathematical tables*: Courier Corporation.
- Akinsanola, A. and Ogunjobi, K. (2015). Recent homogeneity analysis and long-term spatio-temporal rainfall trends in Nigeria. *Theoretical and Applied Climatology*, 1-15.
- Alexandersson, H. (1986). A homogeneity test applied to precipitation data. *Journal of climatology*, 6(6), 661-675.
- Alexandersson, H. and Moberg, A. (1997). Homogenization of Swedish temperature data. Part I: Homogeneity test for linear trends. *International Journal of climatology*, 17(1), 25-34.
- Allen, R. G., Pereira, L., Raes, D. and Smith, M. (1998). *FAO Irrigation and drainage paper No. 56*. Rome: FAO.
- Alley, W. M. (1984). The Palmer drought severity index: limitations and assumptions. *Journal of climate and applied meteorology*, 23(7), 1100-1109.
- Amekudzi, L. K., Yamba, E. I., Preko, K., Asare, E. O., Aryee, J., Baidu, M., et al. (2015). Variabilities in Rainfall Onset, Cessation and Length of Rainy Season for the Various Agro-Ecological Zones of Ghana. *Climate*, 3(2), 416-434.
- Araya, Keesstra, S. and Stroosnijder, L. (2010). A new agro-climatic classification for crop suitability zoning in northern semi-arid Ethiopia. *Agricultural and forest meteorology*, 150(7), 1057-1064.
- Araya and Stroosnijder, L. (2011). Assessing drought risk and irrigation need in northern Ethiopia. *Agricultural and Forest meteorology*, 151(4), 425-436.
- Bannayan, M., Lotfabadi, S. S., Sanjani, S., Mohamadian, A. and Aghaalikhani, M. (2011). Effects of precipitation and temperature on crop production variability in northeast Iran. *International journal of Biometeorology*, 55(3), 387-401.

- Bannayan, M., Sanjani, S., Alizadeh, A., Lotfabadi, S. S. and Mohamadian, A. (2010). Association between climate indices, aridity index, and rainfed crop yield in northeast of Iran. *Field Crops Research*, 118(2), 105-114.
- Batisani, N. (2011). The spatio-temporal-severity dynamics of drought in Botswana. *Journal of Environmental Protection*, 2(06), 803.
- Batisani, N. (2012). Climate variability, yield instability and global recession: the multi-stressor to food security in Botswana. *Climate and Development*, 4(2), 129-140.
- Batisani, N. and Yarnal, B. (2010). Rainfall variability and trends in semi-arid Botswana: implications for climate change adaptation policy. *Applied Geography*, 30(4), 483-489. doi: 10.1016/j.apgeog.2009.10.007
- Beguiría, S., Vicente-Serrano, S. M., Reig, F. and Latorre, B. (2014). Standardized precipitation evapotranspiration index (SPEI) revisited: parameter fitting, evapotranspiration models, tools, datasets and drought monitoring. *International Journal of Climatology*, 34(10), 3001-3023.
- Botswana Central Statistics. (2009). *Botswana water statistics*. Botswana: Department of Printing and Publishing Services Retrieved from [http://www1.eis.gov.bw/EIS/Reports/Botswana%20Water\\_statistics%20report.pdf](http://www1.eis.gov.bw/EIS/Reports/Botswana%20Water_statistics%20report.pdf).
- Bromwich, D. H., Rogers, A. N., Kållberg, P., Cullather, R. I., White, J. W. and Kreutz, K. J. (2000). ECMWF Analyses and Reanalyses Depiction of ENSO Signal in Antarctic Precipitation\*. *Journal of Climate*, 13(8), 1406-1420.
- Brown, M. E. and Funk, C. C. (2008). Food security under climate change.
- Buishand, T. A. (1982). Some methods for testing the homogeneity of rainfall records. *Journal of Hydrology*, 58(1), 11-27.
- Byakatonda, J., Parida, B. and Kenabatho, P. K. (2018a). Relating the dynamics of climatological and hydrological droughts in semiarid Botswana. *Physics and Chemistry of the Earth, Parts A/B/C*.

- Byakatonda, J., Parida, B., Kenabatho, P. K. and Moalafhi, D. (2016). Modelling dryness severity using artificial neural networks at the Okavango delta, Botswana. *GLOBAL NEST JOURNAL*, 18(3), 463-481.
- Byakatonda, J., Parida, B., Kenabatho, P. K. and Moalafhi, D. (2018b). Influence of climate variability and length of rainy season on crop yields in semiarid Botswana. *Agricultural and Forest Meteorology*, 248, 130-144.
- Byakatonda, J., Parida, B., Kenabatho, P. K. and Moalafhi, D. (2018c). Prediction of onset and cessation of austral summer rainfall and dry spell frequency analysis in semiarid Botswana. *Theoretical and Applied Climatology*, 1-17.
- Byakatonda, J., Parida, B., Kenabatho, P. K. and Moalafhi, D. (2018d). Analysis of rainfall and temperature time series to detect long-term climatic trends and variability over semiarid Botswana. *Journal of Earth Systems Science*, 127(25) 1-20.
- Cancelliere, A., Di Mauro, G., Bonaccorso, B. and Rossi, G. (2007). Drought forecasting using the standardized precipitation index. *Water resources management*, 21(5), 801-819.
- Chang, F. J., Chen, P. A., Lu, Y. R., Huang, E. and Chang, K.-Y. (2014). Real-time multi-step-ahead water level forecasting by recurrent neural networks for urban flood control. *Journal of Hydrology*, 517, 836-846.
- Chang, F. J., Tsai, Y. H., Chen, P. A., Coynel, A. and Vachaud, G. (2015). Modeling water quality in an urban river using hydrological factors–Data driven approaches. *Journal of environmental management*, 151, 87-96.
- Chen, X., Wu, J. and Wang, L. (2005). Prediction of climate change impacts on streamflow of lake bosten using artificial neural network model. *Journal of Lake Science*, 3, 004.
- Cooper, P., Dimes, J., Rao, K., Shapiro, B., Shiferaw, B. and Twomlow, S. (2008). Coping better with current climatic variability in the rain-fed farming systems of sub-Saharan Africa: An essential first step in adapting to future climate change? *Agriculture, Ecosystems & Environment*, 126(1), 24-35.

- Costa, A. C. and Soares, A. (2009a). Homogenization of climate data: review and new perspectives using geostatistics. *Mathematical Geosciences*, 41(3), 291-305.
- Costa, A. C. and Soares, A. (2009b). Trends in extreme precipitation indices derived from a daily rainfall database for the South of Portugal. *International Journal of Climatology*, 29(13), 1956-1975.
- Critchley, W., Siegert, K., Chapman, C. and Finkel, M. (1991). *Water Harvesting. A manual for the design and construction of water harvesting schemes for plant production*. Rome: FAO.
- Croarkin, C. and Tobias, P. (2006). *NIST/SEMATECH e-handbook of statistical methods National Institute of Standards and Technology*, URL <http://www.itl.nist.gov/div898/handbook> Retrieved from <http://www.itl.nist.gov/div898/handbook>
- Dai, A. (2011). Characteristics and trends in various forms of the Palmer Drought Severity Index during 1900–2008. *Journal of Geophysical Research: Atmospheres (1984–2012)*, 116(D12).
- Dai, A. (2013). Increasing drought under global warming in observations and models. *Nature Climate Change*, 3(1), 52-58.
- Darby, H. and Lauer, J. (2004). Plant physiology—critical stages in the life of a corn plant. *Field Corn.(online)* <http://www.mn.nrcs.usda.gov/technical/ecs/pest/planningaids> (accessed June 12, 2017), 17-24.
- Dastorani, M. and Afkhami, H. (2011). Application of artificial neural networks on drought prediction in Yazd (Central Iran). *Desert*, 16(1), 39-48.
- De Martonne, E. (1926). A new climatological function: The Aridity Index. *Gauthier-Villars, Paris, France*.
- De Stefano, L., Duncan, J., Dinar, S., Stahl, K., Strzepek, K. M. and Wolf, A. T. (2012). Climate change and the institutional resilience of international river basins. *Journal of Peace Research*, 49(1), 193-209.

- Demuth, H., Beale, M. and Hagan, M. (2009). *Neural network toolbox user's guide*, The MathWorks. Inc., Natick, USA.
- Diaconescu, E. (2008). The use of NARX neural networks to predict chaotic time series. *WSEAS Transactions on Computer Research*, 3(3), 182-191.
- Dikgola, K. (2015). *Spatial and temporal variation of inundation in the Okavango Delta, Botswana; with special reference to areas used for flood recession cultivation*. (PhD Thesis), Western Cape.
- Droogers, P. and Allen, R. G. (2002). Estimating reference evapotranspiration under inaccurate data conditions. *Irrigation and drainage systems*, 16(1), 33-45.
- Edossa, D. C., Woyessa, Y. E. and Welderufael, W. A. (2014). Analysis of Droughts in the Central Region of South Africa and Their Association with SST Anomalies. *International Journal of Atmospheric Sciences*, 2014.
- Engelbrecht, F., Adegoke, J., Bopape, M.-J., Naidoo, M., Garland, R., Thatcher, M., et al. (2015). Projections of rapidly rising surface temperatures over Africa under low mitigation. *Environmental Research Letters*, 10(8), 085004.
- FAO Statistics. (2009). *Statistical data base of Food and Agriculture Organization of the United Nations*.
- FAO, U. (2001). *Drought Impact Mitigation and Prevention in the Limpopo River Basin: A Situation Analysis*: FAO Sub-Regional Office.
- Fauchereau, N., Trzaska, S., Rouault, M. and Richard, Y. (2003). Rainfall variability and changes in southern Africa during the 20th century in the global warming context. *Natural Hazards*, 29(2), 139-154.
- Feidas, H., Makrogiannis, T. and Bora-Senta, E. (2004). Trend analysis of air temperature time series in Greece and their relationship with circulation using surface and satellite data: 1955–2001. *Theoretical and Applied Climatology*, 79(3-4), 185-208.

- Feyen, L. and Dankers, R. (2009). Impact of global warming on streamflow drought in Europe. *Journal of Geophysical Research: Atmospheres*, 114(D17).
- Füssel, H.-M. (2009). An updated assessment of the risks from climate change based on research published since the IPCC Fourth Assessment Report. *Climatic Change*, 97(3-4), 469-482.
- Galarneau Jr, T. J., Bosart, L. F. and Aiyyer, A. R. (2008). Closed anticyclones of the subtropics and midlatitudes: A 54-yr climatology (1950–2003) and three case studies *Synoptic—Dynamic Meteorology and Weather Analysis and Forecasting* (pp. 349-392): Springer.
- Gao, Y. and Meng Joo, E. (2005). NARMAX time series model prediction: feedforward and recurrent fuzzy neural network approaches. *Fuzzy sets and systems*, 150(2), 331-350.
- Gerik, T., Bean, B. W. and Vanderlip, R. (2003). Sorghum growth and development. *Texas FARMER Collection*.
- Giorgi, F. and Lionello, P. (2008). Climate change projections for the Mediterranean region. *Global and planetary change*, 63(2), 90-104.
- GOB-MEWT. (2012). *Second National Communication to the United Nations Framework Convention on Climate Change (UNFCCC)* Gaborone, Botswana: Republic of Botswana.
- GOB-MMEWR. (2006). *National water mater plan review* Gaborone: Government of Botswana.
- Gocic, M. and Trajkovic, S. (2013). Analysis of changes in meteorological variables using Mann-Kendall and Sen's slope estimator statistical tests in Serbia. *Global and Planetary Change*, 100, 172-182.
- Golden gate weather services. (2017). El Niño and La Niña Years and Intensities. Retrieved 3/6/2017, from <http://ggweather.com/enso/oni.htm>



- Gommes, R. and Petrassi, F. (1994). Rainfall variability and drought in Sub-Saharan Africa since 1960. *FAO Agrometeorology Series Working Paper (FAO). no. 9.*
- Granero, M. S., Segovia, J. T. and Pérez, J. G. (2008). Some comments on Hurst exponent and the long memory processes on capital markets. *Physica A: Statistical Mechanics and its Applications*, 387(22), 5543-5551.
- Guha-Sapir, D., Vos, F., Below, R. and Ponserre, S. (2011). Annual disaster statistical review 2010. *Centre for Research on the Epidemiology of Disasters.*
- Hänsel, S., Medeiros, D. M., Matschullat, J., Silva, I. d. M. and Petta, R. A. (2016). Assessing homogeneity and climate variability of temperature and precipitation series in the capitals of northeastern Brazil. *Frontiers in Earth Science*, 4, 29.
- Hansen, J., Sato, M., Ruedy, R., Schmidt, G. A. and Lo, K. (2016). Global Temperature in 2015.
- Hargreaves, G. H. (1994). Defining and using reference evapotranspiration. *Journal of Irrigation and Drainage Engineering*, 120(6), 1132-1139.
- Hayes, M., Svoboda, M., Wall, N. and Widhalm, M. (2011). The Lincoln declaration on drought indices: universal meteorological drought index recommended. *Bulletin of the American Meteorological Society*, 92(4), 485-488.
- Hecht-Nielsen, R. (1987). *Kolmogorov's mapping neural network existence theorem*. Paper presented at the Proceedings of the international conference on Neural Networks.
- Heim Jr, R. R. (2002). A review of twentieth-century drought indices used in the United States. *Bulletin of the American Meteorological Society*, 83(8), 1149-1165.
- Hoell, A., Funk, C., Magadzire, T., Zinke, J. and Husak, G. (2015). El Niño–Southern Oscillation diversity and southern Africa teleconnections during austral summer. *Climate Dynamics*, 45(5-6), 1583-1599.
- Hosking, J. R. M. and Wallis, J. R. (2005). *Regional frequency analysis: an approach based on L-moments*: Cambridge University Press.

- Huang, J., Ji, M., Xie, Y., Wang, S., He, Y. and Ran, J. (2016). Global semi-arid climate change over last 60 years. *Climate Dynamics*, 46(3-4), 1131-1150.
- Huang, S., Li, P., Huang, Q., Leng, G., Hou, B. and Ma, L. (2017). The propagation from meteorological to hydrological drought and its potential influence factors. *Journal of Hydrology*, 547, 184-195.
- Huang, W., Wang, S., Yu, L., Bao, Y. and Wang, L. (2006). A new computational method of input selection for stock market forecasting with neural networks *Computational Science–ICCS 2006* (pp. 308-315): Springer.
- Hulme, M. (1992). Rainfall changes in Africa: 1931–1960 to 1961–1990. *International Journal of Climatology*, 12(7), 685-699. doi: 10.1002/joc.3370120703
- Hurst, H. E. (1951). Long-term storage capacity of reservoirs. *Trans. Amer. Soc. Civil Eng.*, 116, 770-808.
- Iglesias, A., Garrote, L., Cancelliere, A., Cubillo, F. and Wilhite, D. A. (2009). *Coping with drought risk in agriculture and water supply systems: Drought management and policy development in the Mediterranean* (Vol. 26): Springer Science & Business Media.
- Illeperuma, G. and Sonnadara, U. (2009). Forecasting Droughts using Artificial Neural Networks. *Promoting Knowledge Transfer to Strengthen Disaster Risk Reduction & Climate Change Adaptation*, 100.
- IPCC. (2012). *Managing the risks of extreme events and disasters to advance climate change adaptation: Special report of the intergovernmental panel on climate change* (C. B. Field, V. Barro T.F. Stocker, D. Qin, D.J. Dokken, K.L. Ebi, M.D. Mastrandrea, K.J. Mach, G.-K. Plattner, S.K. Allen, M. Tignor & P. M. Midgley Eds.): Cambridge University Press.
- Jiang, F.-q., Hu, R.-j., Zhang, Y.-w., Li, X.-m. and Tong, L. (2011). Variations and trends of onset, cessation and length of climatic growing season over Xinjiang, NW China. *Theoretical and applied climatology*, 106(3-4), 449-458.

- Jones, P., Trenberth, K., Ambenje, P., Bojariu, R., Easterling, D., Klein, T., et al. (2007). Observations: surface and atmospheric climate change. *IPCC, Climate change*, 235-336.
- Jung, M., Reichstein, M., Ciais, P., Seneviratne, S. I., Sheffield, J., Goulden, M. L., et al. (2010). Recent decline in the global land evapotranspiration trend due to limited moisture supply. *Nature*, 467(7318), 951-954.
- Kebede, A., Diekkrüger, B. and Edossa, D. C. (2016). Dry spell, onset and cessation of the wet season rainfall in the Upper Baro-Akobo Basin, Ethiopia. *Theoretical and Applied Climatology*, 1-10.
- Kenabatho, P., Parida, B. and Moalafhi, D. (2012). The value of large-scale climate variables in climate change assessment: the case of Botswana's rainfall. *Physics and Chemistry of the Earth, Parts A/B/C*, 50, 64-71.
- Kenabatho, P., Parida, B., Moalafhi, D. and Segosebe, T. (2015). Analysis of rainfall and large-scale predictors using a stochastic model and artificial neural network for hydrological applications in southern Africa. *Hydrological Sciences Journal*, 60(11), 1943-1955.
- Kendall, M. (1975). Rank auto-correlation methods. *Charles Griffin, London*.
- Keyantash, J. and Dracup, J. A. (2002). The quantification of drought: an evaluation of drought indices. *Bulletin of the American Meteorological Society*, 83(8), 1167-1180.
- Khan, M. I., Liu, D., Fu, Q., Dong, S., Liaqat, U. W., Faiz, M. A., et al. (2016). Recent Climate Trends and Drought Behavioral Assessment Based on Precipitation and Temperature Data Series in the Songhua River Basin of China. *Water Resources Management*, 1-21.
- Khan, S. A., Kumar, S., Hussain, M. and Kalra, N. (2009). Climate change, climate variability and Indian agriculture: impacts vulnerability and adaptation strategies *Climate Change and Crops* (pp. 19-38): Springer.

- Kottegoda, N. T. and Rosso, R. (2008). *Applied statistics for civil and environmental engineers*: Blackwell Chichester, UK.
- Koutsoyiannis, D. (2003). Climate change, the Hurst phenomenon, and hydrological statistics. *Hydrological Sciences Journal*, 48(1), 3-24.
- Kundzewicz, Z. W. and Kaczmarek, Z. (2000). Coping with hydrological extremes. *Water International*, 25(1), 66-75.
- Lahmiri, S. (2016). On Simulation Performance of Feedforward and NARX Networks Under Different Numerical Training Algorithms. In F. Miranda & C. Abreu (Eds.), *Handbook of Research on Computational Simulation and Modeling in Engineering* (pp. 171-183): Hershey PA: Engineering Science Reference.
- Laux, P., Jäckel, G., Tingem, R. M. and Kunstmann, H. (2010). Impact of climate change on agricultural productivity under rainfed conditions in Cameroon—a method to improve attainable crop yields by planting date adaptations. *Agricultural and Forest Meteorology*, 150(9), 1258-1271.
- LaViola, J. J. (2003). *Double exponential smoothing: an alternative to Kalman filter-based predictive tracking*. Paper presented at the Proceedings of the workshop on Virtual environments 2003.
- Le Barbé, L., Lebel, T. and Tapsoba, D. (2002). Rainfall variability in West Africa during the years 1950-90. *Journal of climate*, 15(2), 187-202.
- Lettenmaier, D. P. (1976). Detection of trends in water quality data from records with dependent observations. *Water Resources Research*, 12(5), 1037-1046.
- Li-hua, X. (2006). Relationship Between Calibration and Verification Objective Functions in the Optimization of Hydrological Model Parameters. *Journal of Shihezi University (Natural Science)*, 1, 000.

- Li, Y., Ye, W., Wang, M. and Yan, X. (2009). Climate change and drought: a risk assessment of crop-yield impacts. *Climate research (Open Access for articles 4 years old and older)*, 39(1), 31.
- Lim, C. and McAleer, M. (2001). Forecasting tourist arrivals. *Annals of Tourism Research*, 28(4), 965-977.
- Liu, Z., Peng, C., Xiang, W., Tian, D., Deng, X. and Zhao, M. (2010). Application of artificial neural networks in global climate change and ecological research: An overview. *Chinese Science Bulletin*, 55(34), 3853-3863.
- Livada, I. and Assimakopoulos, V. (2007). Spatial and temporal analysis of drought in Greece using the Standardized Precipitation Index (SPI). *Theoretical and applied climatology*, 89(3-4), 143-153.
- Lloyd-Hughes, B. (2012). A spatio-temporal structure-based approach to drought characterisation. *International Journal of Climatology*, 32(3), 406-418.
- Lobell, D. B., Burke, M. B., Tebaldi, C., Mastrandrea, M. D., Falcon, W. P. and Naylor, R. L. (2008). Prioritizing climate change adaptation needs for food security in 2030. *Science*, 319(5863), 607-610.
- Lorenzo-Lacruz, J., Vicente-Serrano, S. M., López-Moreno, J. I., Beguería, S., García-Ruiz, J. M. and Cuadrat, J. M. (2010). The impact of droughts and water management on various hydrological systems in the headwaters of the Tagus River (central Spain). *Journal of Hydrology*, 386(1), 13-26.
- Lourakis, M. I. (2005). A brief description of the Levenberg-Marquardt algorithm implemented by levmar. *Foundation of Research and Technology*, 4, 1-6.
- Maier, H. R. and Dandy, G. C. (2000). Neural networks for the prediction and forecasting of water resources variables: a review of modelling issues and applications. *Environmental modelling & software*, 15(1), 101-124.

- Maier, H. R. and Dandy, G. C. (2001). Neural network based modelling of environmental variables: a systematic approach. *Mathematical and Computer Modelling*, 33(6), 669-682.
- Malesu, M. M., Oduor, A. R. and Odhiambo, O. J. (2007). *Green water management handbook: Rainwater harvesting for agricultural production and ecological sustainability*: SearNet Secretariat, World Agroforestry Centre.
- Maliva, R. and Missimer, T. (2012). Aridity and drought *Arid lands water evaluation and management* (pp. 21-39): Springer.
- Mann, H. B. (1945). Nonparametric tests against trend. *Econometrica: Journal of the Econometric Society*, 245-259.
- Masih, I., Maskey, S., Mussá, F. and Trambauer, P. (2014). A review of droughts on the African continent: a geospatial and long-term perspective. *Hydrology and Earth System Sciences*, 18(9), 3635.
- Masinde, M. (2014). Artificial neural networks models for predicting effective drought index: factoring effects of rainfall variability. *Mitigation and Adaptation Strategies for Global Change*, 19(8), 1139-1162.
- Matalas, N. C. and Langbein, W. (1962). Information content of the mean. *Journal of Geophysical Research*, 67(9), 3441-3448.
- Mbululo, Y. and Nyihirani, F. (2012). Climate characteristics over southern highlands Tanzania. *Atmospheric and Climate Sciences*, 2(04), 454.
- McEvoy, D. J., Huntington, J. L., Abatzoglou, J. T. and Edwards, L. M. (2012). An evaluation of multiscalar drought indices in Nevada and Eastern California. *Earth Interactions*, 16(18), 1-18.
- McKee, T. B., Doesken, N. J. and Kleist, J. (1993). *The relationship of drought frequency and duration to time scales*. Paper presented at the Eighth Conference on Applied Climatology, Anaheim, CA, Boston.

- Menezes, J. M. P. and Barreto, G. A. (2008). Long-term time series prediction with the NARX network: an empirical evaluation. *Neurocomputing*, 71(16), 3335-3343.
- Menzel, A., Sparks, T. H., Estrella, N., Koch, E., Aasa, A., Ahas, R., et al. (2006). European phenological response to climate change matches the warming pattern. *Global change biology*, 12(10), 1969-1976.
- Ministry of Finance and Development Planning. (2009). *National Development Plan 10 ( April 2009-March 2016)*. Botswana: Government Printing and Publishing Services.
- Ministry of Finance and Development Planning. (2017). *National Development Plan 11 ( April 2017-March 2023)*. Botswana: Government Printing and Publishing Services.
- Mishra and Desai, V. (2005). Drought forecasting using stochastic models. *Stochastic Environmental Research and Risk Assessment*, 19(5), 326-339.
- Mishra and Desai, V. (2006). Drought forecasting using feed-forward recursive neural network. *Ecological Modelling*, 198(1), 127-138.
- Mishra, Desai, V. and Singh, V. (2007). Drought forecasting using a hybrid stochastic and neural network model. *Journal of Hydrologic Engineering*.
- Mishra and Singh, V. P. (2010). A review of drought concepts. *Journal of Hydrology*, 391(1), 202-216.
- Mishra and Singh, V. P. (2011). Drought modeling—A review. *Journal of Hydrology*, 403(1), 157-175.
- Mishra, A., K, Sivakumar, B. and Singh, V. P. (2015). Drought processes, modeling, and mitigation. *Journal of Hydrology*, 526, 1-2.
- Moalafhi, D. B., Tshoko, R., Athopheng, J. R., Odirile, P. T. and Masike, S. (2012). Implications of climate change on water resources of Botswana.
- Modarres, R. and da Silva, V. d. P., Rodrigues. (2007). Rainfall trends in arid and semi-arid regions of Iran. *Journal of Arid Environments*, 70(2), 344-355.

- Moeletsi, M. and Walker, S. (2012). Rainy season characteristics of the Free State Province of South Africa with reference to rain-fed maize production. *Water SA*, 38(5), 775-782.
- Morán-Tejeda, E., Bazo, J., López-Moreno, J. I., Aguilar, E., Azorín-Molina, C., Sanchez-Lorenzo, A., et al. (2016). Climate trends and variability in Ecuador (1966–2011). *International Journal of Climatology*.
- Morid, S., Smakhtin, V. and Bagherzadeh, K. (2007). Drought forecasting using artificial neural networks and time series of drought indices. *International Journal of Climatology*, 27(15), 2103-2111.
- Morid, S., Smakhtin, V. and Moghaddasi, M. (2006). Comparison of seven meteorological indices for drought monitoring in Iran. *International journal of climatology*, 26(7), 971-985.
- Mugalavai, E. M., Kipkorir, E. C., Raes, D. and Rao, M. S. (2008). Analysis of rainfall onset, cessation and length of growing season for western Kenya. *Agricultural and forest meteorology*, 148(6), 1123-1135.
- Munshi, J. (2014). There is no chaos in stock markets. Available at SSRN 2448648.
- Mupangwa, W., Walker, S. and Twomlow, S. (2011). Start, end and dry spells of the growing season in semi-arid southern Zimbabwe. *Journal of Arid Environments*, 75(11), 1097-1104.
- Nalbantis, I. and Tsakiris, G. (2009). Assessment of hydrological drought revisited. *Water Resources Management*, 23(5), 881-897.
- Narasimhan, B. and Srinivasan, R. (2005). Development and evaluation of Soil Moisture Deficit Index (SMDI) and Evapotranspiration Deficit Index (ETDI) for agricultural drought monitoring. *Agricultural and Forest Meteorology*, 133(1), 69-88.
- Nath, R., Nath, D., Li, Q., Chen, W. and Cui, X. (2017). Impact of drought on agriculture in the Indo-Gangetic Plain, India. *Advances in Atmospheric Sciences*, 34(3), 335-346.



- Naumann, G., Dutra, E., Barbosa, P., Pappenberger, F., Wetterhall, F. and Vogt, J. (2014). Comparison of drought indicators derived from multiple data sets over Africa. *Hydrology and Earth System Sciences*, 18(5), 1625-1640.
- Nazemosadat, M., Samani, N. and Barry, D. (2006). ENSO forcing on climate change in Iran: Precipitation analysis. *Iranian Journal of Science and Technology, Transaction B: Engineering*, 30(ECOL-ARTICLE-2007-006), 555-565.
- Neog, P., Bhuyan, J. and Baruah, N. (2008). Thermal indices in relation to crop phenology and seed yield of soybean (*Glycine max* L. Merrill). *Journal of Agrometeorology*, 10, 388-392.
- Ngetich, K., Mucheru-Muna, M., Mugwe, J., Shisanya, C., Diels, J. and Mugendi, D. (2014). Length of growing season, rainfall temporal distribution, onset and cessation dates in the Kenyan highlands. *Agricultural and Forest Meteorology*, 188, 24-32.
- Nicholson, S. E. and Kim, J. (1997). The relationship of the El Nino-Southern oscillation to African rainfall. *International Journal of Climatology*, 17(2), 117-135.
- Nicholson, S. E., Leposo, D. and Grist, J. (2001). The relationship between El Niño and drought over Botswana. *Journal of Climate*, 14(3), 323-335.
- NOAA-NCDC. (2016). Southern Oscillation Index (SOI). Retrieved 16/10/2016, from [www.ncdc.noaa.gov/teleconnections/enso/indicators/soi/data.csv](http://www.ncdc.noaa.gov/teleconnections/enso/indicators/soi/data.csv)
- NOAA-NCEP. (2016). Average sea surface temperature (SST) anomalies in region 3.4 of the Equatorial Pacific Retrieved 16/10/2016, from [http://www.cpc.ncep.noaa.gov/products/analysis\\_monitoring/ensostuff/ONI\\_change.shtml](http://www.cpc.ncep.noaa.gov/products/analysis_monitoring/ensostuff/ONI_change.shtml)
- Nsubuga, F. W., Botai, O., Olwoch, J. M., Rautenbach, C. d., Bevis, Y. and Adetunji, A. O. (2014). The nature of rainfall in the main drainage sub-basins of Uganda. *Hydrological Sciences Journal*, 59(2), 278-299. doi: 10.1080/02626667.2013.804188

- Nyenzi, B. and Lefale, P. (2006). Nyenzi B, Lefale P (2006) El Nino southern oscillation (ENSO) and global warming Advances in Geosciences 6:95-101. *Advances in Geosciences*, 6(6), 95-101.
- Odekunle, T. (2006). Determining rainy season onset and retreat over Nigeria from precipitation amount and number of rainy days. *Theoretical and applied climatology*, 83(1-4), 193-201.
- Omondi, P. (2011). *Agricultural Drought Indices in the Greater Horn of Africa (GHA) Countries*. Paper presented at the Agricultural drought indices proceedings of an expert meeting.
- Omoyo, N. N., Wakhungu, J. and Oteng'i, S. (2015). Effects of climate variability on maize yield in the arid and semi arid lands of lower eastern Kenya. *Agriculture & Food Security*, 4(1), 1.
- Pachauri, R. and Reisinger, A. (2007). IPCC fourth assessment report. *IPCC, Geneva*.
- Pachauri, R. and Reisinger, A. (2008). IPCC, 2007: Climate Change 2007: Synthesis Report. Contribution of Working Groups I, II and III to the Fourth Assessment Report of the Intergovernmental Panel on Climate Change. In: *IPCC*, 104.
- Parida, B. P. and Moalafhi, D. B. (2008). Regional rainfall frequency analysis for Botswana using L-Moments and radial basis function network. *Physics and Chemistry of the Earth, Parts A/B/C*, 33(8), 614-620.
- Parlos, A. G., Rais, O. T. and Atiya, A. F. (2000). Multi-step-ahead prediction using dynamic recurrent neural networks. *Neural networks*, 13(7), 765-786.
- Parry, M. L. (2007). *Climate Change 2007: impacts, adaptation and vulnerability: contribution of Working Group II to the fourth assessment report of the Intergovernmental Panel on Climate Change (Vol. 4)*: Cambridge University Press.
- Partal, T. and Kahya, E. (2006). Trend analysis in Turkish precipitation data. *Hydrological processes*, 20(9), 2011-2026.

- Pettit, A. (1979). Anon-parametric approach to the change-point detection. *Appl. Stat*, 28, 126-135.
- Potop, V., Türkott, L., Kožnarová, V. and Možný, M. (2010). Drought episodes in the Czech Republic and their potential effects in agriculture. *Theoretical and applied climatology*, 99(3-4), 373-388.
- Preece, D. J. (2008). *Decadal rainfall variability over Southern Africa*. UCL (University College London).
- Rahman, M. R. and Lateh, H. (2015). Climate change in Bangladesh: a spatio-temporal analysis and simulation of recent temperature and rainfall data using GIS and time series analysis model. *Theoretical and Applied Climatology*, 1-15.
- Rajasekaran, P., Prabakaran, R. and Thanigaiselvan, R. (2011). *Implementation of EN-Elman Backprop for Dynamic Power Management*. Paper presented at the Devices and Communications (ICDeCom), 2011 International Conference on.
- Rao, A. R. and Padmanabhan, G. (1984). Analysis and modeling of Palmer's drought index series. *Journal of hydrology*, 68(1), 211-229.
- Recha, C., Makokha, G., Traore, P., Shisanya, C., Lodoun, T. and Sako, A. (2012). Determination of seasonal rainfall variability, onset and cessation in semi-arid Tharaka district, Kenya. *Theoretical and Applied Climatology*, 108(3-4), 479-494.
- Report, I. P. o. C. C. W. g. I. t. t. F. A., Adger, W. N., Kajfež-Bogataj, L., Parry, M. L., Canziani, O. and Palutikof, J. (2007). *Climate change 2007: impacts, adaptation and vulnerability*: Cambridge University Press.
- Reza, Y. M., Javad, K. D., Mohammad, M. and Ashish, S. (2011). Trend detection of the rainfall and air temperature data in the Zayandehrud basin. *Journal of Applied Sciences*, 11, 2125-2134.

- Richard, Y., Trzaska, S., Roucou, P. and Rouault, M. (2000). Modification of the southern African rainfall variability/ENSO relationship since the late 1960s. *Climate Dynamics*, 16(12), 883-895.
- Rimkus, E., Stonevičius, E., Korneev, V., Kažys, J., Valiuškevičius, G. and Pakhomau, A. (2013). Dynamics of meteorological and hydrological droughts in the Neman river basin. *Environmental Research Letters*, 8(4), 045014.
- Rocha, A. and Simmonds, I. (1997). Interannual variability of south-eastern African summer rainfall. Part I: Relationships with air-sea interaction processes. *International Journal of Climatology*, 17(3), 235-265.
- Rockström, J., Falkenmark, M., Karlberg, L., Hoff, H., Rost, S. and Gerten, D. (2009). Future water availability for global food production: the potential of green water for increasing resilience to global change. *Water Resources Research*, 45(7).
- Rojas, O., Li, Y. and Cumani, R. (2014). Understanding the Drought Impact of El Niño on the Global Agricultural Areas: An assessment using FAO's Agricultural Stress Index (ASI): FAO.
- Rowhani, P., Lobell, D. B., Linderman, M. and Ramankutty, N. (2011). Climate variability and crop production in Tanzania. *Agricultural and Forest Meteorology*, 151(4), 449-460.
- Sabzevari, A. A., Zarenistanak, M., Tabari, H. and Moghimi, S. (2015). Evaluation of precipitation and river discharge variations over southwestern Iran during recent decades. *Journal of Earth System Science*, 124(2), 335-352.
- Sakalauskienė, G. (2003). The Hurst phenomenon in hydrology. *Environmental research, engineering and management*, 3(25), 16-20.
- Saldarriaga, J. and Yevjevich, V. (1970). *Application of run-lengths to hydrologic series*: Colorado State University.
- Sen, P. K. (1968). Estimates of the regression coefficient based on Kendall's tau. *Journal of the American Statistical Association*, 63(324), 1379-1389.

- Shahid, S. (2010). Rainfall variability and the trends of wet and dry periods in Bangladesh. *International Journal of climatology*, 30(15), 2299-2313.
- Sheffield, J., Wood, E. F. and Roderick, M. L. (2012). Little change in global drought over the past 60 years. *Nature*, 491(7424), 435-438.
- Shukla, S., Steinemann, A. C. and Lettenmaier, D. P. (2011). Drought monitoring for Washington State: Indicators and applications. *Journal of Hydrometeorology*, 12(1), 66-83.
- Sivakumar, M. (1988). Predicting rainy season potential from the onset of rains in Southern Sahelian and Sudanian climatic zones of West Africa. *Agricultural and Forest Meteorology*, 42(4), 295-305.
- Sivakumar, M. (1992). Empirical analysis of dry spells for agricultural applications in West Africa. *Journal of Climate*, 5(5), 532-539.
- Sivakumar, M. (2010). *Agricultural Drought—WMO Perspectives*. Paper presented at the Agricultural Drought Indices: Proceedings of an Expert Meeting.
- Smakhtin, V. U. and Hughes, D. (2004). *Review, automated estimation and analyses of drought indices in South Asia* (Vol. 83): Iwmi.
- Solomon, S. (2007). *Climate change 2007-the physical science basis: Working group I contribution to the fourth assessment report of the IPCC* (Vol. 4): Cambridge University Press.
- Some'e, B. S., Ezani, A. and Tabari, H. (2012). Spatiotemporal trends and change point of precipitation in Iran. *Atmospheric Research*, 113, 1-12. doi: 10.1016/j.atmosres.2012.04.016
- Some'e, B. S., Ezani, A. and Tabari, H. (2013). Spatiotemporal trends of aridity index in arid and semi-arid regions of Iran. *Theoretical and applied climatology*, 111(1-2), 149-160.
- Sorjamaa, A., Hao, J., Reyhani, N., Ji, Y. and Lendasse, A. (2007). Methodology for long-term prediction of time series. *Neurocomputing*, 70(16), 2861-2869.

- Stagge, J. H., Tallaksen, L. M., Gudmundsson, L., Van Loon, A. F. and Stahl, K. (2015). Candidate distributions for climatological drought indices (SPI and SPEI). *International Journal of Climatology*.
- Stagge, J. H., Tallaksen, L. M., Xu, C. and Van Lanen, H. (2014). Standardized precipitation-evapotranspiration index (SPEI): Sensitivity to potential evapotranspiration model and parameters. *Proceedings of FRIEND-Water*.
- Stathakis, D. (2009). How many hidden layers and nodes? *International Journal of Remote Sensing*, 30(8), 2133-2147.
- Statistics Botswana. (2015). *Annual Agricultural Survey Report 2013*. Gaborone, Botswana: Government of Botswana Printing and Publishing services Retrieved from [www.cso.gov.bw](http://www.cso.gov.bw).
- Stocker, T. F., Qin, D., Plattner, G., Tignor, M., Allen, S., Boschung, J., et al. (2013). Climate change 2013: the physical science basis. Intergovernmental panel on climate change, working group I Contribution to the IPCC fifth assessment report (AR5). *New York*.
- Tabari, H., Somee, B. S. and Zadeh, M. R. (2011). Testing for long-term trends in climatic variables in Iran. *Atmospheric Research*, 100(1), 132-140.
- Tabari, H. and Talaei, P. H. (2011). Temporal variability of precipitation over Iran: 1966–2005. *Journal of Hydrology*, 396(3), 313-320. doi: 10.1016/j.jhydrol.2010.11.034
- Tadross, M., Hewitson, B. and Usman, M. (2005). The interannual variability of the onset of the maize growing season over South Africa and Zimbabwe. *Journal of climate*, 18(16), 3356-3372.
- Thiel, H. (1950). *A rank-invariant method of linear and polynomial regression analysis, Part 3*. Paper presented at the Proceedings of Koninklijke Nederlandse Akademie van Wetenschappen A.
- Tirado, R. and Cotter, J. (2010). Ecological farming: Drought-resistant agriculture. *Exeter, UK: Greenpeace Research Laboratories*.

- Troup, A. (1965). The 'southern oscillation'. *Quarterly Journal of the Royal Meteorological Society*, 91(390), 490-506.
- Tsheko, R. (2004). Rainfall reliability, drought and flood vulnerability in Botswana. *Water SA*, 29(4), 389-392.
- Usman, M. T. and Reason, C. (2004). Dry spell frequencies and their variability over southern Africa. *Climate research.*, 26(3), 199-211.
- Van Loon. (2013). *On the propagation of drought: how climate and catchment characteristics influence hydrological drought development and recovery*. (PhD Thesis), Wageningen WUR.
- Van Loon and Laaha, G. (2015). Hydrological drought severity explained by climate and catchment characteristics. *Journal of Hydrology*, 526, 3-14.
- Vicente-Serrano, S. M., Beguería, S. and López-Moreno, J. I. (2010). A multiscalar drought index sensitive to global warming: the standardized precipitation evapotranspiration index. *Journal of Climate*, 23(7), 1696-1718.
- Vicente-Serrano, S. M., Beguería, S., Lorenzo-Lacruz, J., Camarero, J. J., López-Moreno, J. I., Azorin-Molina, C., et al. (2012). Performance of drought indices for ecological, agricultural, and hydrological applications. *Earth Interactions*, 16(10), 1-27.
- Vicente-Serrano, S. M. and López-Moreno, J. I. (2005). Hydrological response to different time scales of climatological drought: an evaluation of the Standardized Precipitation Index in a mountainous Mediterranean basin. *Hydrology and Earth System Sciences Discussions*, 9(5), 523-533.
- Vicente-Serrano, S., Chura, O., López-Moreno, J., Azorin-Molina, C., Sanchez-Lorenzo, A., Aguilar, E., et al. (2015). Spatio-temporal variability of droughts in Bolivia: 1955–2012. *International Journal of Climatology*, 35(10), 3024-3040.
- Vicente-Serrano, S. M., López-Moreno, J. I., Gimeno, L., Nieto, R., Morán-Tejeda, E., Lorenzo-Lacruz, J., et al. (2011). A multiscalar global evaluation of the impact of

- ENSO on droughts. *Journal of Geophysical Research: Atmospheres (1984–2012)*, 116(D20).
- Von Neumann, J. (1941). Distribution of the ratio of the mean square successive difference to the variance. *The Annals of Mathematical Statistics*, 12(4), 367-395.
- Voss, J. (2013). Rescaled Range Analysis: A Method for Detecting Persistence, Randomness, or Mean Reversion in Financial Markets. *CFA Blog*.
- Wada, Y., Van Beek, L. and Bierkens, M. F. (2011). Modelling global water stress of the recent past: on the relative importance of trends in water demand and climate variability. *Hydrology and Earth System Sciences*, 15(12), 3785-3808.
- Wang, W., Zhu, Y., Xu, R. and Liu, J. (2015). Drought severity change in China during 1961–2012 indicated by SPI and SPEI. *Natural Hazards*, 75(3), 2437-2451.
- White, D. and Walcott, J. (2009). The role of seasonal indices in monitoring and assessing agricultural and other droughts: a review. *Crop and Pasture Science*, 60(7), 599-616.
- Wijngaard, J., Klein Tank, A. and Können, G. (2003). Homogeneity of 20th century European daily temperature and precipitation series. *International Journal of Climatology*, 23(6), 679-692.
- Wilhite, D. A. (2000). Drought as a natural hazard: concepts and definitions. *Drought, a global assessment*, 1, 3-18.
- Wilhite, D. A., Svoboda, M. D. and Hayes, M. J. (2007). Understanding the complex impacts of drought: a key to enhancing drought mitigation and preparedness. *Water resources management*, 21(5), 763-774.
- WMO. (2000). *Detecting trend and other changes in hydrological data* (Z. W. Kundzewicz & A. Robson Eds. Vol. WCDMP – 45). Geneva: WMO.
- WMO. (2009). Guidelines on analysis of extremes in a changing climate in support of informed decisions for adaptation (Vol. WCDMP - No. 72. WMO – TD No. 1500): World meteorological Organization.



- WMO and GWP. (2016). *Handbook of Drought Indicators and Indices* (M. Svoboda and B.A. Fuchs). *Integrated Drought Management Programme (IDMP), Integrated Drought Management Tools and Guidelines* Geneva: WMO and GWP.
- World Bank. (2005). *Agricultural growth for the poor: an agenda for development* (D. Byerlee, C. de Haan, S. Kane, E. Pehu, C. Ragasa & A. Winters-Nelson Eds.): World Bank-Washington.
- Yu, M., Li, Q., Hayes, M. J., Svoboda, M. D. and Heim, R. R. (2014). Are droughts becoming more frequent or severe in China based on the standardized precipitation evapotranspiration index: 1951–2010? *International Journal of Climatology*, 34(3), 545-558.
- Yuan, J. and Hartmann, D. L. (2008). Spatial and temporal dependence of clouds and their radiative impacts on the large-scale vertical velocity profile. *Journal of Geophysical Research: Atmospheres*, 113(D19).
- Yue, S. and Hashino, M. (2003). Long term trends of annual and monthly precipitation in Japan: Wiley Online Library.
- Yue, S., Pilon, P., Phinney, B. and Cavadias, G. (2002). The influence of autocorrelation on the ability to detect trend in hydrological series. *Hydrological Processes*, 16(9), 1807-1829.
- Yue, S. and Wang, C. (2004). The Mann-Kendall test modified by effective sample size to detect trend in serially correlated hydrological series. *Water Resources Management*, 18(3), 201-218.
- Zargar Yaghoobi, A. H. (2012). *Handling uncertainty in hydrologic analysis and drought risk assessment using Dempster-Shafer theory*. (Doctor of Philosophy), University of British Columbia, Canada.

- Zaroug, M. A., Eltahir, E. A. and Giorgi, F. (2013). Droughts and floods over the upper catchment of the Blue Nile and their connections to the timing of El Niño and La Niña Events. *Hydrology and Earth System Sciences Discussions*, 10(8), 10971-10995.
- Zealand, C. M., Burn, D. H. and Simonovic, S. P. (1999). Short term streamflow forecasting using artificial neural networks. *Journal of hydrology*, 214(1), 32-48.
- Zhang, Q., Xu, C.-Y. and Zhang, Z. (2009). Observed changes of drought/wetness episodes in the Pearl River basin, China, using the standardized precipitation index and aridity index. *Theoretical and Applied Climatology*, 98(1-2), 89-99.

## **AUTHOR'S BIOGRAPHICAL INFORMATION**

### **Personal information**

Name: Jimmy Byakatonda

Date of Birth: 28<sup>th</sup> August 1976

Nationality: Ugandan

Contact: byakatondaj@hotmail.com

### **Education background**

Oct 2014-Oct 2018	Univ. of Botswana	PhD. Civil Eng.
Oct 2006-Apr 2008	UNESCO-IHE Delft, Netherlands	MSc. Water Science & Eng.
Sept 1996- Jun 2000	Makerere Unv., Uganda	Bsc. Agric Engineering

### **Professional experience**

Sept 2008-Todate	Gulu University	Lecturer Hydraulic & Irrign Eng
Oct 2000-2006	Belgian Tech. Corp	Irrigation Engineer

### **Research interests**

Prediction of extreme weather conditions, hydro-climatology, drought modelling, water resource management under scarce conditions and artificial intelligence.

## **Selected peer reviewed journal publications and conference papers**

### **Journal papers**

1. **Byakatonda J**, Parida BP, Moalafhi DB, Kenabatho PK, (2018) Analysis of long term drought severity characteristics and trends across semiarid Botswana using two drought indices, *Atmospheric Research* 213C:492-508.
2. **Byakatonda J**, Parida BP, Kenabatho PK (2018). Relating dynamics of climatological and hydrological drought in Semiarid Botswana; *Journal of Physics and Chemistry of the earth* 105C:12-24..
3. **Byakatonda J**, Parida BP, Kenabatho PK, Moalafhi DB (2018) Prediction of onset and cessation of austral summer rainfall and dry spell frequency analysis in semi-arid Botswana, *Theoretical and Applied Climatology*, 1–17.
4. **Byakatonda J**, Parida BP, Kenabatho PK, Moalafhi DB (2018) Influence of climate variability and length of rainy season on crop yields in semiarid Botswana. *Agricultural and Forest Meteorology* 248C:130–144.
5. **Byakatonda J**, Parida BP, Kenabatho PK, Moalafhi DB (2018) Analysis of rainfall and temperature time series to detect long-term climatic trends and variability over semiarid Botswana, *Journal of Earth Systems Science*, 127(25).
6. **Byakatonda J**, Parida BP, Kenabatho PK, Moalafhi DB (2016) Modelling dryness severity using artificial neural networks at the Okavango delta, Botswana, *GNEST* 18:463-481.

### **Conference papers**

1. **Byakatonda J**, Parida BP, Kenabatho PK (2016). Aridity changes and its association with drought severity in Botswana; Preceding of the 5<sup>th</sup> African Higher Education Week and RUFORUM Biennial Conference, Cape Town, South Africa, 17-21 October, 2016.

2. **Byakatonda J**, Parida BP, Kenabatho PK (2015) Climate Variability and Trends in Meteorological Time Series in Semi-Arid Botswana, Preceding of the 10<sup>th</sup> Alexander von Humboldt International Conference Addis Ababa ,Ethiopia, 18 – 20 November 2015.